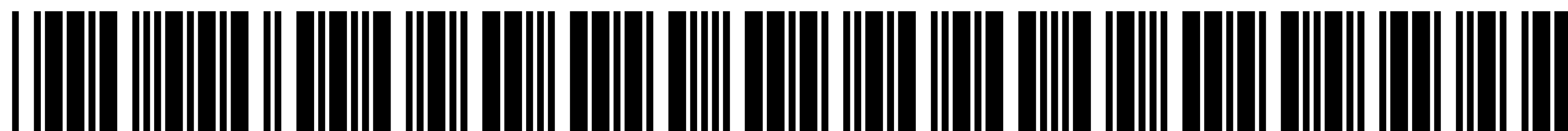

(19) **United States**
(12) **Patent Application Publication**
Golovchenko et al.
(10) **Pub. No.: US 2005/0126905 A1**
(43) **Pub. Date: Jun. 16, 2005**

(54) **HIGH-PRECISION FEEDBACK CONTROL FOR ION SCULPTING OF SOLID STATE FEATURES**

(75) Inventors: **Jene A. Golovchenko**, Lexington, MA (US); **Derek M. Stein**, Delft (NL); **George E. Yefchak**, Santa Clara, CA (US); **Richard J. Pittaro**, San Carlos, CA (US); **Curt Flory**, Los Altos, CA (US)

Correspondence Address:
Theresa A. Lober
T. A. Lober Patent Services
45 Walden Street
Concord, MA 01742 (US)

(73) Assignees: **President and Fellows of Harvard College**, Cambridge, MA (US); **Agilent Technologies, Inc.**, Palo Alto, CA (US)

(21) Appl. No.: **10/960,176**

(22) Filed: **Oct. 7, 2004**

Related U.S. Application Data

(63) Continuation-in-part of application No. 10/695,381, filed on Oct. 28, 2003, and which is a continuation-in-part of application No. 10/186,105, filed on Jun. 27, 2002, now Pat. No. 6,783,643, and which is a continuation-in-part of application No. 09/599,137, filed on Jun. 22, 2000, now Pat. No. 6,464,842.

(60) Provisional application No. 60/509,656, filed on Oct. 8, 2003. Provisional application No. 60/421,908, filed on Oct. 29, 2002. Provisional application No. 60/301,400, filed on Jun. 27, 2001. Provisional application No. 60/140,201, filed on Jun. 22, 1999.

Publication Classification

(51) **Int. Cl.**[7] **C23C 14/32**
(52) **U.S. Cl.** **204/192.34**; 204/298.36

(57) **ABSTRACT**

The invention provides a method for controlled fabrication of a solid state structural feature. In the method, a solid state structure is provided and the structure is exposed to an ion beam, under fabrication process conditions for producing the structural feature. A physical detection species is directed toward a designated structure location, and the rate at which the detection species proceeds from the designated structure location is measured. Detection species rate measurements are fit to a mathematical model, and the fabrication process conditions are controlled, based on the fitted detection species rate measurements, to fabricate the structural feature.

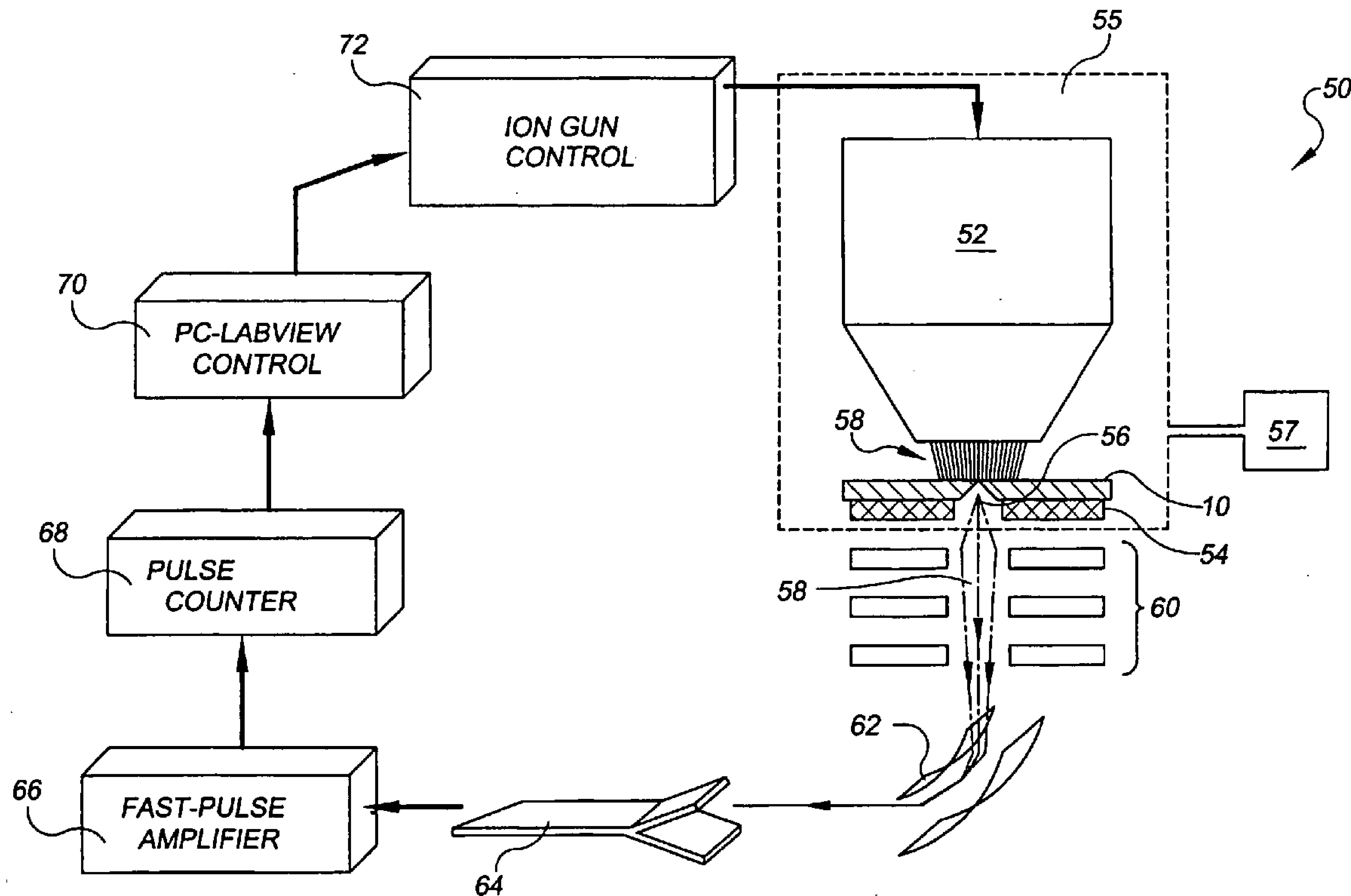

FIG. 1A

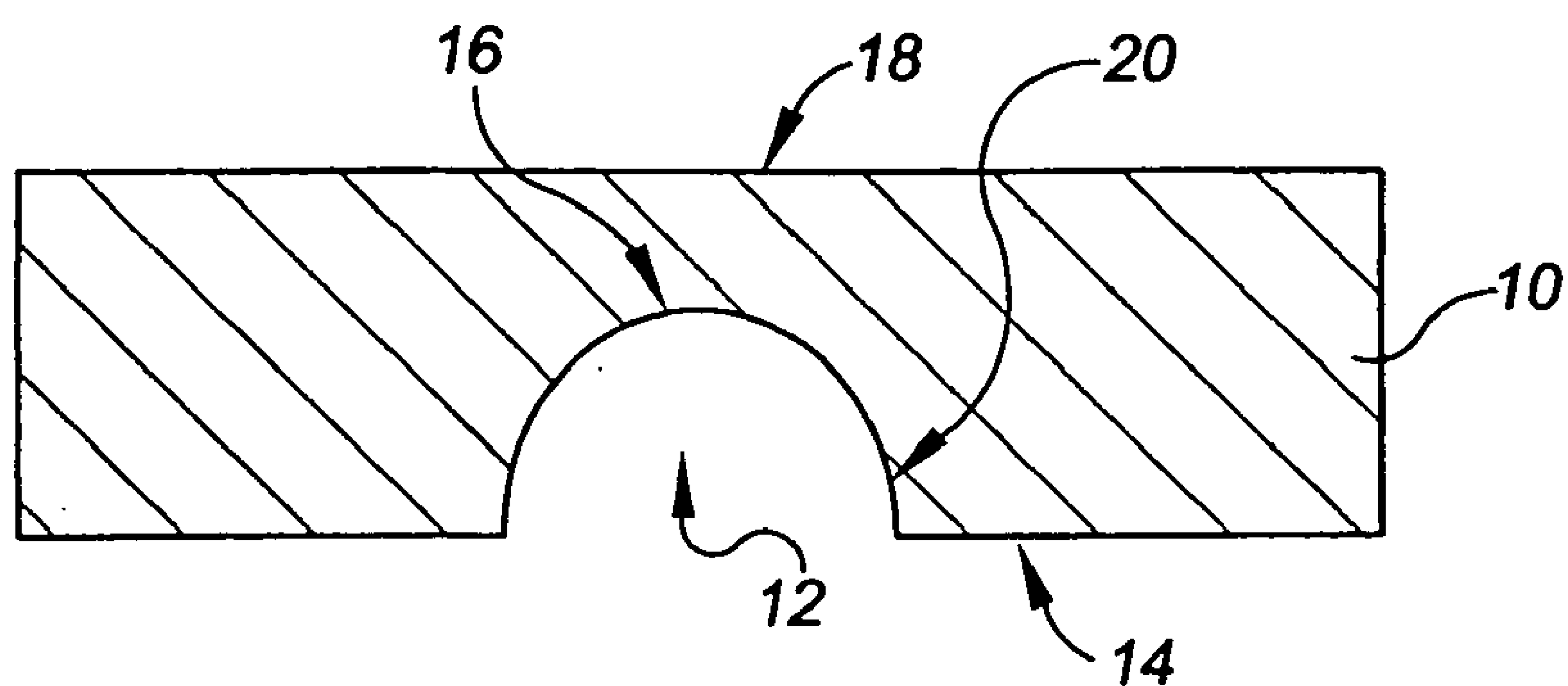

FIG. 1B

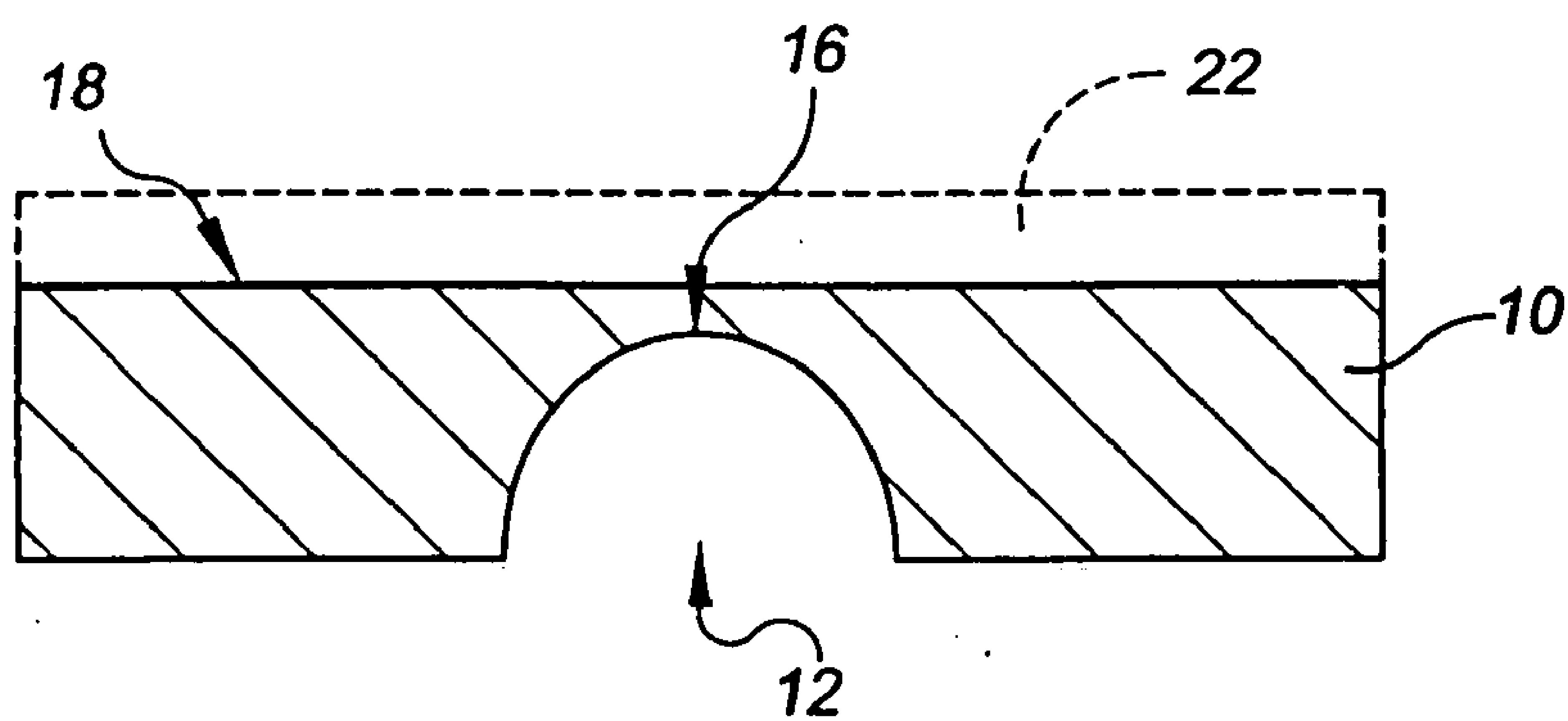

FIG. 1C

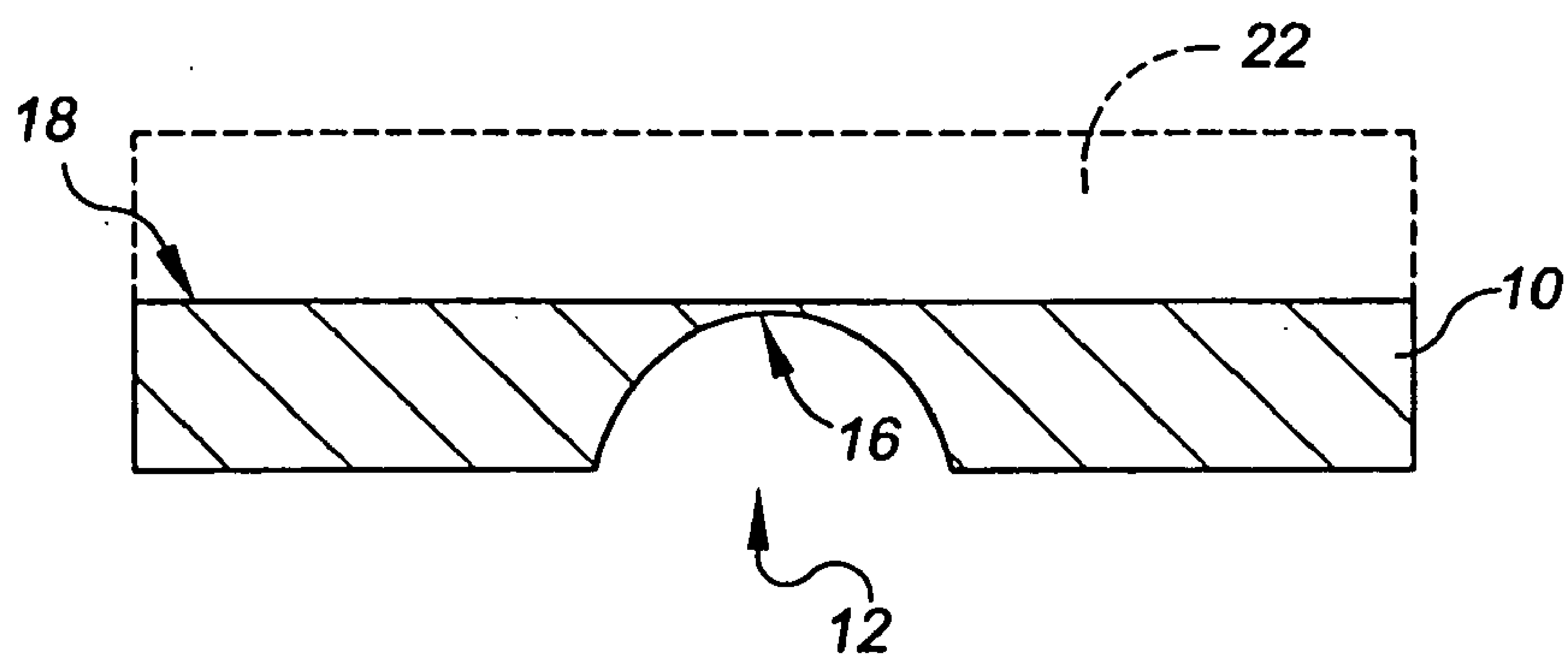

FIG. 1D

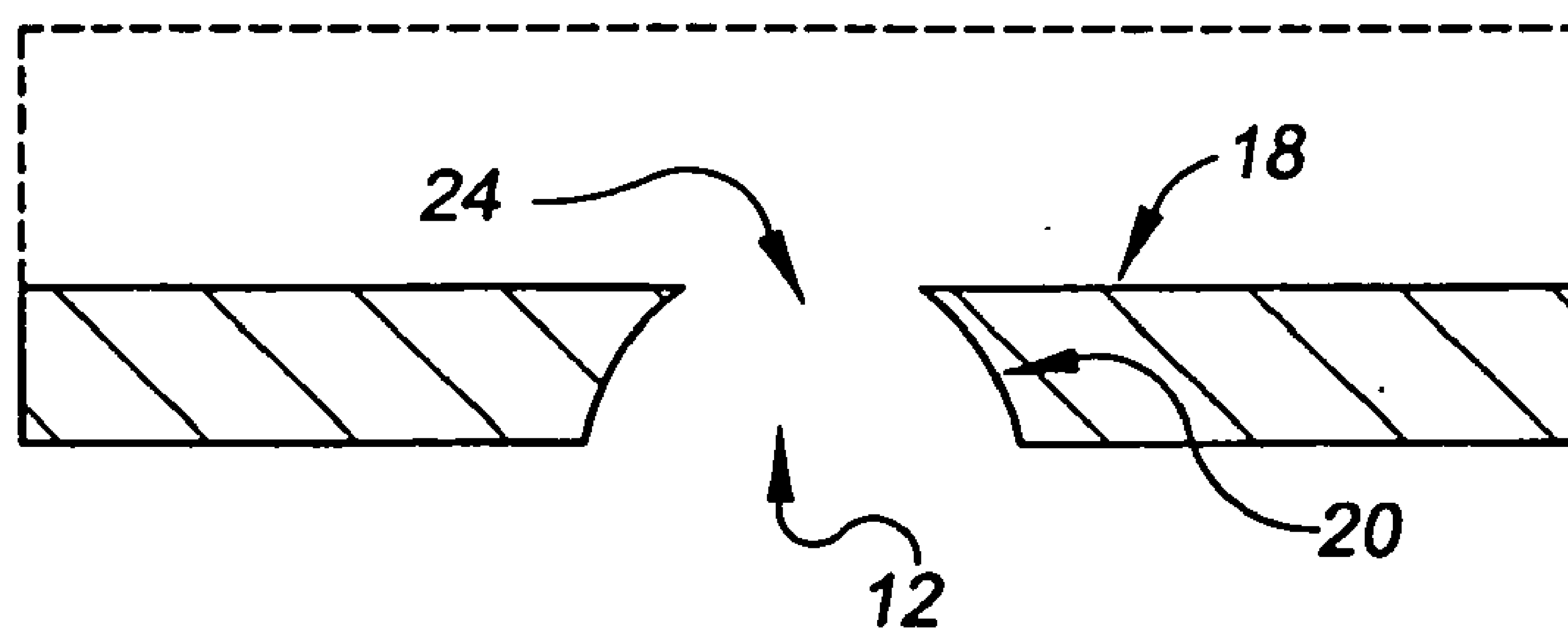

FIG.2A

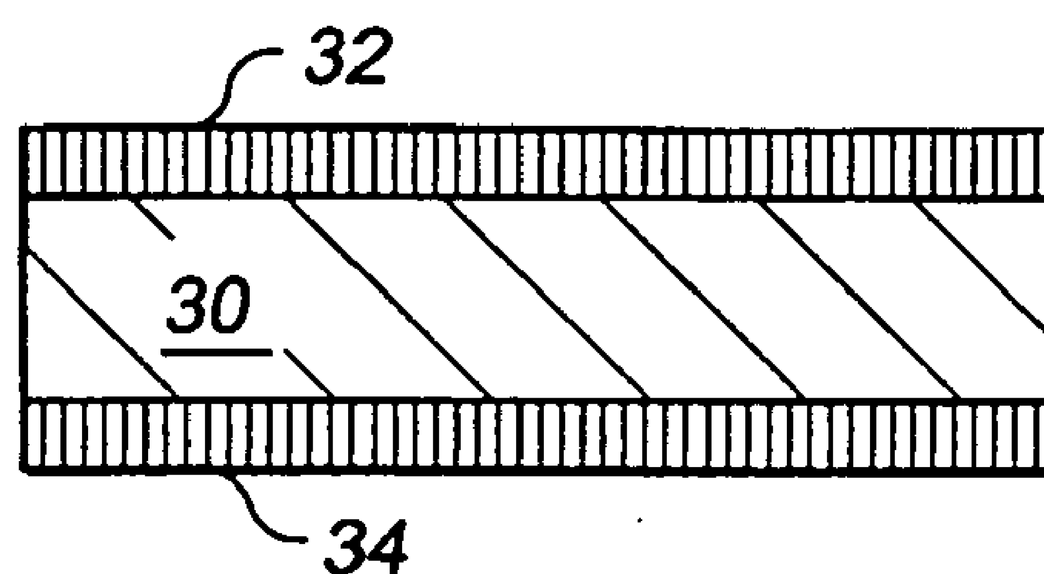

FIG.2B

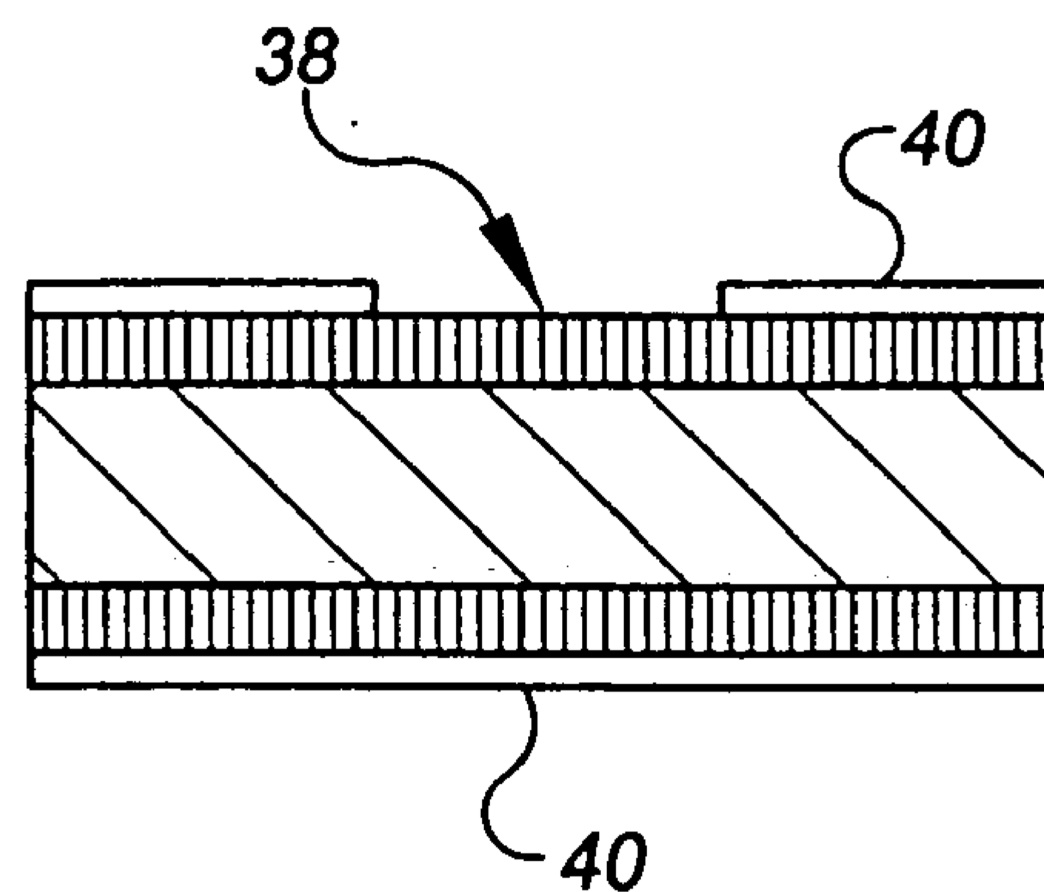

FIG.2C

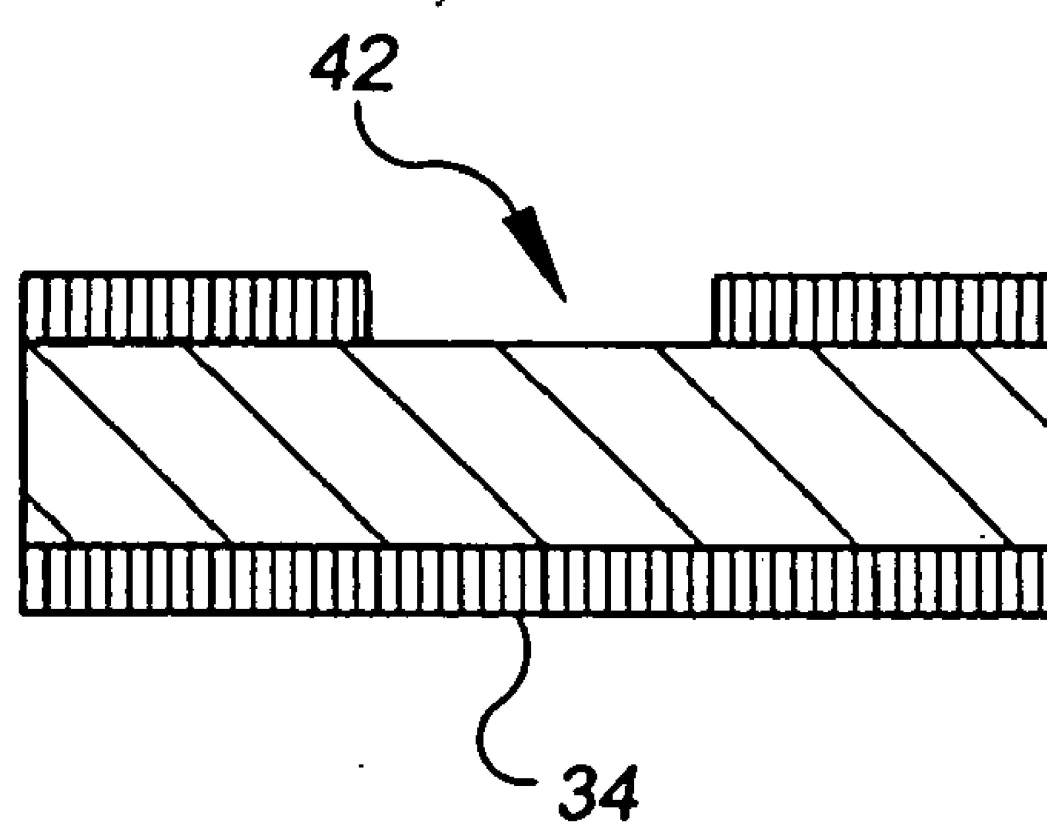

FIG.2D

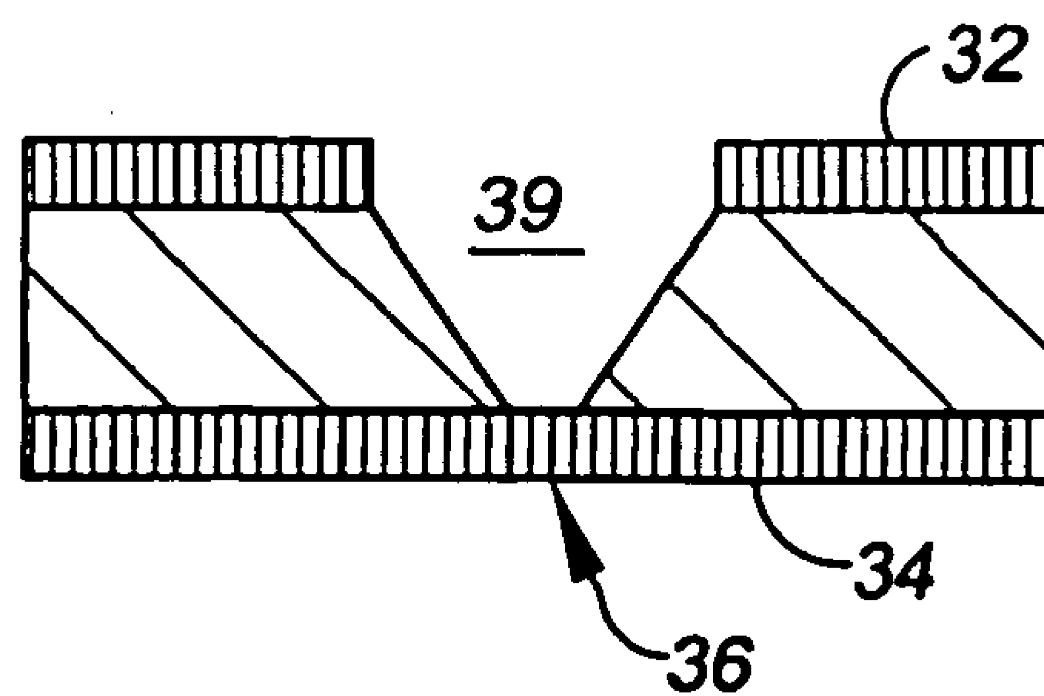

FIG.2E

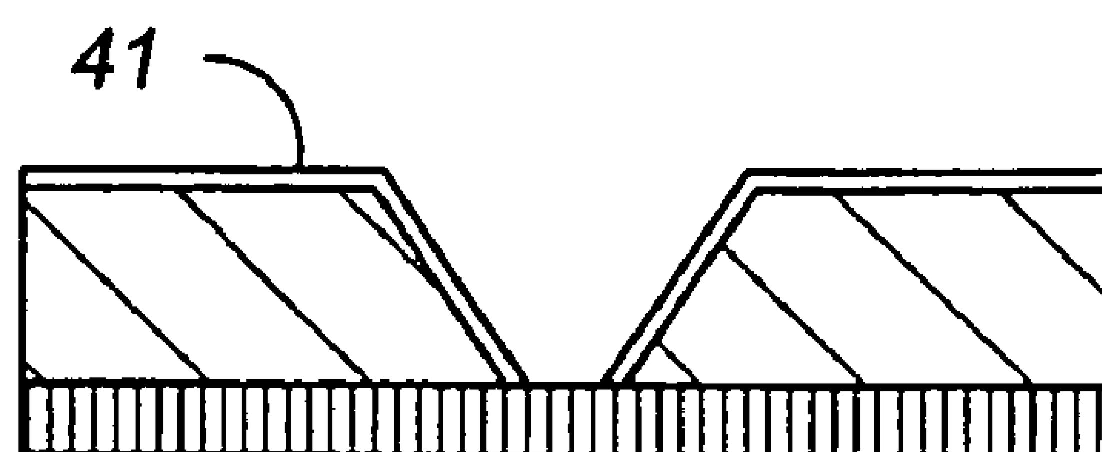

FIG.2F

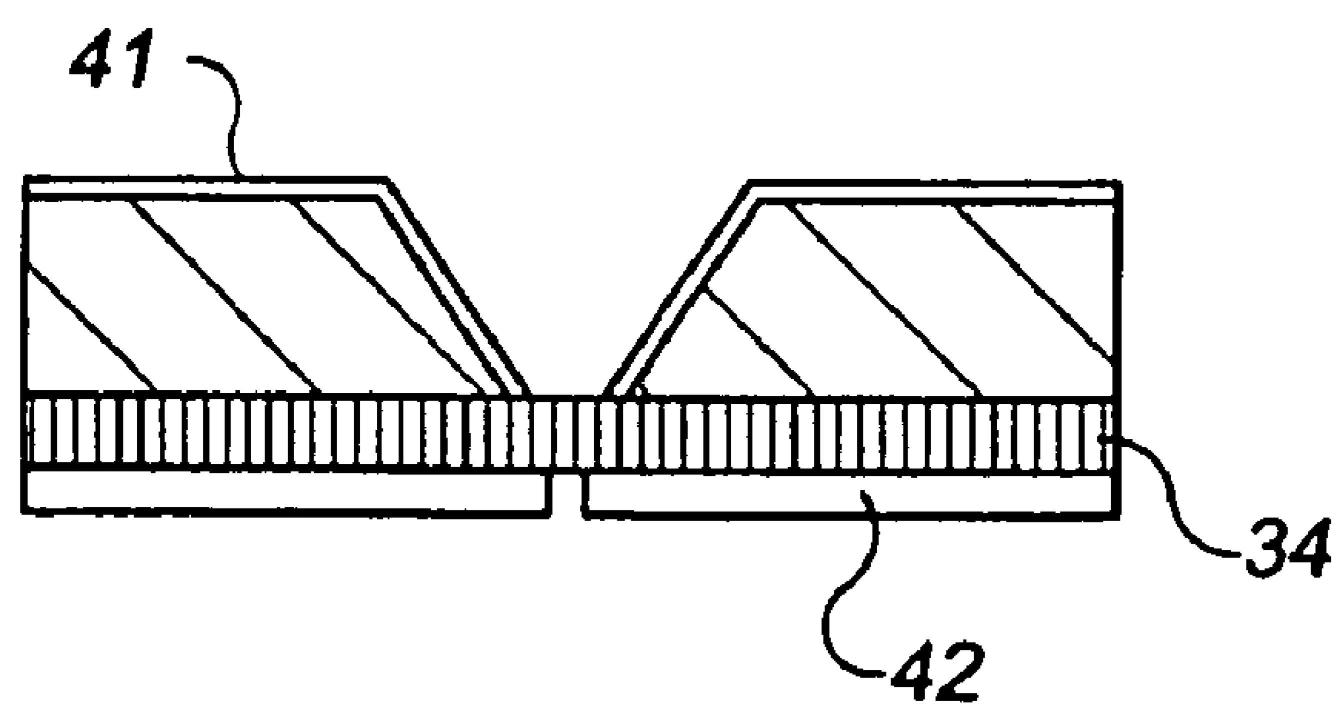

FIG.2G

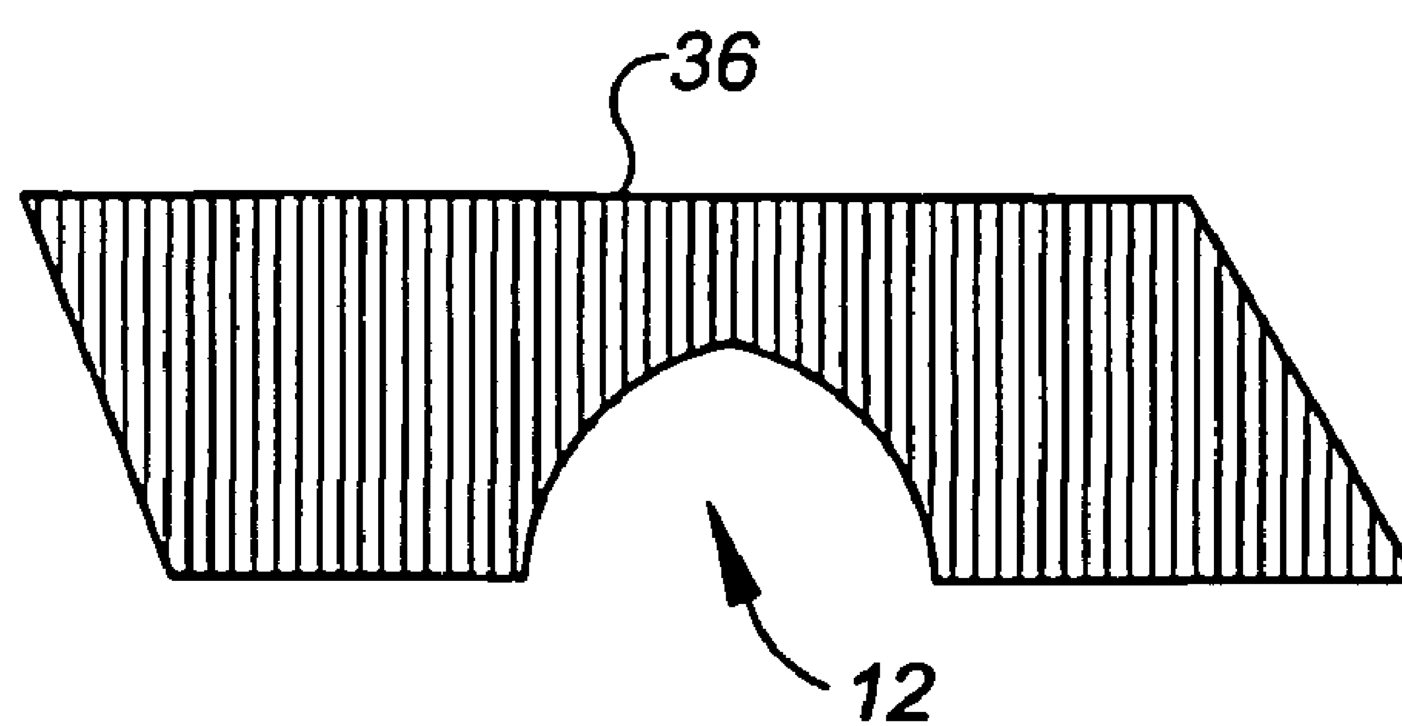

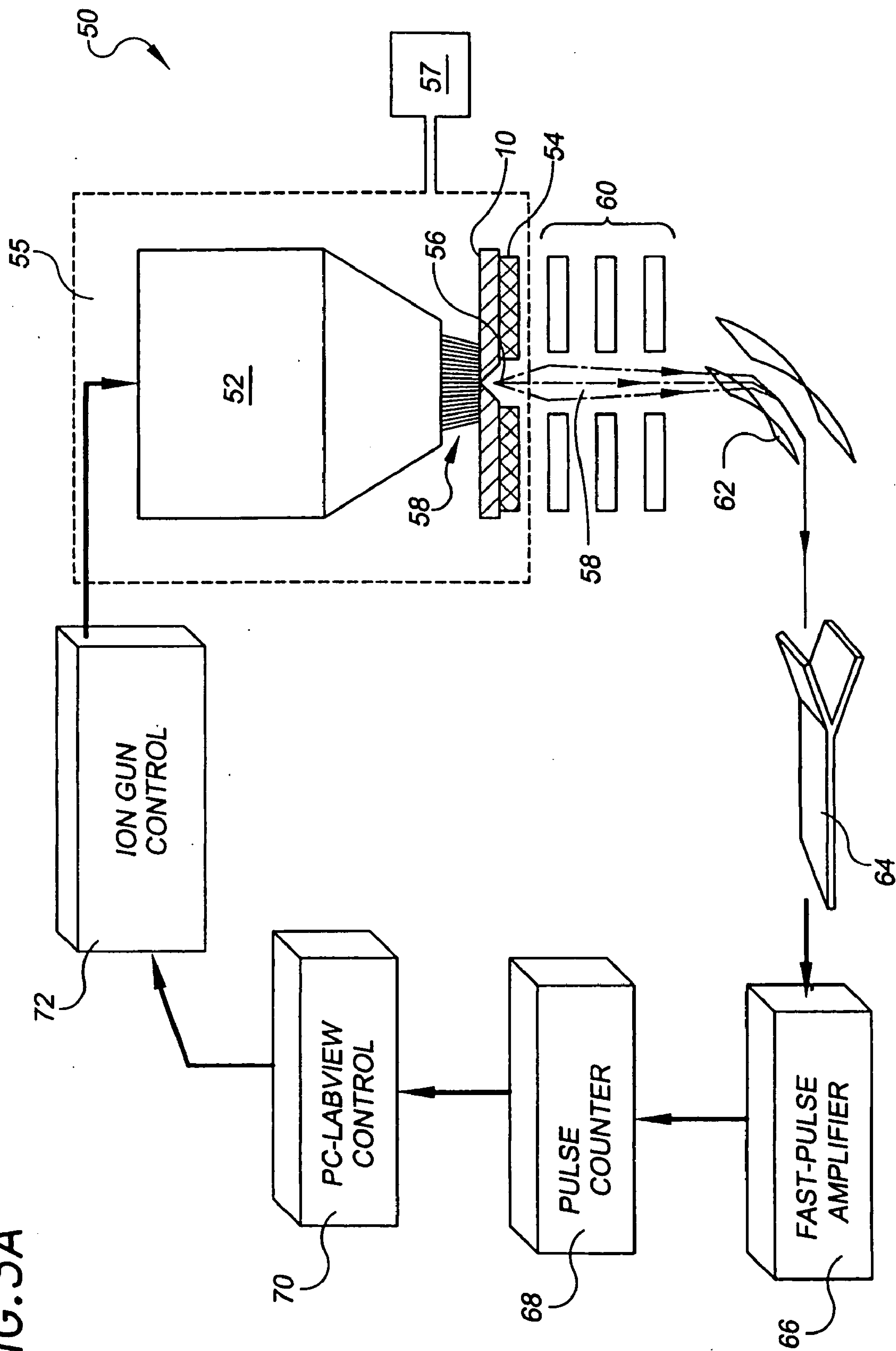

FIG. 3A

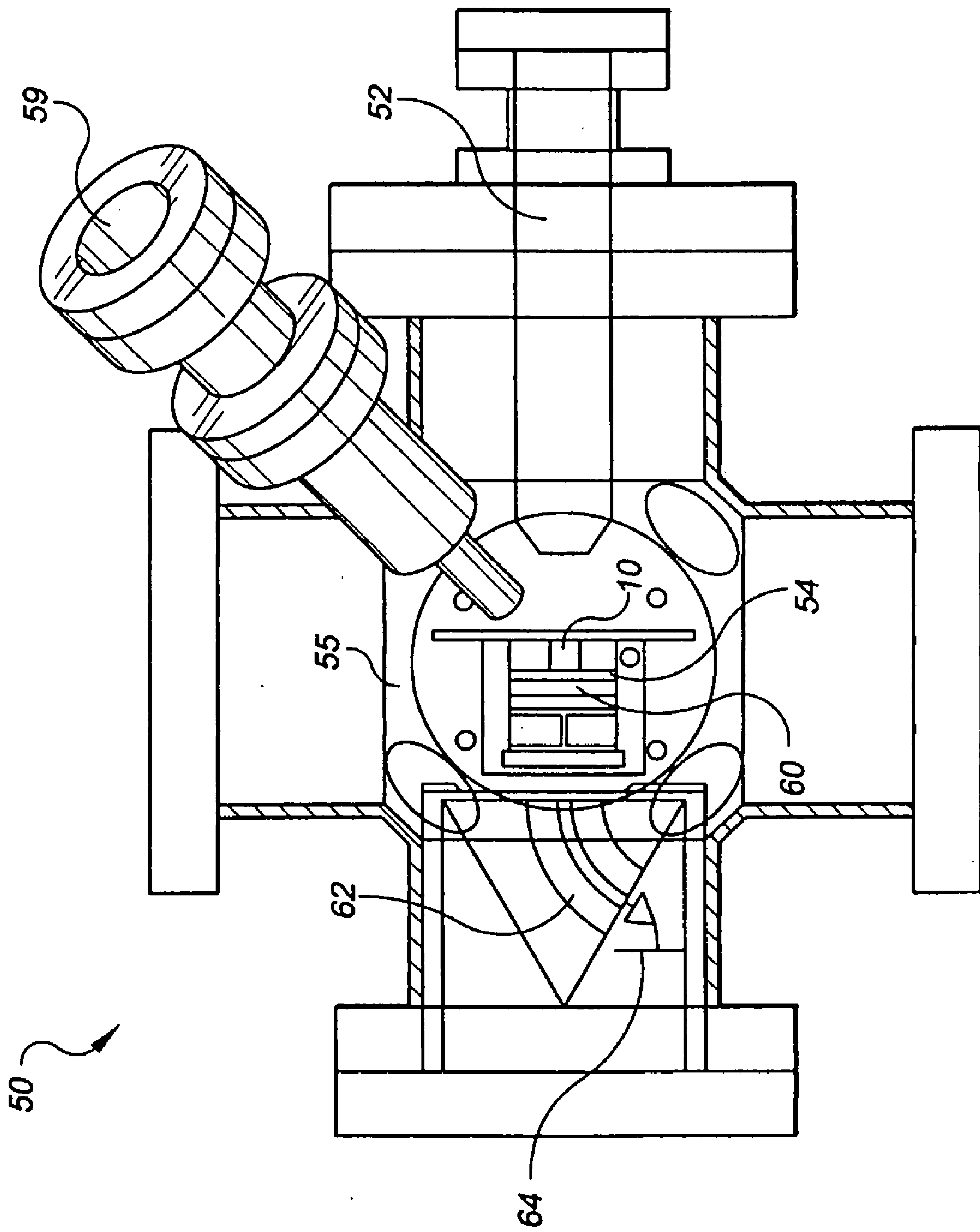

FIG.3B

FIG.4A

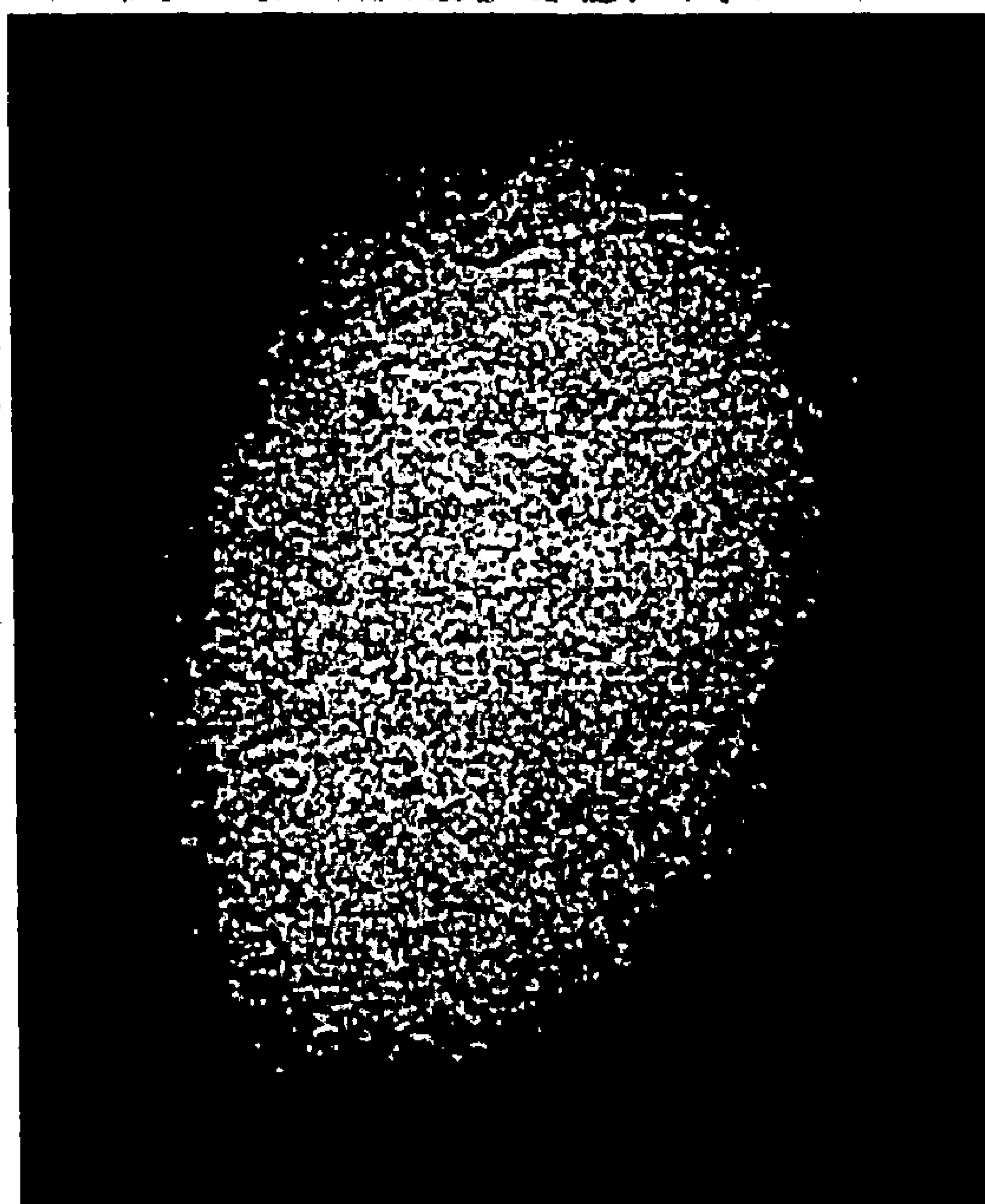

FIG.4B

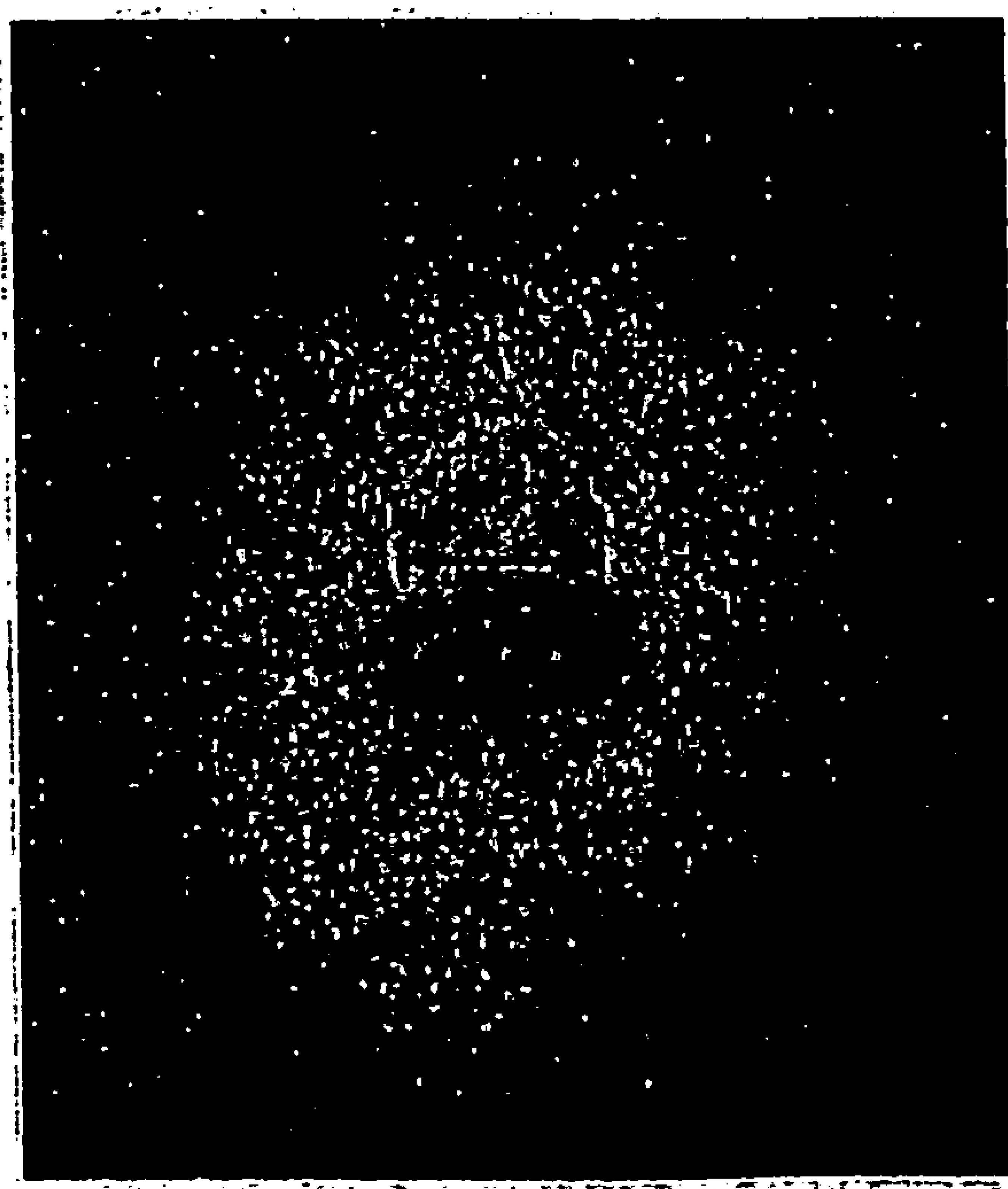

FIG. 4C

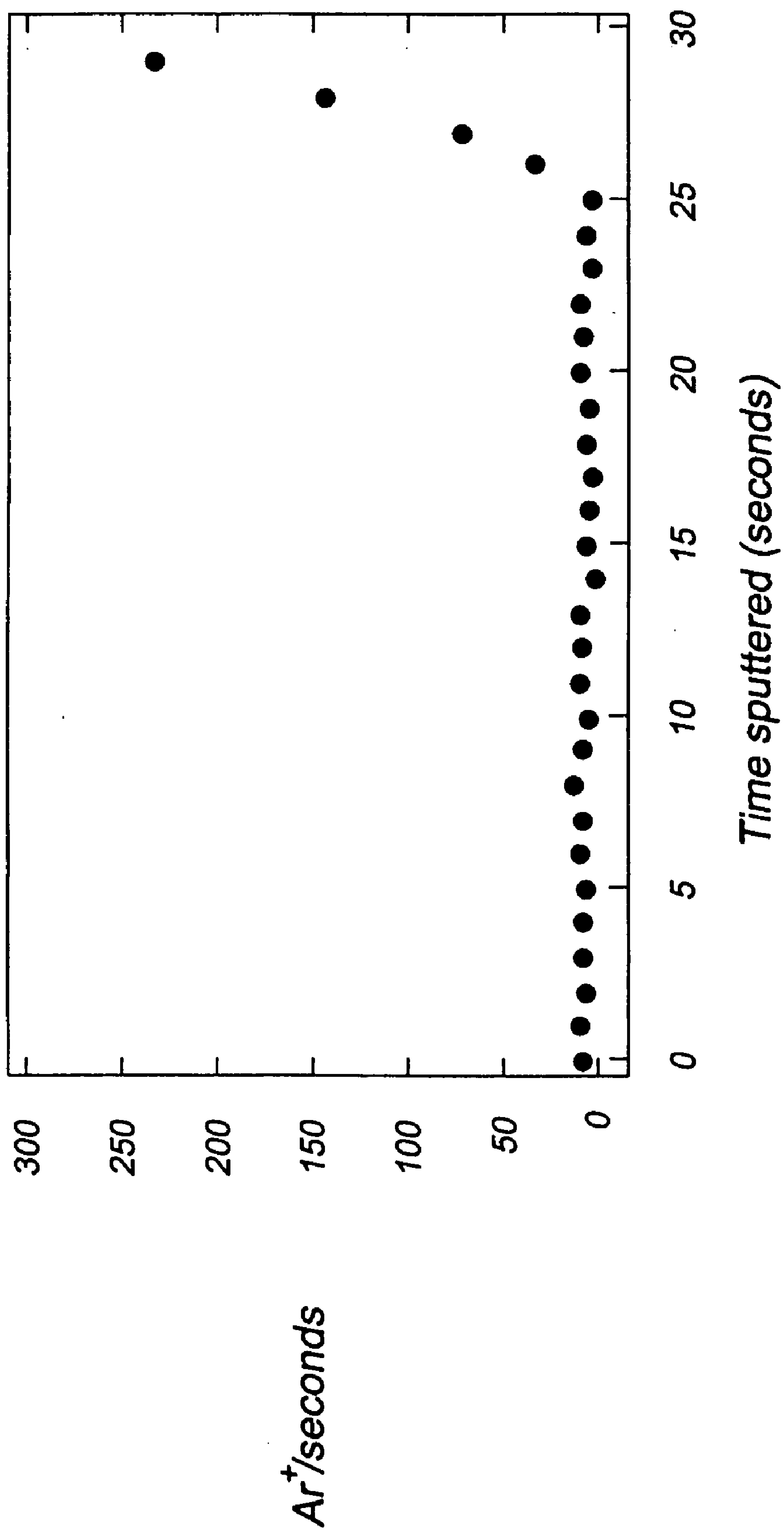

FIG.5A

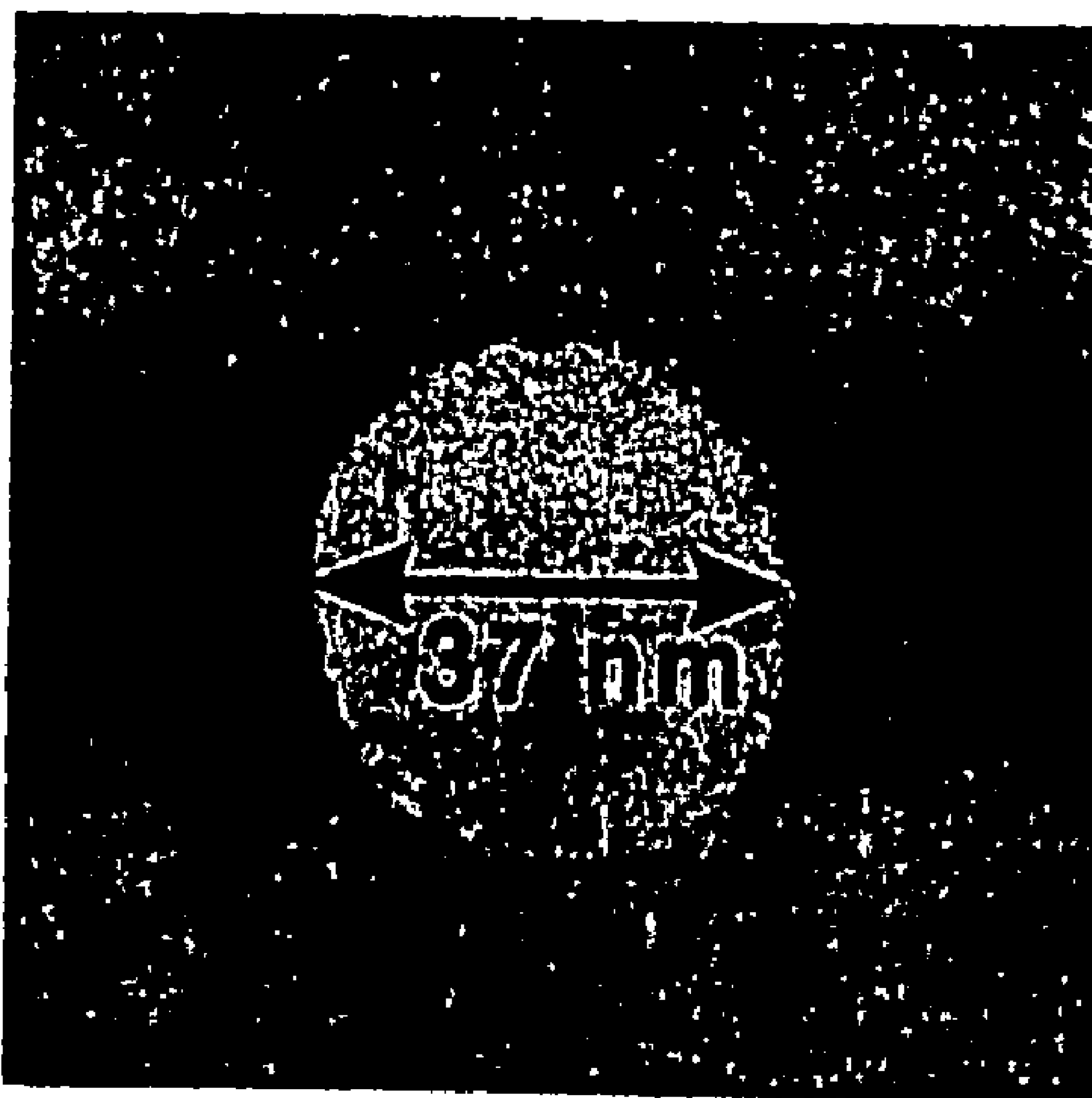

FIG.5B

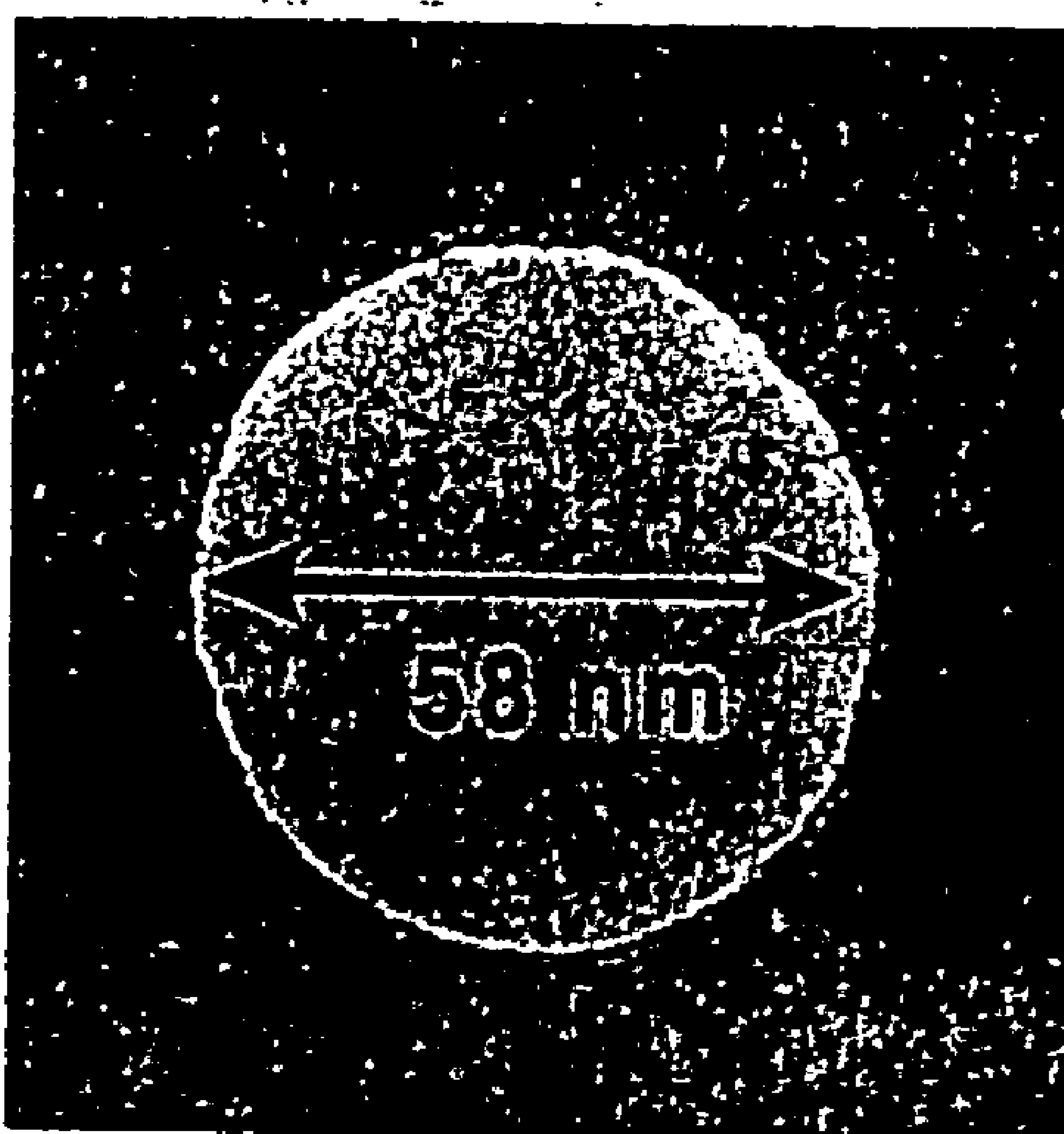

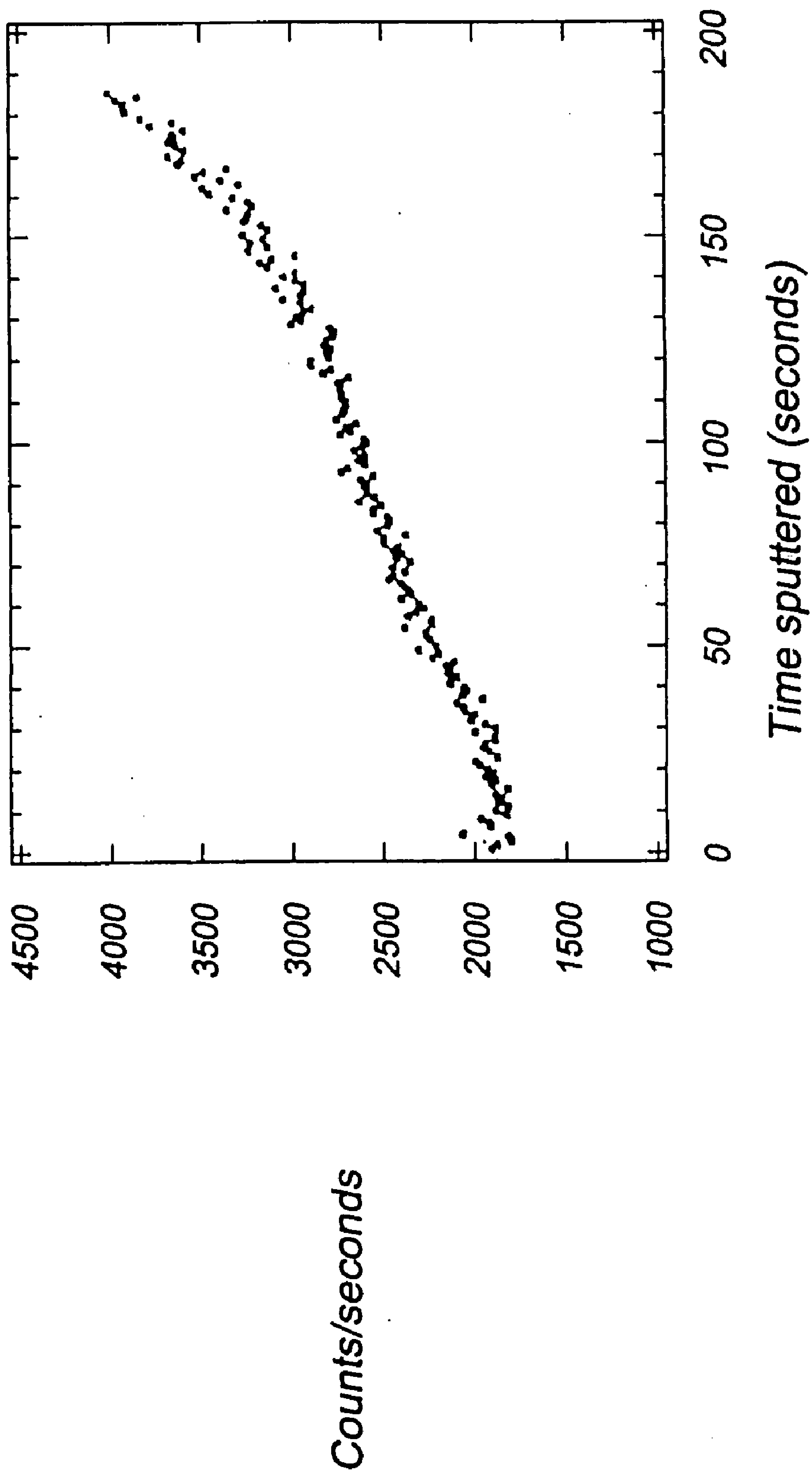

FIG.5C

FIG. 6A

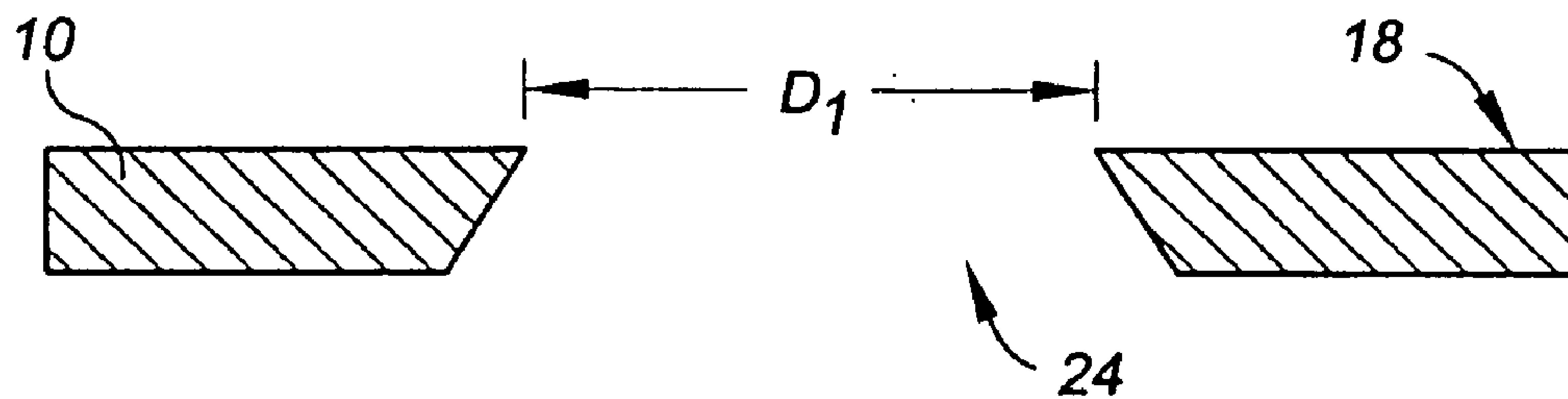

FIG. 6B

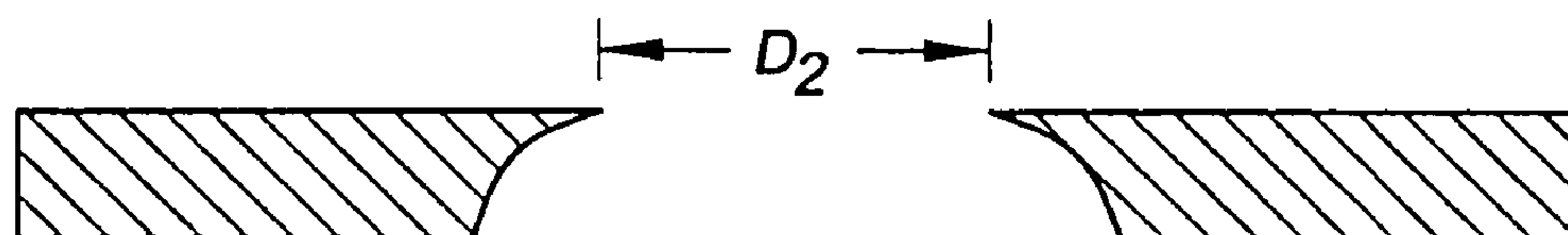

FIG. 6C

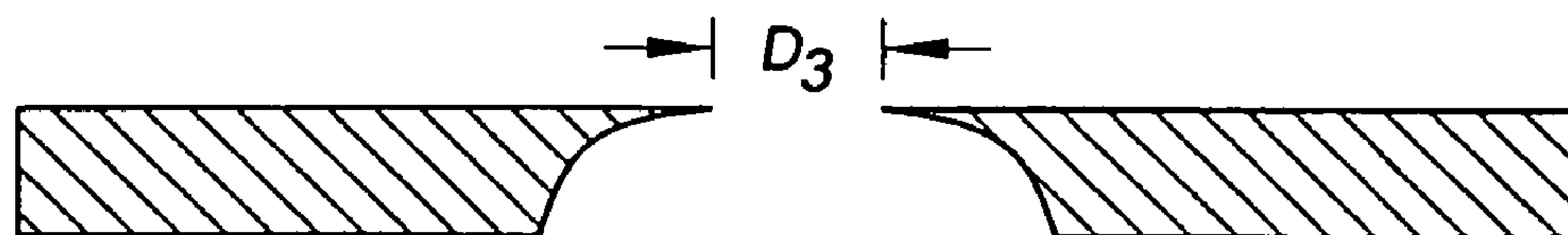

FIG. 7A

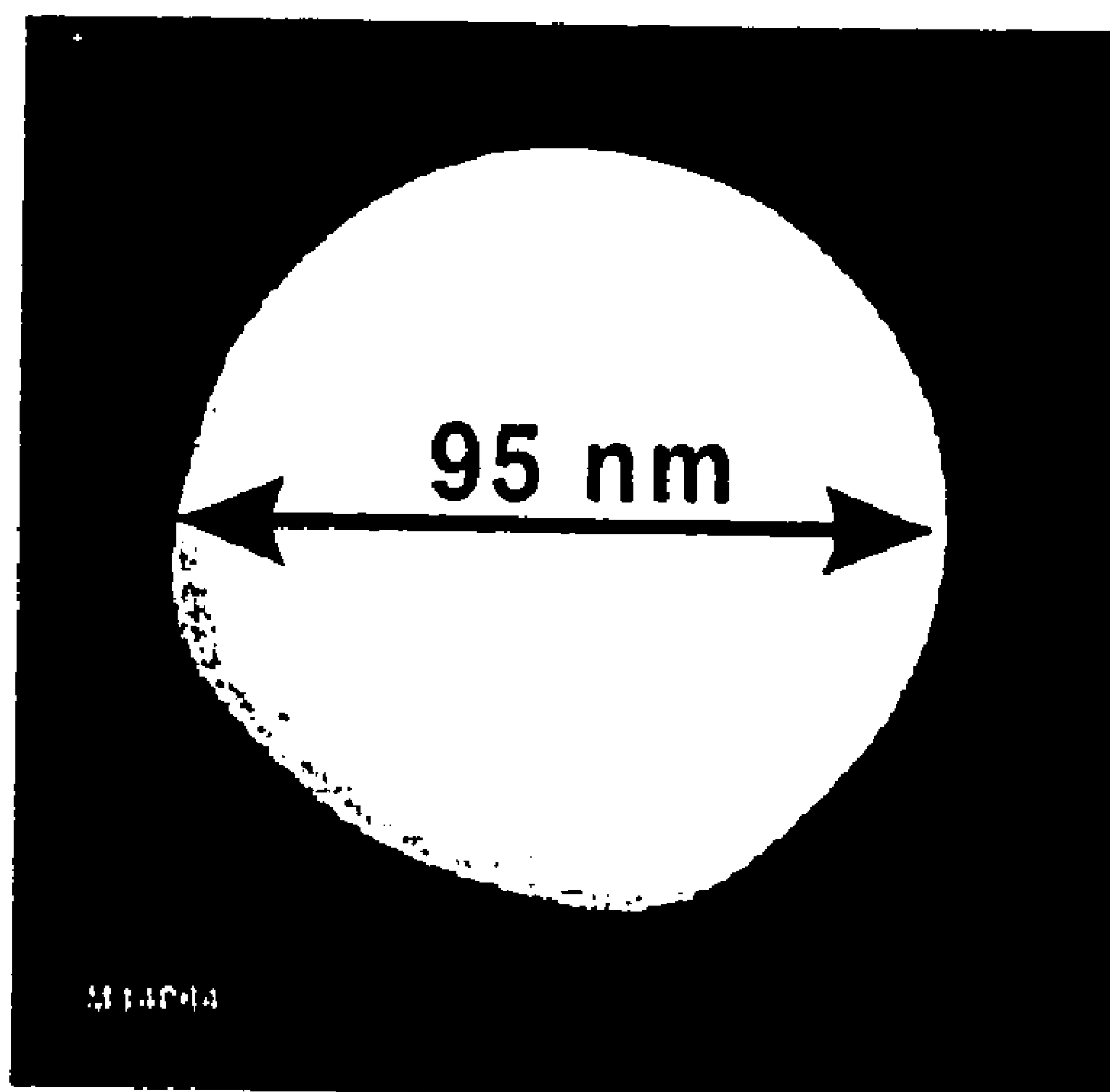

FIG. 7B

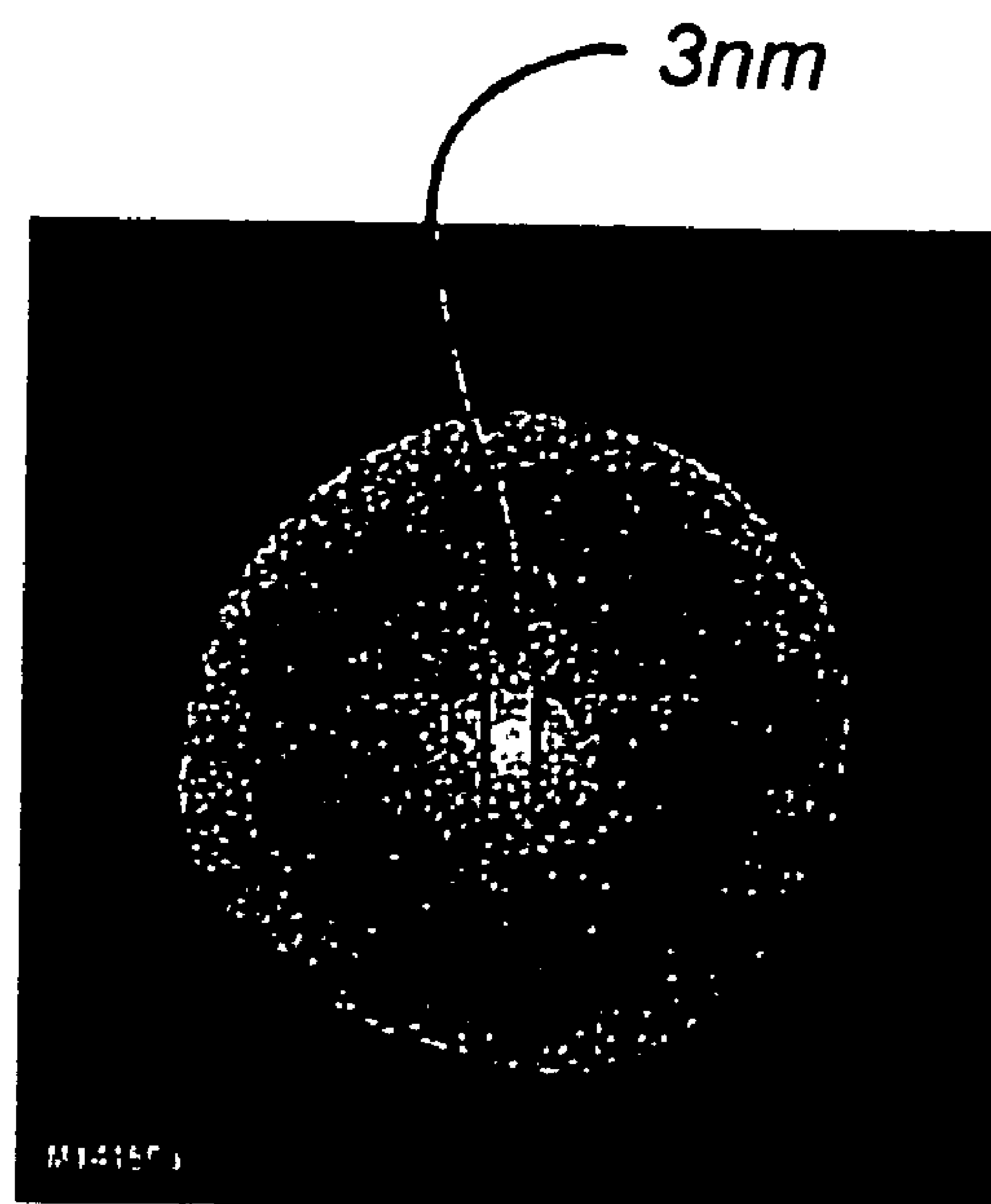

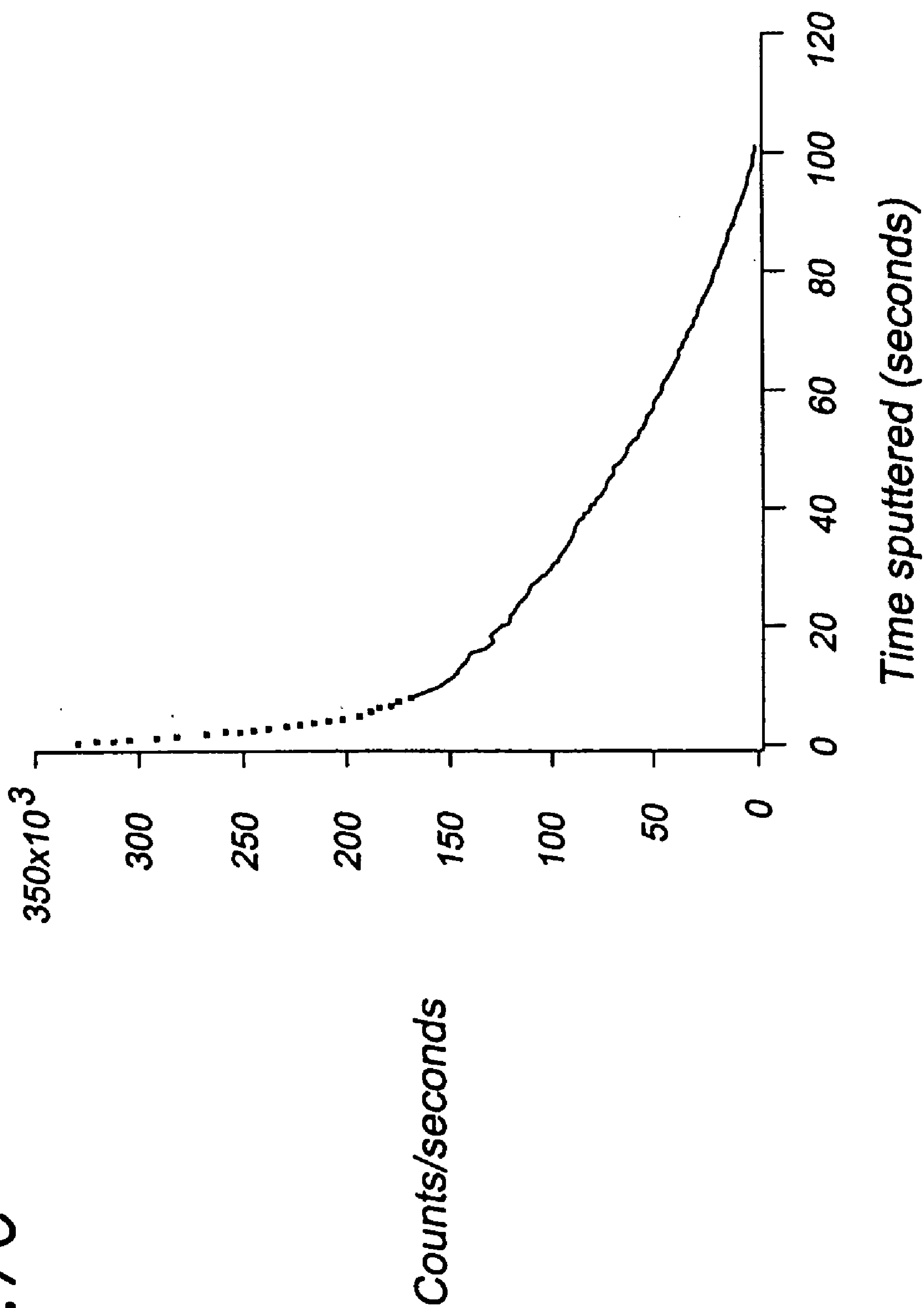

FIG. 7C

FIG.8

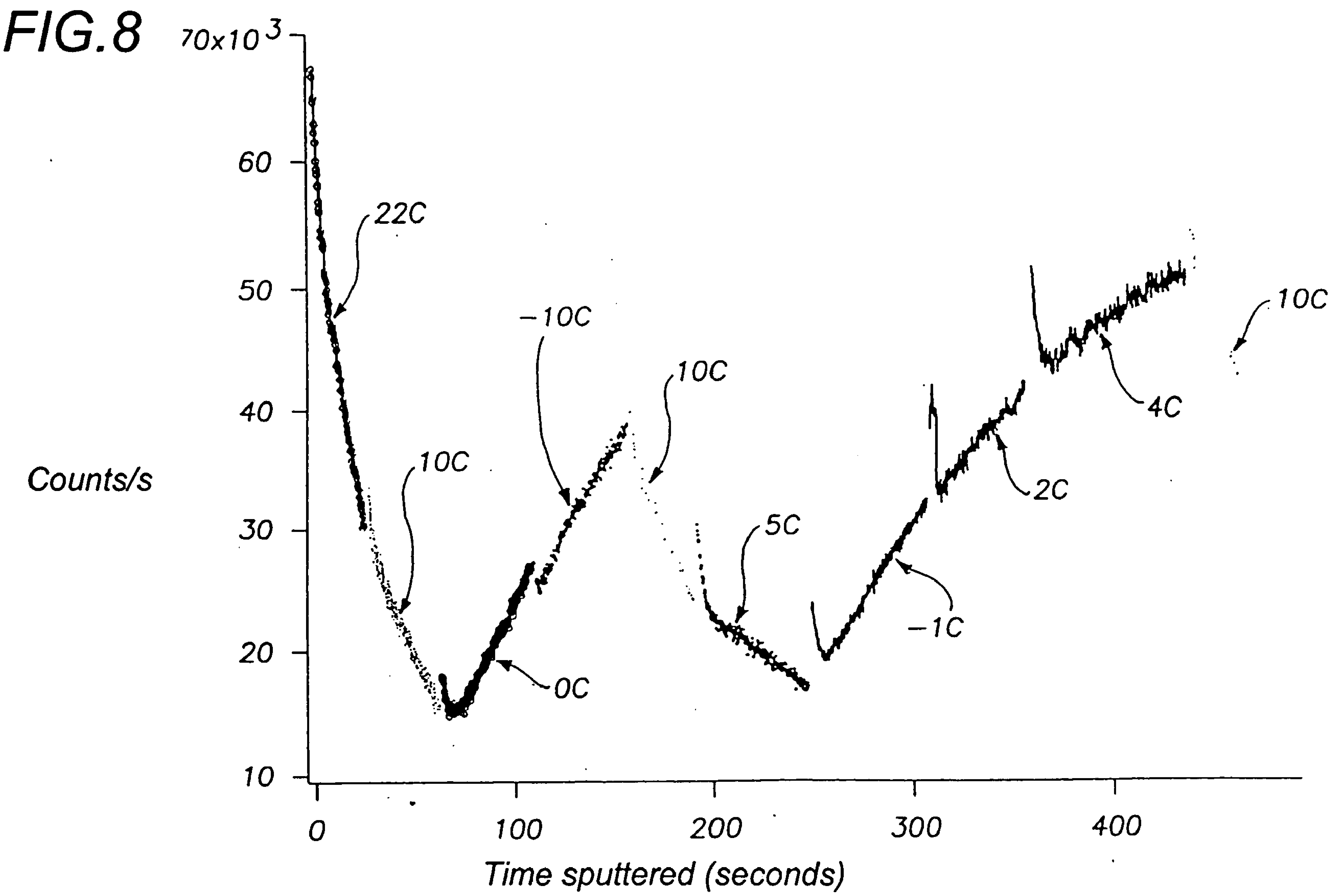

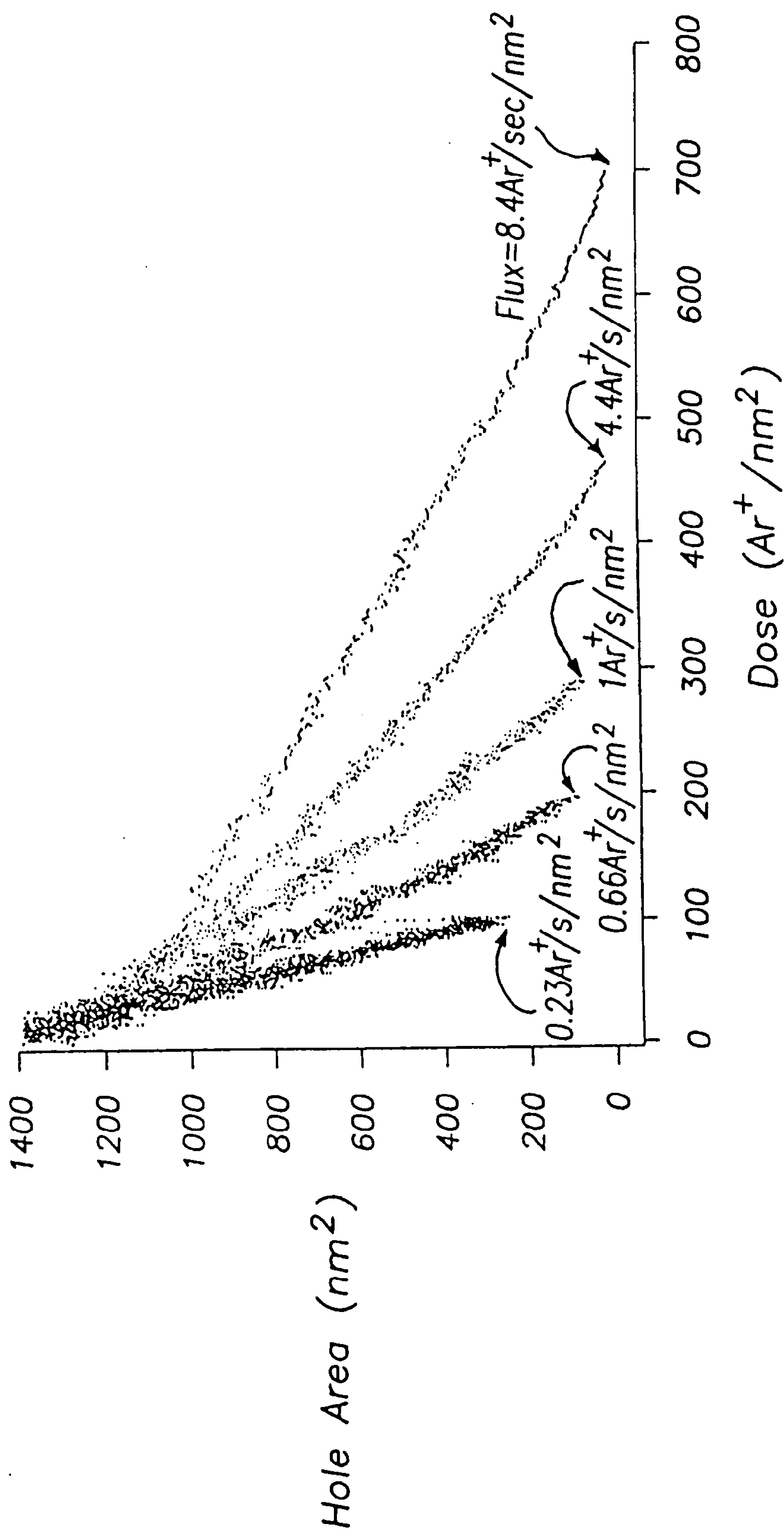

FIG.9A

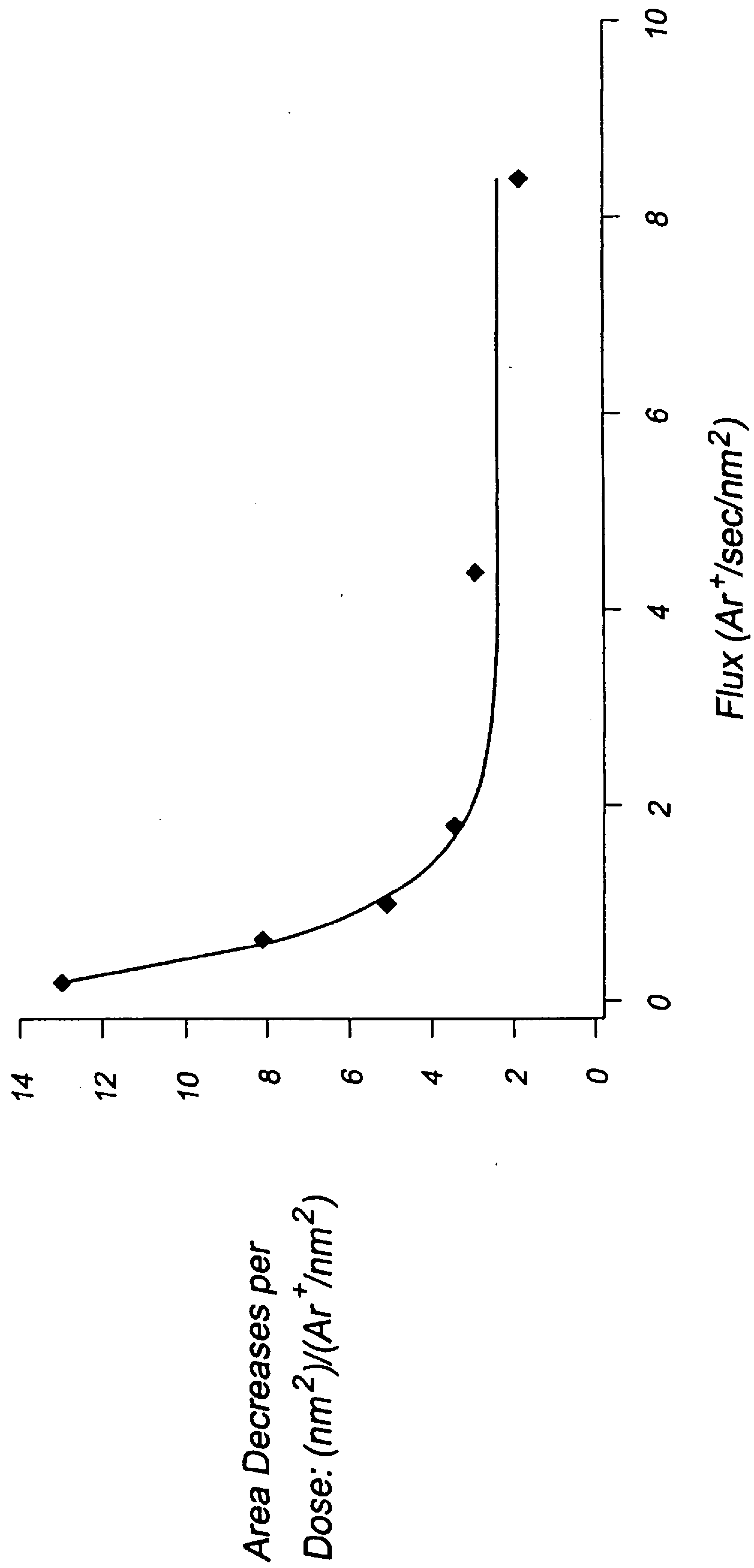

FIG.9B

FIG. 10A

FIG. 10B

Closing Trenches

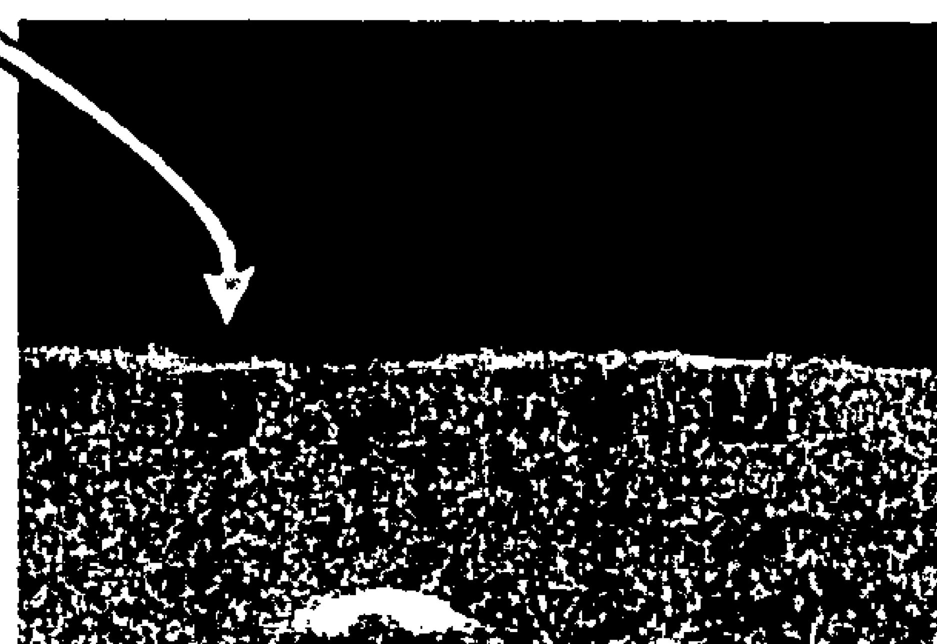

3 KeV, 20°C

3 KeV, 20°C

FIG. 10C

Opening Trenches

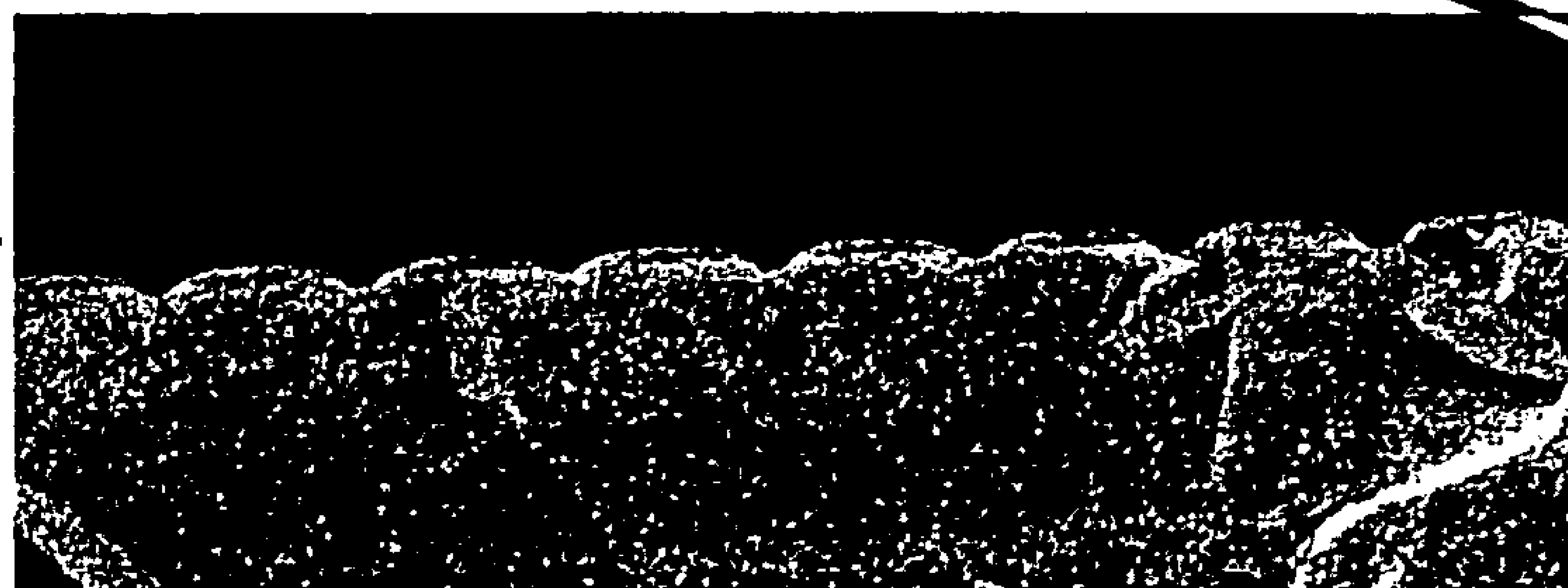

3 KeV, −100°C

3 KeV, −100°C

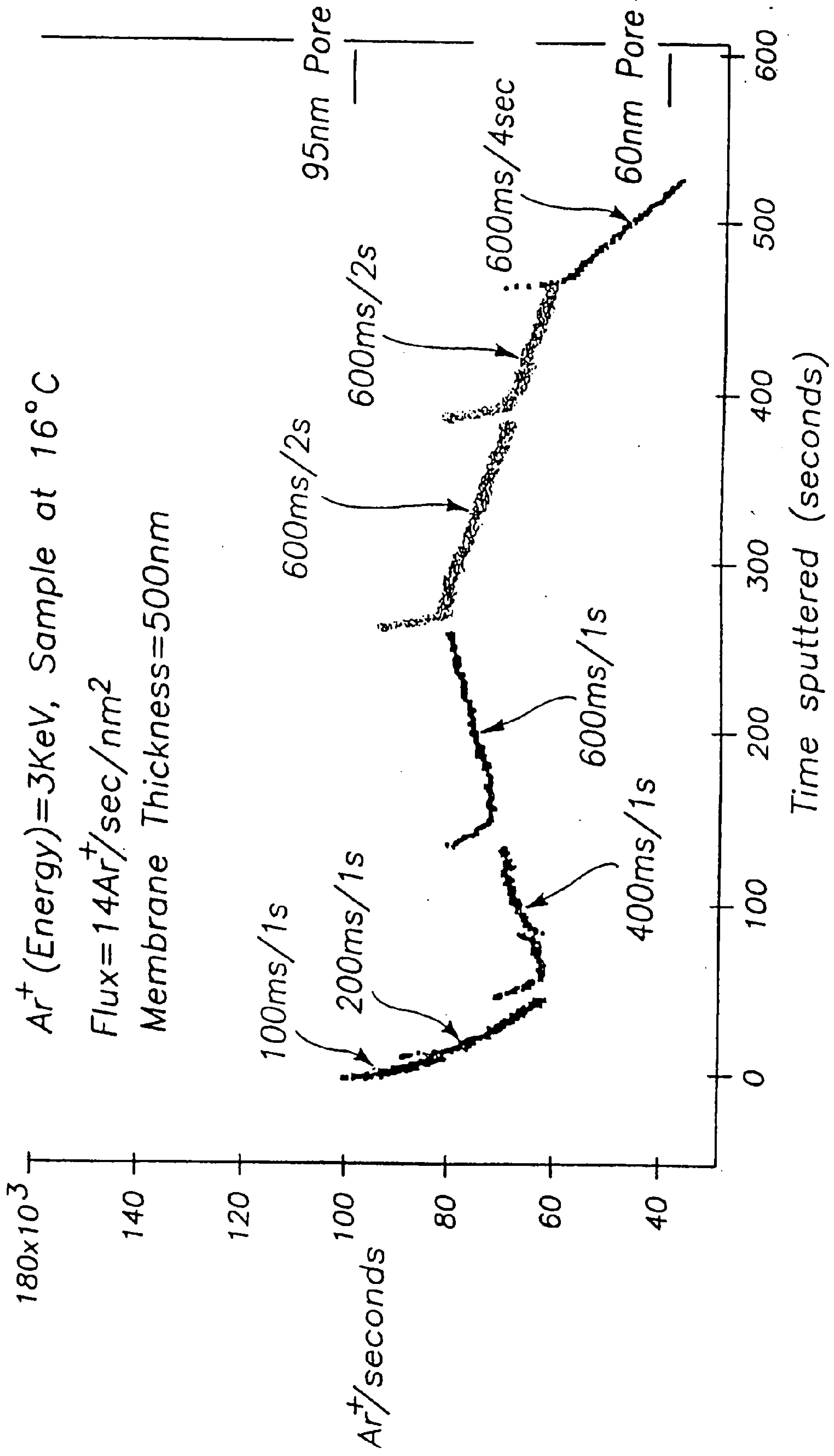
FIG.11A
Ar+ (Energy)=3KeV, Sample at 16°C
Flux=14Ar+/sec/nm2
Membrane Thickness=500nm
Ar+/seconds
180x10^3
140
120
100
80
60
40
100ms/1s
200ms/1s
400ms/1s
600ms/1s
600ms/2s
600ms/2s
600ms/4sec
95nm Pore
60nm Pore
0
100
200
300
400
500
600
Time sputtered (seconds)

FIG. 12

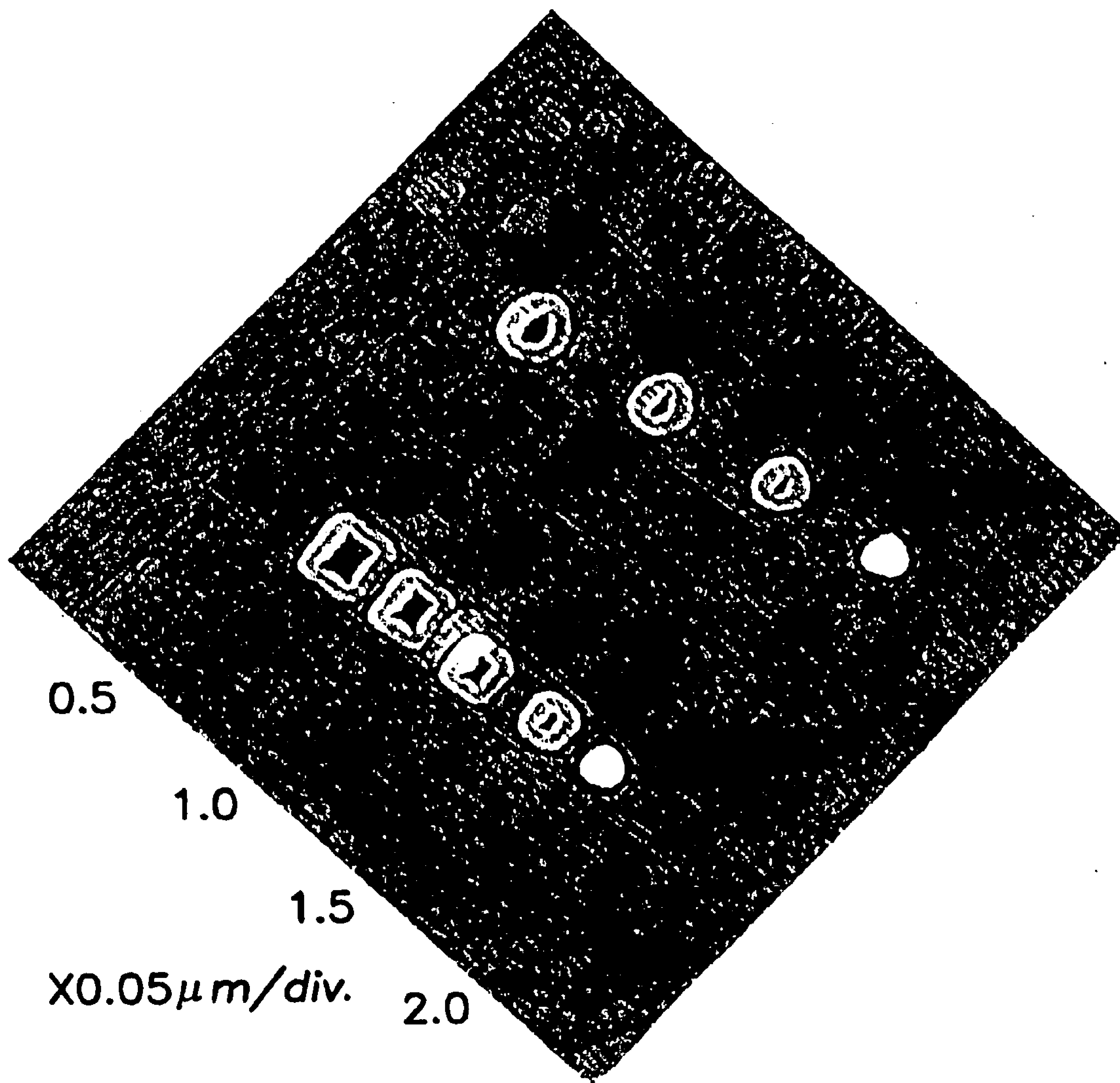

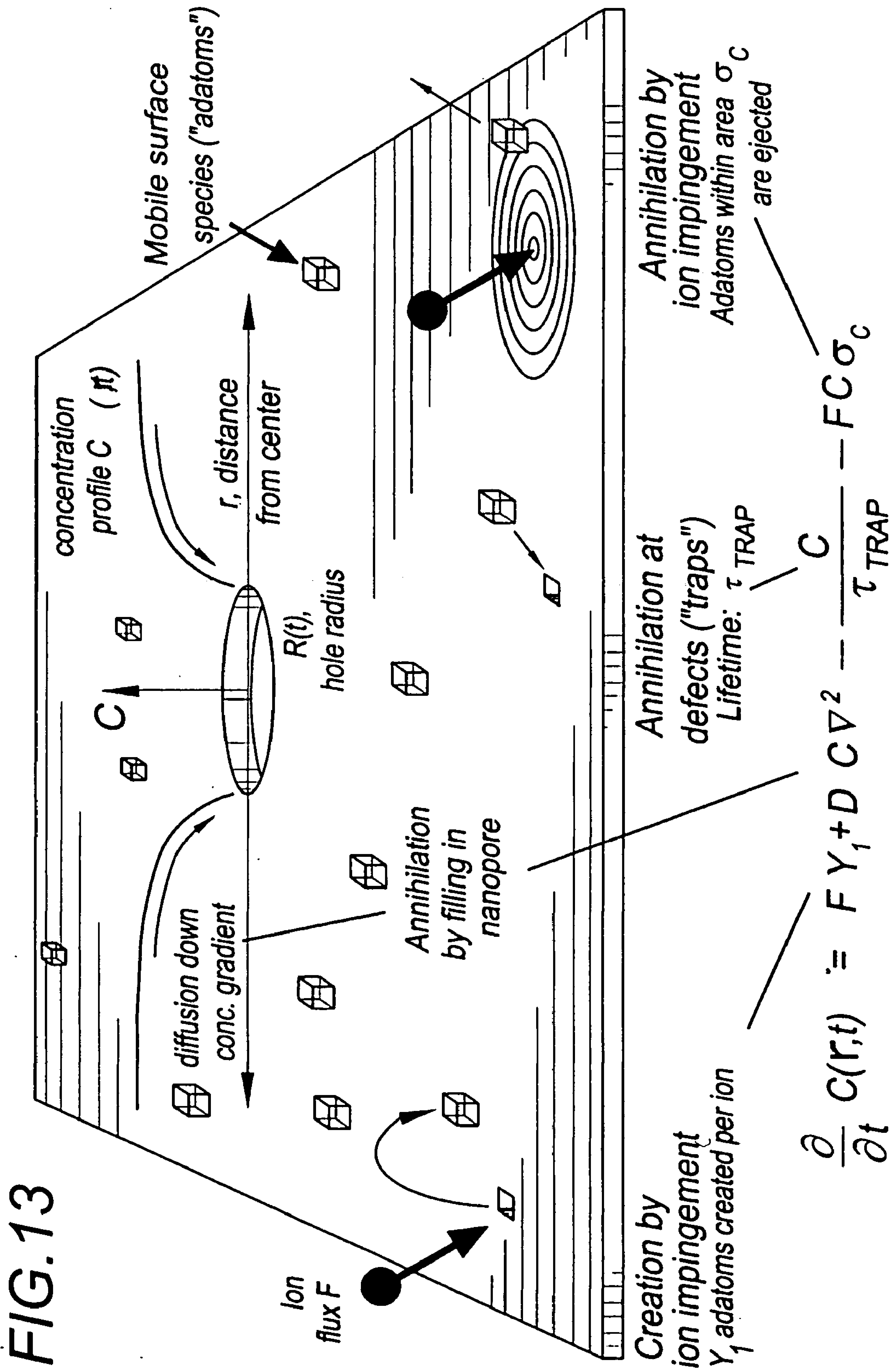

FIG.13
Ion
flux F
Creation by
ion impingement
Y_1 adatoms created per ion
diffusion down
conc. gradient
Annihilation
by filling in
nanopore
C
R(t),
hole radius
concentration
profile C (r,t)
r, distance
from center
Mobile surface
species ("adatoms")
Annihilation at
defects ("traps")
Lifetime: τ_{TRAP}
Annihilation by
ion impingement
Adatoms within area σ_C
are ejected
$\frac{\partial}{\partial t} C(r,t) = F Y_1 + D C \nabla^2 - \frac{C}{\tau_{TRAP}} - F C \sigma_C$

FIG. 14A

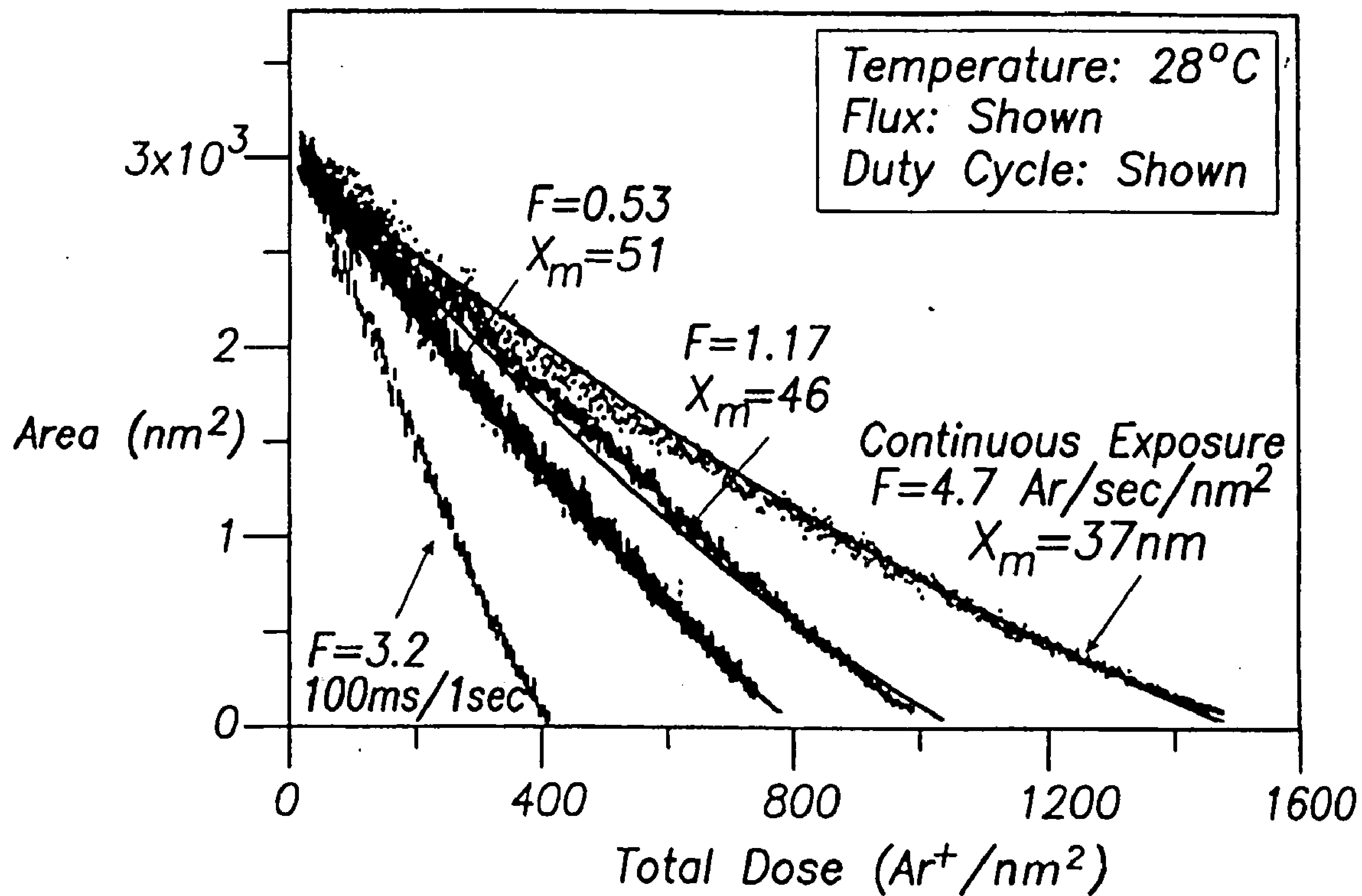

FIG. 14B

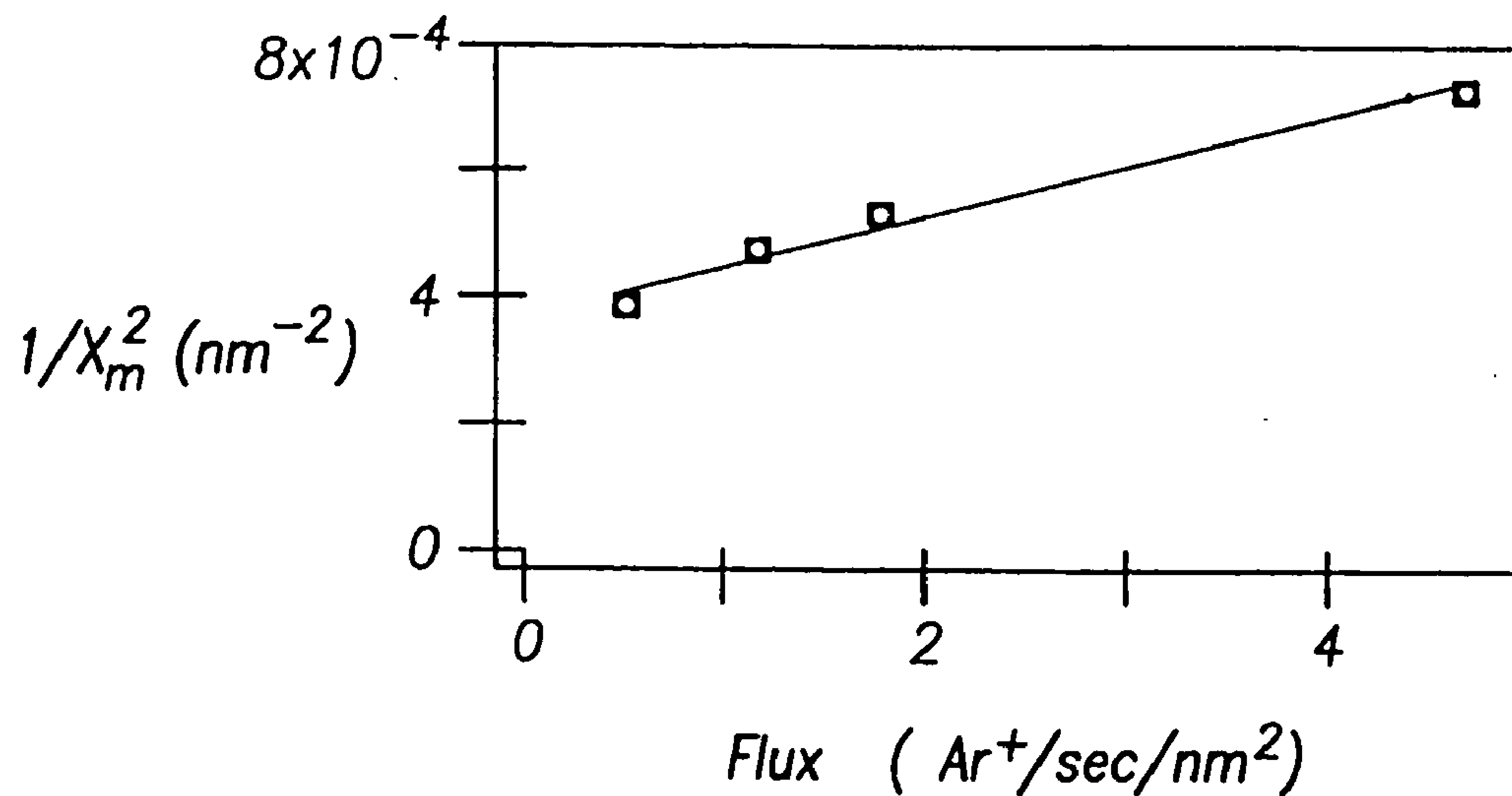

FIG. 15

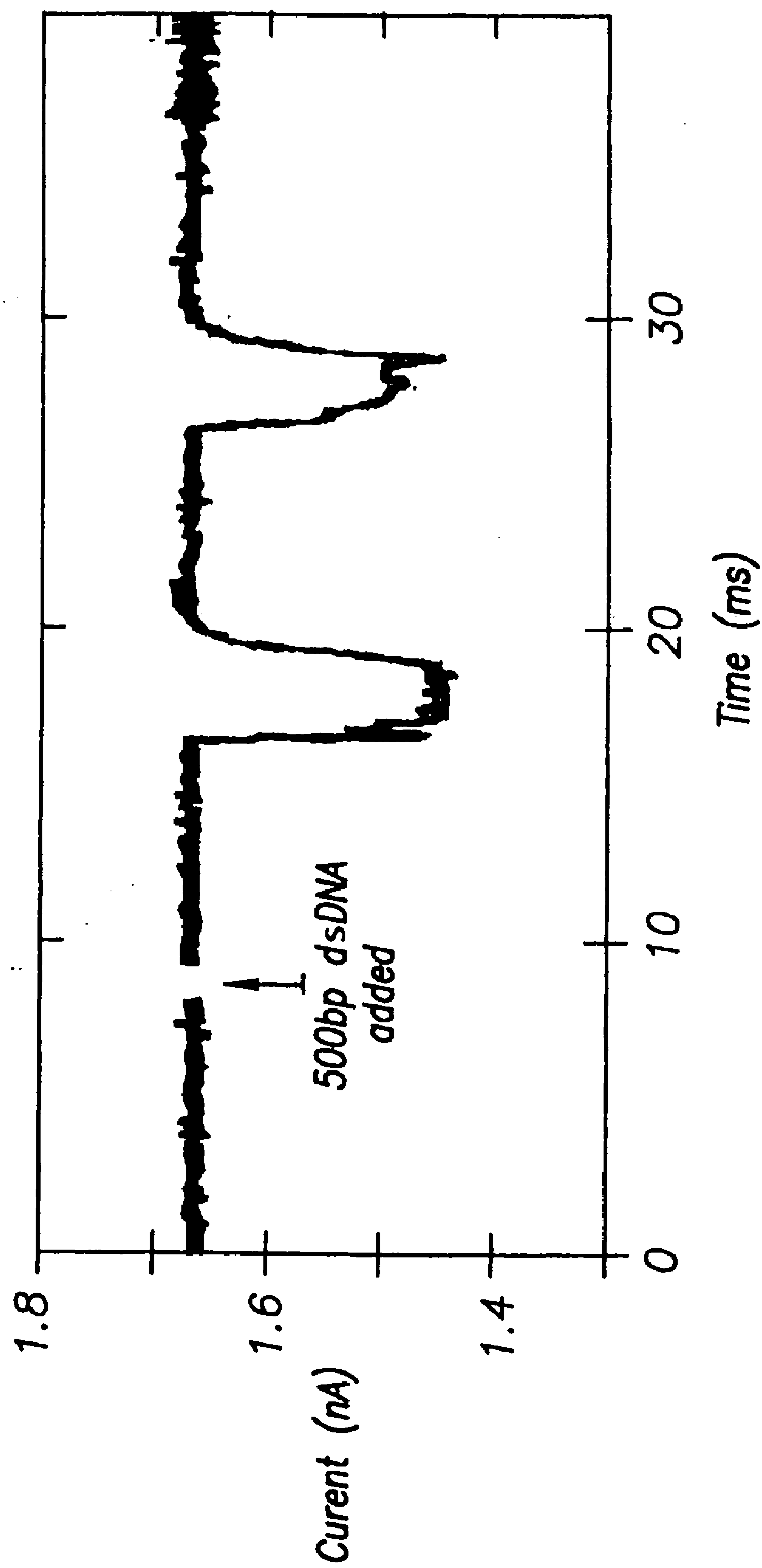

FIG. 16

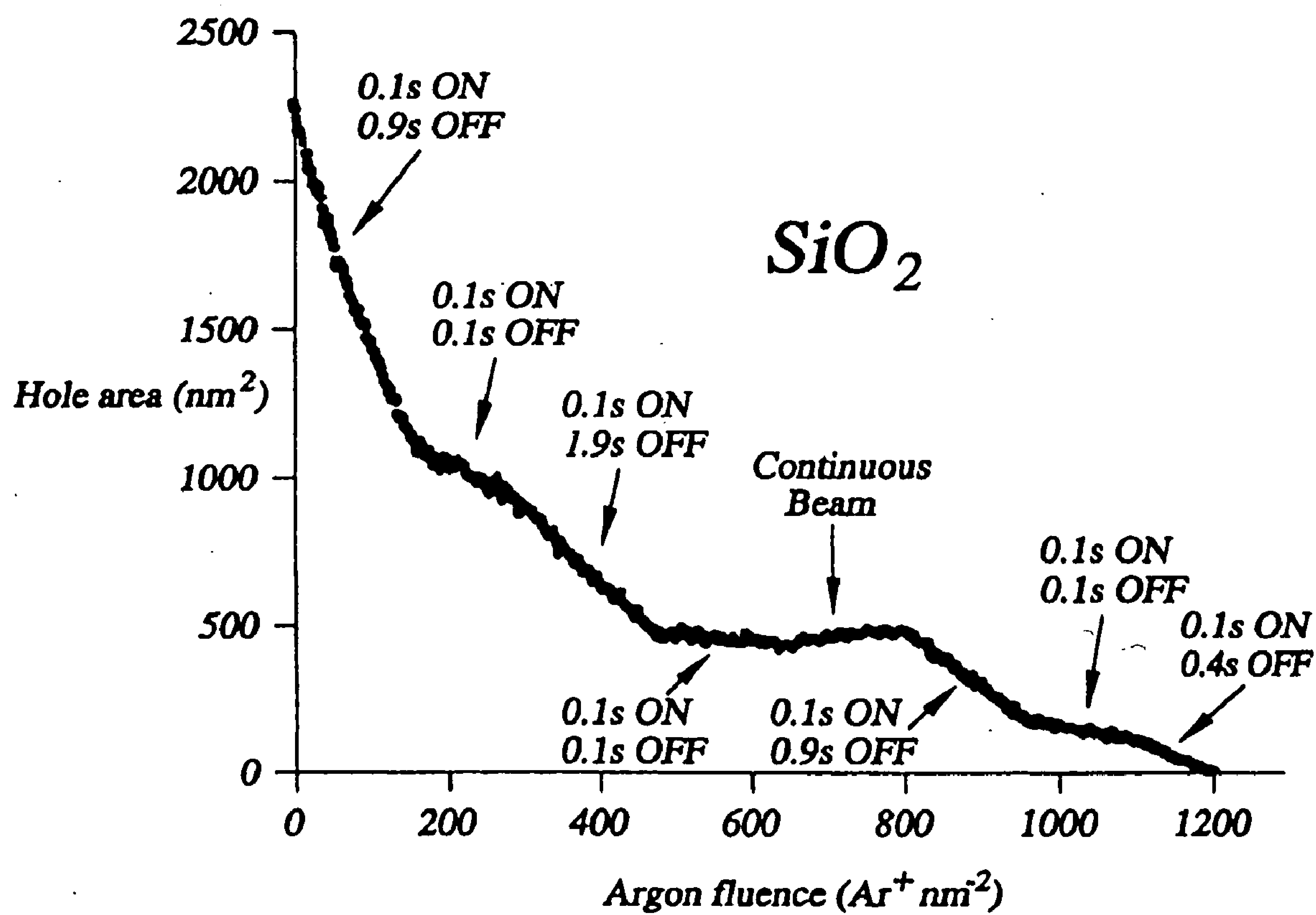

FIG. 17

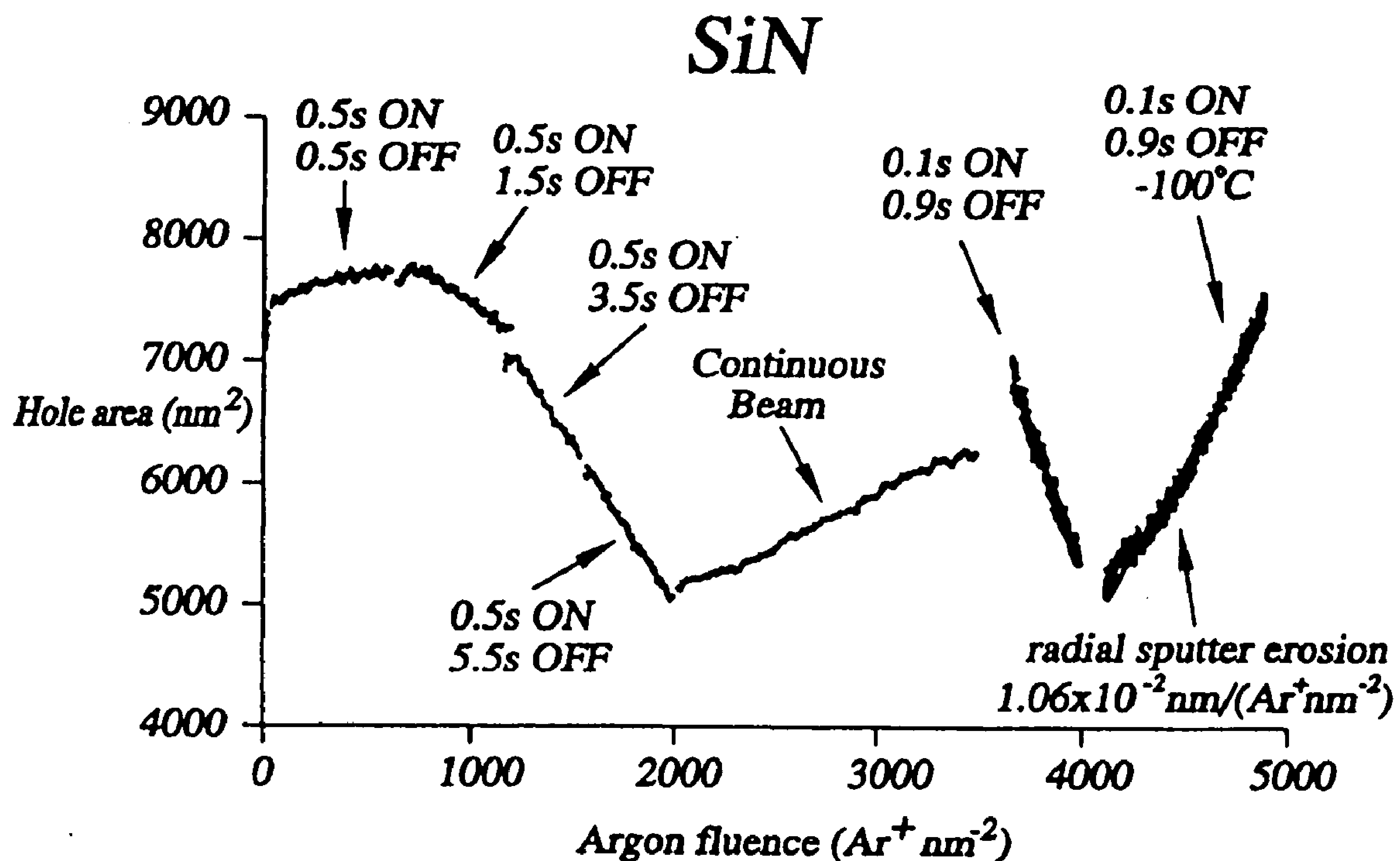

FIG. 18

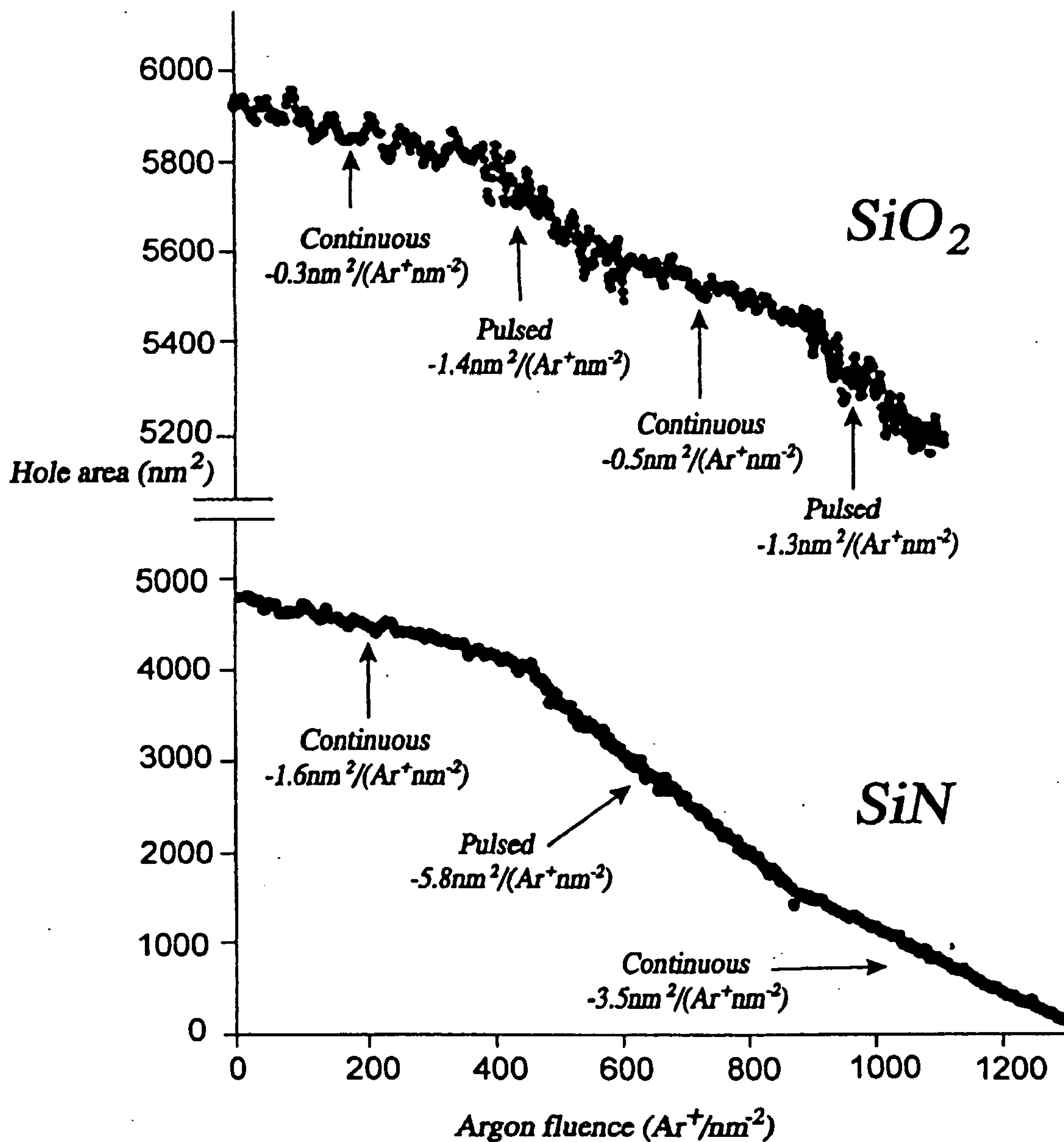

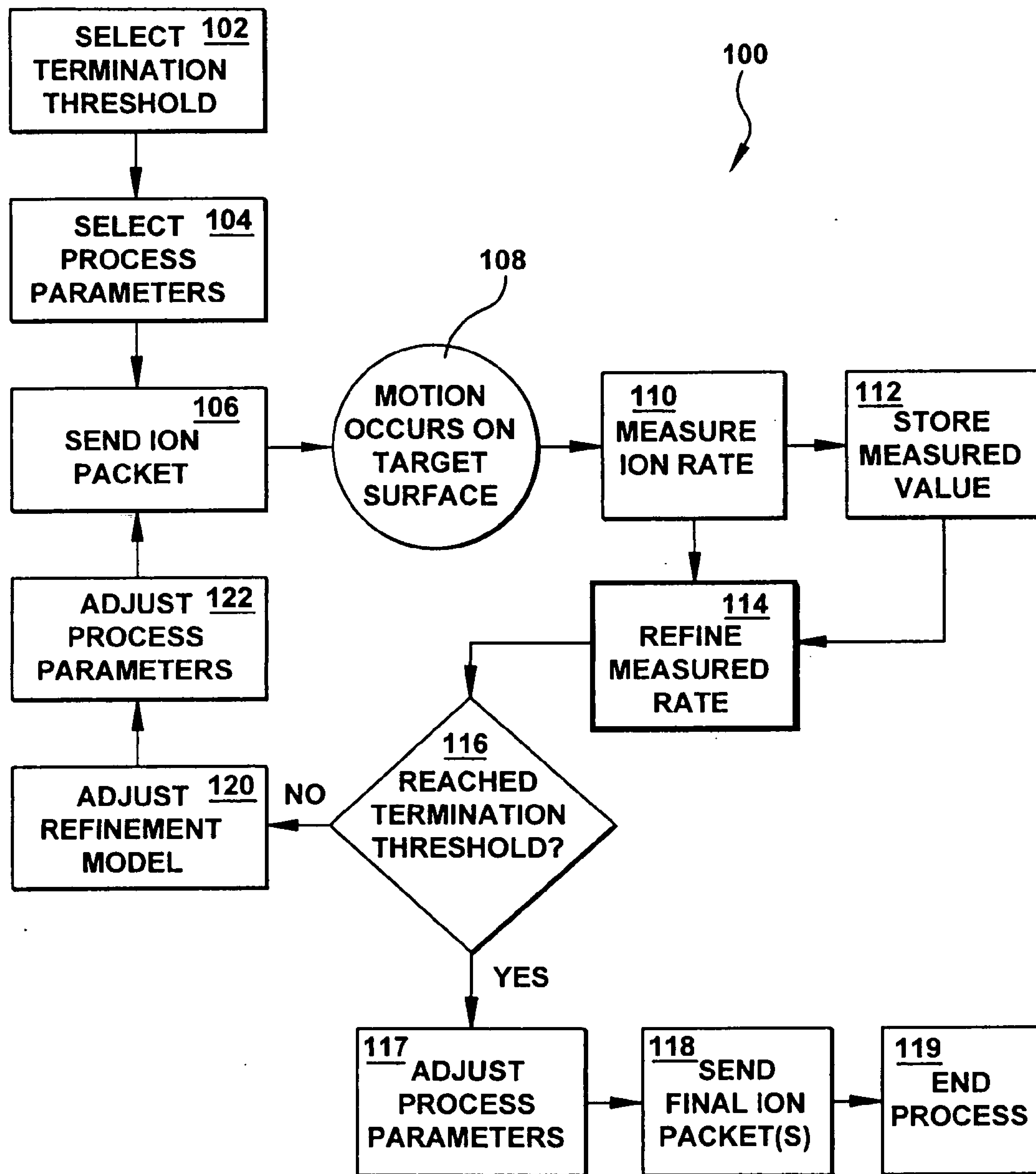
FIG.19A
100
SELECT TERMINATION THRESHOLD 102
SELECT PROCESS PARAMETERS 104
SEND ION PACKET 106
108
MOTION OCCURS ON TARGET SURFACE
110 MEASURE ION RATE
112 STORE MEASURED VALUE
114 REFINE MEASURED RATE
116 REACHED TERMINATION THRESHOLD?
NO
YES
ADJUST REFINEMENT MODEL 120
ADJUST PROCESS PARAMETERS 122
117 ADJUST PROCESS PARAMETERS
118 SEND FINAL ION PACKET(S)
119 END PROCESS

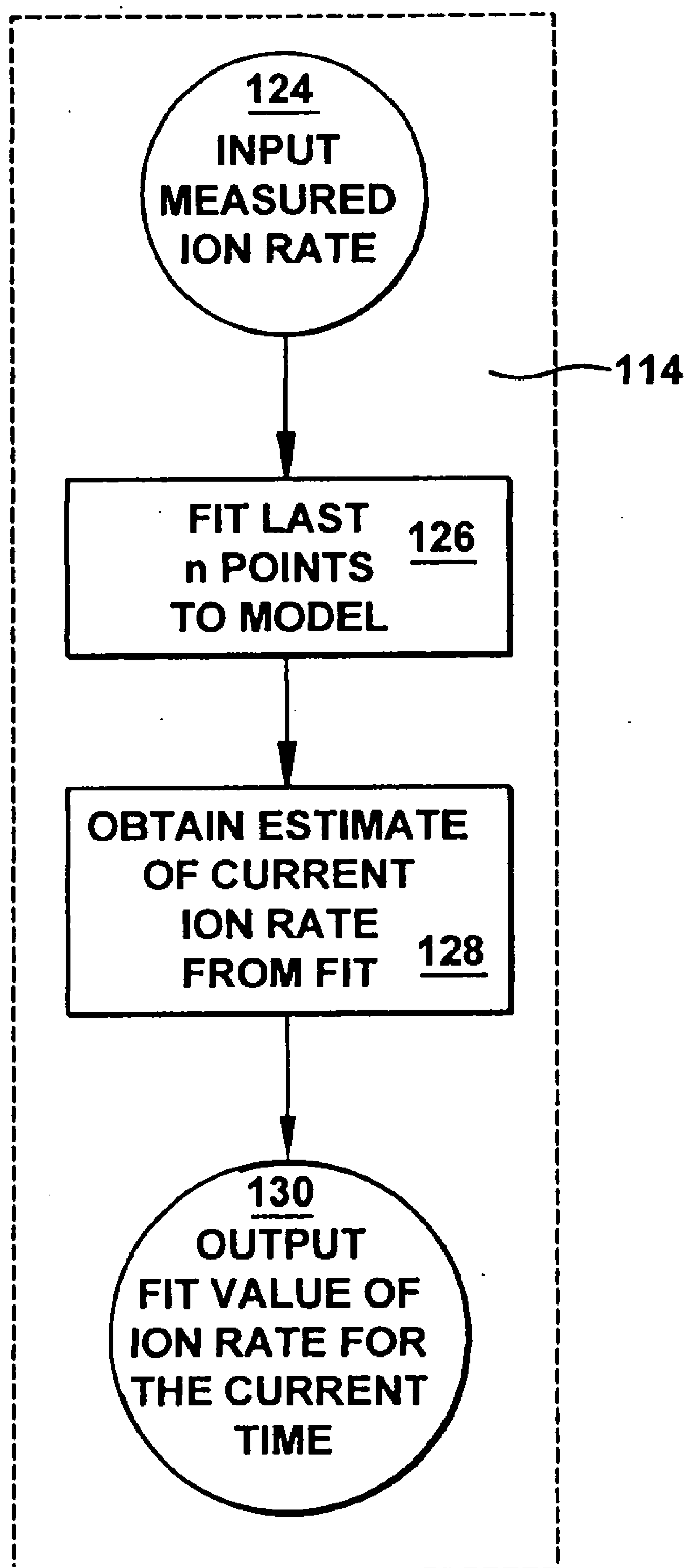
FIG.19B
124
INPUT MEASURED ION RATE
114
FIT LAST n POINTS TO MODEL
126
OBTAIN ESTIMATE OF CURRENT ION RATE FROM FIT
128
130
OUTPUT FIT VALUE OF ION RATE FOR THE CURRENT TIME

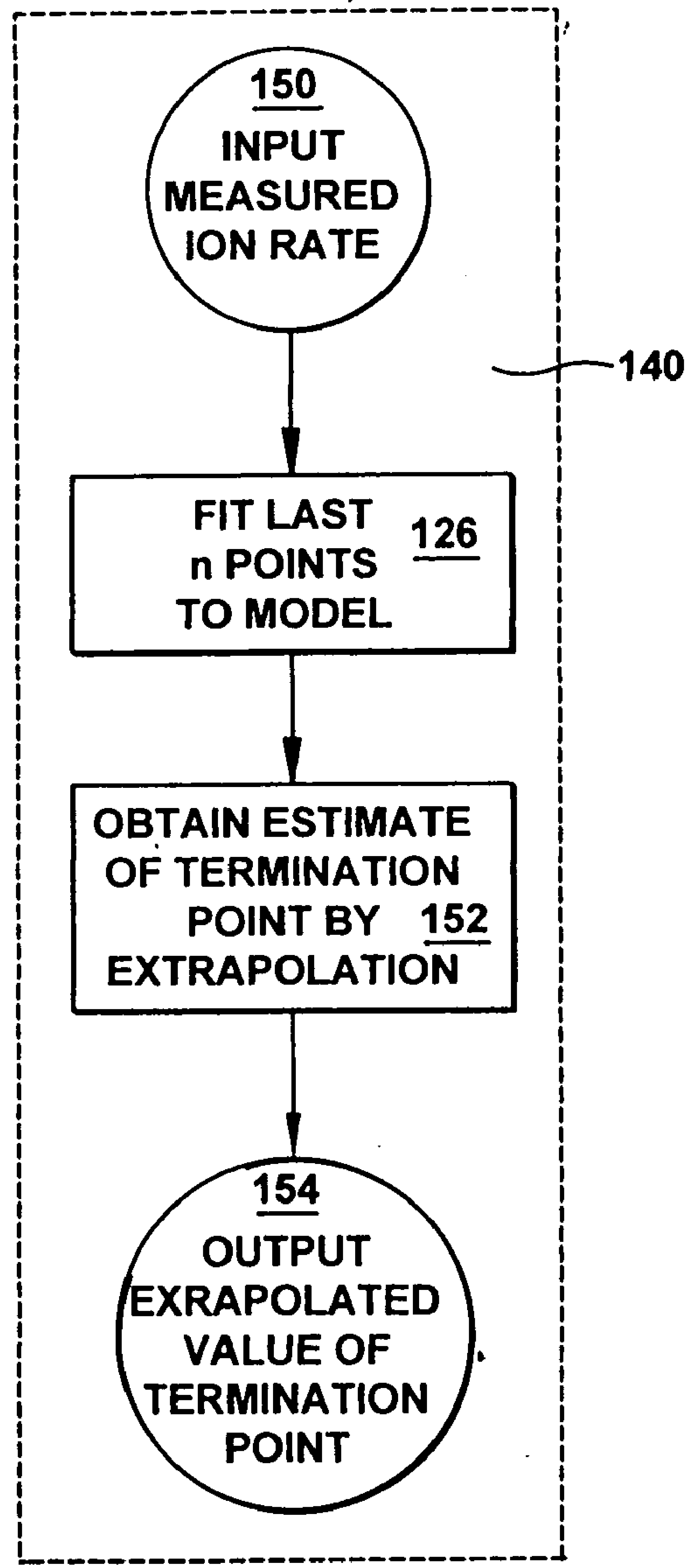
FIG.20B
150
INPUT MEASURED ION RATE
140
FIT LAST n POINTS TO MODEL
126
OBTAIN ESTIMATE OF TERMINATION POINT BY EXTRAPOLATION
152
154
OUTPUT EXRAPOLATED VALUE OF TERMINATION POINT

FIG. 20A

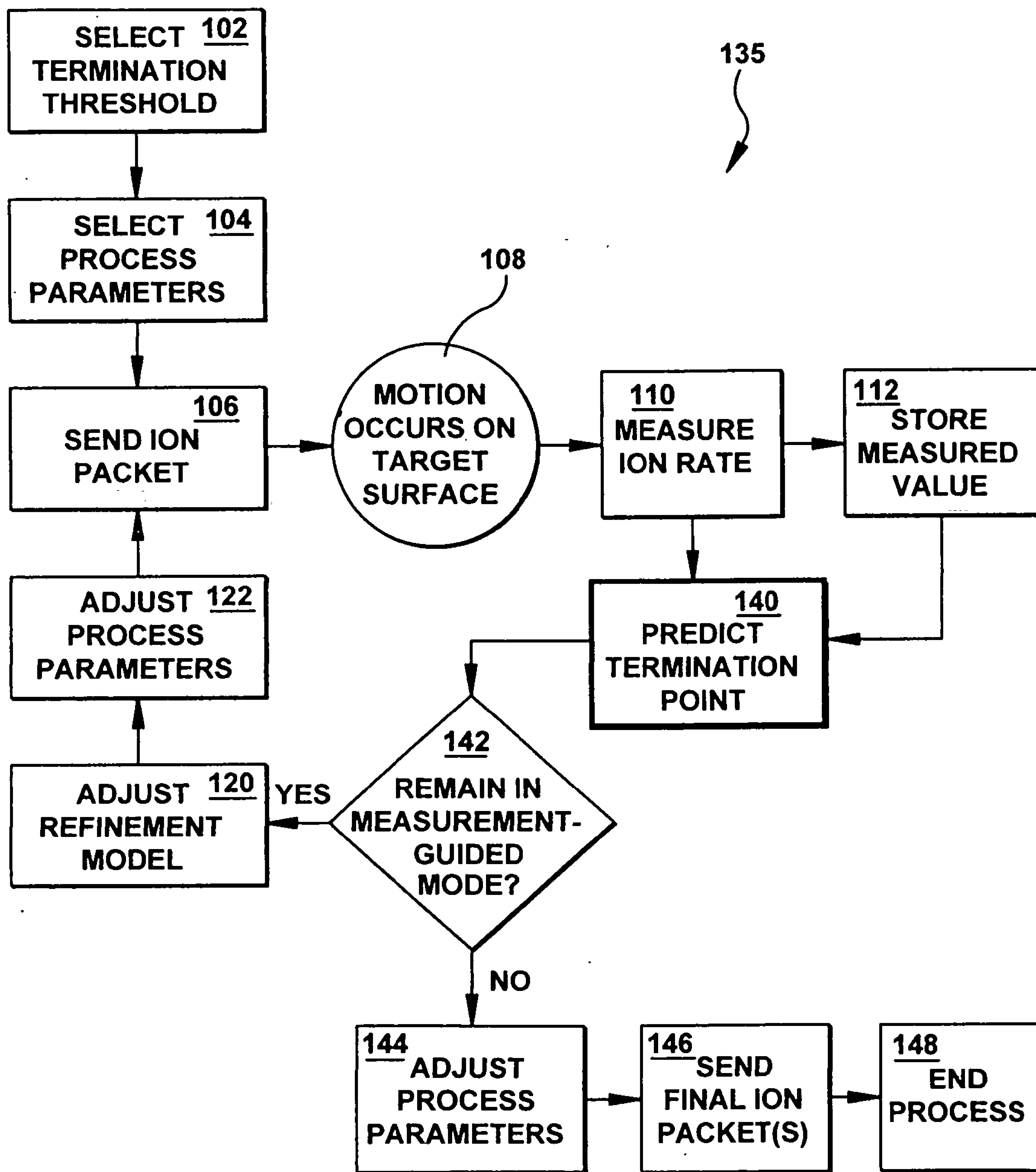

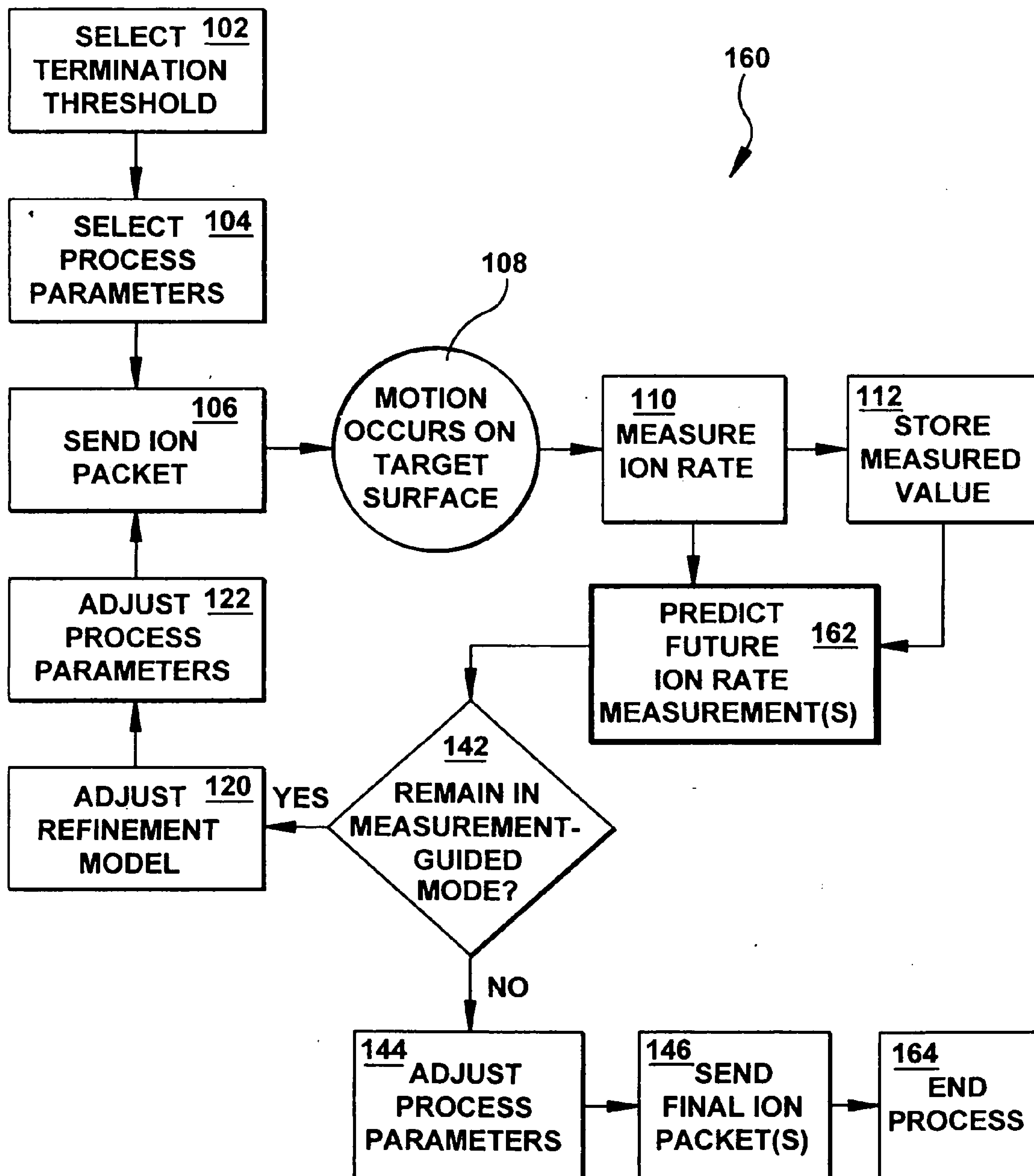
FIG.21A
160
SELECT TERMINATION THRESHOLD 102
SELECT PROCESS PARAMETERS 104
SEND ION PACKET 106
108
MOTION OCCURS ON TARGET SURFACE
110 MEASURE ION RATE
112 STORE MEASURED VALUE
PREDICT FUTURE ION RATE MEASUREMENT(S) 162
ADJUST PROCESS PARAMETERS 122
ADJUST REFINEMENT MODEL 120
YES
142 REMAIN IN MEASUREMENT-GUIDED MODE?
NO
144 ADJUST PROCESS PARAMETERS
146 SEND FINAL ION PACKET(S)
164 END PROCESS

FIG.21B

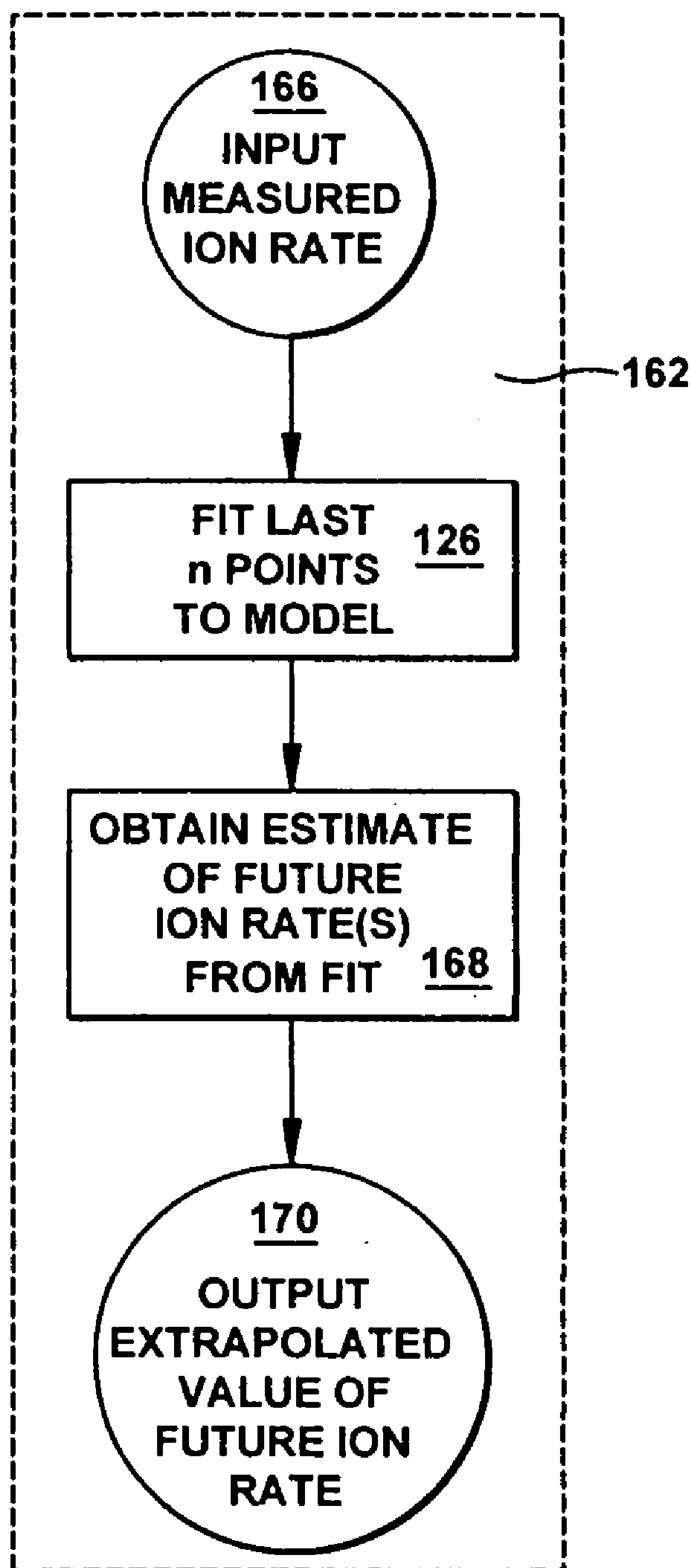

HIGH-PRECISION FEEDBACK CONTROL FOR ION SCULPTING OF SOLID STATE FEATURES

[0001] This application claims the benefit of U.S. Provisional Application No. 60/509,656, filed Oct. 8, 2003, the entirety of which is hereby incorporated by reference. This application is a continuation-in-part of co-pending U.S. Non-provisional Application No. 10/695,381, filed Oct. 28, 2003, which claims the benefit of U.S. Provisional Application No. 60/421,908, filed Oct. 29, 2002, the entirety of which is hereby incorporated by reference, and which is a continuation-in-part of co-pending U.S. Non-provisional Application No. 10/186,105, filed Jun. 27, 2002, now issued as U.S. Pat. No. 6,783,643, which claims the benefit of U.S. Provisional Application No. 60/301,400, filed Jun. 27, 2001, the entirety of both of which are hereby incorporated by reference, and which is a continuation-in-part of co-pending U.S. Non-provisional application Ser. No. 09/599,137, filed Jun. 22, 2000, now issued as U.S. Pat. No. 6,464,842, which claims the benefit of U.S. Provisional Application No. 60/140,021, filed Jun. 22, 1999, the entirety of which is hereby incorporated by reference.

CROSS REFERENCE TO RELATED APPLICATION

[0002] This application is related to co-pending U.S. Non-provisional application Ser. No. 09/602,650, now issued as U.S. Pat. No. 6,627,067, entitled "Molecular and Atomic Scale Evaluation of Biopolymers," filed Jun. 22, 2000, and hereby incorporated by reference in its entirety.

STATEMENT REGARDING FEDERALLY SPONSORED RESEARCH

[0003] This invention was made with Government support under Contract No. F49620-01-1-0467, awarded by DARPA. under Contract No. DMR-0073590, awarded by NSF, and under Contract No. DE-FG02-01ER45922, awarded by DOE. The Government has certain rights in the invention.

BACKGROUND OF THE INVENTION

[0004] This invention relates to fabrication of solid state structures, and more particularly relates to dimensional control of solid state structural features.

[0005] Precise dimensional control of solid state structural features is essential for many applications in fields ranging from biology and chemistry to physics, optics, and microelectronics. The term "solid state" is here meant to refer to non-biological materials generally. Frequently the successful fabrication of a solid state system critically depends on an ability to articulate specific structural features, often of miniature dimensions, within very tight tolerances. Accordingly, as solid state systems evolve to the micro-regime and further to the nano-regime, nanometric dimensional feature control is increasingly a primary concern for system feasibility.

[0006] There have been established a wide range of microfabrication techniques for producing and controlling structural feature dimensions in micromechanical and microelectromechanical systems. For example, high resolution lithographic techniques and high-precision additive and subtractive material processing techniques have been proposed to enable small-scale feature fabrication. But in the fabrication of many nano-regime systems, in which structural feature dimensions of a few nanometers are of importance, it is generally found that conventionally-proposed techniques often cannot form the requisite nano-scale features reproducibly or predictably, and often cannot be controlled on a time scale commensurate with production of such nano-scale features. As a result, volume manufacture of many systems that include nanometric feature dimensions and/or tolerances is not practical or economical.

SUMMARY OF THE INVENTION

[0007] The invention provides processes and corresponding process control methodology that enable reproducible and predictable production of structural features for solid state mechanical and electromechanical systems. The processes of the invention can be controlled to produce, control, and/or change feature dimensions in the nano-regime.

[0008] The invention provides a method for controlled fabrication of a solid state structural feature. In the method, a solid state structure is provided and the structure is exposed to an ion beam, under fabrication process conditions for producing the structural feature. A physical detection species is directed toward a designated structure location during the ion beam exposure of the structure or at a time when the structure is not exposed to the ion beam, and the rate at which the detection species proceeds from the designated structure location is measured. Detection species rate measurements are fit to a mathematical model, and the fabrication process conditions are controlled, based on the fitted detection species rate measurements, to fabricate the structural feature.

[0009] The processes of the invention enable fabrication of a wide range of structural features in a manner that is reproducible, controllable, and efficient. Applications in fields ranging from biology to microelectronics are enabled by these processes, and can be carried out in a manner that is commercially viable. Other features and advantages of the invention will be apparent from the following description and accompanying drawings, and from the claims.

BRIEF DESCRIPTION OF THE DRAWINGS

[0010] **FIGS. 1A-1D** are schematic cross-sectional views of fabrication sequence steps for the production of an aperture in accordance with the invention;

[0011] **FIGS. 2A-2G** are schematic cross-sectional views of an example fabrication sequence of steps for the production of the cavity of **FIG. 1A** in a membrane;

[0012] **FIGS. 3A-3B** are schematic diagrams of an ion beam sputtering system configured in accordance with the invention to implement precision feedback control;

[0013] **FIG. 4A** is an electron micrograph of a cavity formed in a 500 nm-thick silicon nitride membrane in accordance with the invention;

[0014] **FIG. 4B** is an electron micrograph of a 10 nm-wide aperture formed in a silicon nitride membrane by a process provided by the invention;

[0015] **FIG. 4C** is a plot of detected ion counts as a function of time for the aperture etch process that resulted in the aperture shown in **FIG. 4B**;

[0016] **FIG. 5A** is an electron micrograph of a 37 nm-wide aperture formed in a 500 nm-thick silicon nitride membrane in accordance with the invention;

[0017] **FIG. 5B** is an electron micrograph of the aperture of **FIG. 5A** enlarged to 58 nm in width by a process provided by the invention;

[0018] **FIG. 5C** is a plot of detected ion counts as a function of time for the aperture etch process that resulted in the aperture increase from that shown in **FIG. 5A** to that shown in **FIG. 5B**;

[0019] **FIGS. 6A-6C** are schematic cross-sectional views of stages in the reduction of a limiting aperture diameter by a process provided by the invention;

[0020] **FIG. 7A** is an electron micrograph of a 95 nm-wide aperture formed in a 500 nm-thick silicon nitride membrane in accordance with the invention;

[0021] **FIG. 7B** is an electron micrograph of the aperture of **FIG. 5A** reduced to 3 nm in width by a process provided by the invention;

[0022] **FIG. 7C** is a plot of detected ion counts as a function of time for the aperture etch process that resulted in the aperture decrease from that shown in **FIG. 7A** to that shown in **FIG. 7B**;

[0023] **FIG. 8** is a plot of detected ion counts per second as a function of ion sputtering time of a square aperture, initially of about 72 nm×72 nm in area, in a silicon nitride membrane of 500 nm in thickness, subjected to the mass transport processes of the invention under various temperatures;

[0024] **FIGS. 9A-9B** are plots of aperture area as a function of total ion dose for five different ion fluxes and aperture area decrease per dose as a function of ion flux, respectively, for an aperture having an initial area of about 1400 nm^2, for the material transport processes provided by the invention;

[0025] **FIGS. 10A-10C** are scanning electron micrographs of a trenched silicon nitride layer exposing the underlying silicon wafer on which the layer was deposited, partial fill-in of the silicon nitride trenches as a result of the material transport process conditions provided by the invention, and partial sputter etch removal of the upper trench layer as a result of the sputtering conditions provided by the invention;

[0026] **FIG. 11** is a plot of counted ions/second traversing an aperture as a function of time for various ion beam exposure cycles;

[0027] **FIG. 12** is an atomic force micrograph of a silicon nitride membrane one surface of which was exposed to a focused ion beam to produce apertures and protrusions on the membrane surface opposite that exposed to the ion beam;

[0028] **FIG. 13** is a schematic view of a solid state structure surface undergoing a material transport and ion sculpting process provided by the invention, identifying physical mechanisms corresponding to various terms of an ion sculpting model provided by the invention;

[0029] **FIG. 14A** is a plot of aperture area as a function of total ion dose for four different ion fluxes and for continuous as well as periodic ion flux exposure, for the material transport processes provided by the invention;

[0030] **FIG. 14B** is a plot of the inverse of adatom diffusion distance as a function of incident argon ion flux;

[0031] **FIG. 15** is a plot of measured current as a function of time produced as negatively charged DNA molecules were drawn through a nanopore produced in accordance with the invention in a silicon nitride membrane.

[0032] **FIG. 16** is a plot of the area of a hole in a silicon dioxide membrane experimentally measured as a function of argon ion beam fluence, for the indicated duty cycles of pulsed beam exposure and for a continuous beam;

[0033] **FIG. 17** is a plot of the area of a hole in a silicon nitride membrane experimentally measured as a function of argon ion beam fluence, for the indicated duty cycles of pulsed beam exposure and for a continuous beam, and for a temperature of −100° C.;

[0034] **FIG. 18** is a plot of the area of a hole in a silicon nitride membrane and a plot of the area of a hole in a silicon dioxide membrane experimentally measured as a function of argon ion beam fluence, as the ion exposure is switched between continuous beam exposure and pulsed beam exposure having a 50% duty cycle of pulsed ion beam exposure at 10 ms beam "on" and 10 ms beam "off;"

[0035] FIGS. **19**A-B are flow diagrams of a feedback control technique provided by the invention for refining measured indications of progress of an ion sculpting process;

[0036] FIGS. **20**A-B are flow diagrams of a first feedback control technique provided by the invention for enabling measured data extrapolation to future ion sculpting process conditions; and

[0037] FIGS. **21**A-B are flow diagrams of a second feedback control technique provided by the invention for enabling measured data extrapolation to future ion sculpting process conditions.

DETAILED DESCRIPTION OF THE INVENTION

[0038] The processes for dimensional feature control provided by the invention can be directed to a wide range of materials and structural configurations. The example processes here described are meant to be illustrative but not to represent specific limitations in materials or configurations. The processes of the invention are particularly well-suited for precisely controlling structural feature dimensions, and for enabling such control on the scale of nanometers. This control can be especially advantageous for the precise formation and definition of nanometric-sized features and spaces, such as gaps existing as an aperture, e.g., pores, slits, orifices, vents, and holes, as well as trenches, channels, troughs, and in general, the spacing between two or more distinct feature edges.

[0039] Referring to **FIG. 1**, in one example implementation of a method provided by the invention for precisely and reproducibly defining the spacing of features, there is carried out a process for forming an aperture of a prespecified extent, e.g., diameter, in a structural layer. In a first process step, referring to **FIG. 1A**, a starting structure **10** is pro-

vided, shown in cross-section in the figure. Such starting structure **10** can be supplied as, e.g., a substrate, a thick or thin layer provided on a support such as a substrate, a membrane, or suitable structure. A cavity **12** is formed in the structure **10** on a selected surface **14** of the structure and in a region at which an aperture is desired.

[**0040**] The cavity **12** extends into the bulk of the structure **10** for only a fraction of the structure's thickness, rather than through the entire thickness of the structure, to an opposing surface **18**. As a result, the deepest level, i.e., the bottom **16**, of the formed cavity lies at some midpoint in the structure's bulk. As explained in more detail below, the geometry of the cavity bottom **16** and the cavity sidewalls **20** are preferably selected to enable controlled formation of a limiting aperture of controlled transverse and longitudinal dimensions in later processing steps. In the example illustrated, a bowl-shaped cavity is employed.

[**0041**] Referring to **FIGS. 1B and 1C**, once the cavity is produced, the structure is progressively thinned from the cavity-free surface **18**. As the thinning is continued, a portion **22** of the structure is increasingly removed, shown by dotted lines. This causes the cavity-free surface **18** of the structure to advance toward the bottom **16** of the cavity.

[**0042**] Continued thinning of the structure results in the intersection of the cavity-free surface **18** with the bottom **16** of the cavity, as shown in **FIG. 1D**. When this intersection occurs, a limiting aperture **24** is formed which transforms the cavity **12** to an aperture extending through the thickness of the structure. Further thinning of the structure causes the cavity-free surface **18** to intersect upper sidewall locations of the cavity, whereby the limiting aperture **24** takes on that profile of the sidewalls which exists at a given cavity intersection depth. In the example illustrated, the diameter of the limiting aperture **24** increases as thinning is continued, given the bowl shape of the cavity. It is to be recognized, however, that the diameter of the limiting aperture can be made to decrease as thinning is continued, for a corresponding cavity sidewall profile. In addition, asperities or other distinct profile features or geometry can be provided along the cavity sidewalls for controlling limiting aperture geometry.

[**0043**] This aperture forming process provides distinct advantages in that it does not rely on direct lithographic techniques for defining final limiting aperture and wall dimensions. As a result, the aperture forming process is not constrained by lithographic resolution limits. The process enables production of a limiting aperture dimension or diameter as small as 1-2 nanometers or less without the need for exotic or expensive processing apparatus.

[**0044**] As explained above, this aperture formation process can be carried out on any of a wide range of structures, such as substrates, layers, and films provided on a supporting structure or free-standing as, e.g., membranes. Solid state materials in general can be employed as the structural material in which an aperture is formed; microelectronic or semiconductor materials can be particularly effective in enabling efficient processing techniques, as described below. For example, the broad classes of inorganic and organic glassy materials, such as oxides, glasses, plastics, polymers, and organic films, e.g., PMMA, as well as crystalline materials, such as semiconductors, e.g., silicon and silicon nitride, and metals, as well as other materials can be employed. The invention is not limited to a particular structural material or class of structural materials. Preferably, the structural material is selected to meet the criteria of the application specified for the aperture.

[**0045**] The method is particularly well-suited for enabling formation of apertures in membranes, and for providing the nano-regime control of aperture formation that is required for many membrane applications. In the formation of a membrane aperture, microelectronic and semiconductor materials and fabrication processes can be advantageously exploited in accordance with the invention to enable cost-effective and efficient manufacturability.

[**0046**] Referring to **FIG. 2**, in an example microfabrication process provided by the invention for forming an aperture in a membrane, a starting substrate **30**, e.g., a silicon wafer, is provided, as shown in **FIG. 2A**. A selected membrane material, e.g., silicon nitride, is provided as a coating layer **32**, **34** on the upper and lower surfaces, respectively, of the wafer. The thickness of the coating layer **34** is that thickness selected for the membrane to be formed. In one example, a silicon-rich, low-stress, silicon nitride layer of about 50 nm in thickness is deposited on the silicon wafer by conventional chemical vapor deposition (CVD) processing. It is recognized that additional membrane materials, e.g., silicon dioxide, can be deposited before or after deposition of the silicon nitride layers for mechanical stress control or other consideration. The silicon nitride layer can also be further processed, e.g., by ion implantation, to control mechanical membrane stress or adjust electrical or thermal conductivity of the membrane as desired for a given application.

[**0047**] As shown in **FIG. 2B**, a layer of photoresist **40** is formed on one of the deposited nitride layers and patterned to define a nitride etch window **38**. The opposing surface of the wafer is blanket coated with a photoresist layer **40**. Then, as shown in **FIG. 2C**, the silicon nitride exposed by the nitride etch window **38** is removed by, e.g., conventional reactive ion etching techniques. This exposes a substrate etch window **42**. The opposing nitride layer **34** is protected from this etch by the blanket photoresist layer **40**, which is removed at the etch completion.

[**0048**] Next, referring to **FIG. 2D**, the silicon wafer is bulk micromachined by a suitable etch procedure, e.g., a conventional anisotropic wet etch process employing KOH. Preferably, the bulk wafer etch process employed is characterized by a high selectivity to the wafer material over the membrane material. In the example illustrated, the KOH etch substantially does not attack the silicon nitride layers. Continuation of the etch through the thickness of the wafer thereby produces a self-supporting nitride membrane **36** in a nitride layer **34**. The nitride membrane forms the bottom of a pyramidal well **39** etched out of the silicon wafer due to the anisotropic, crystallographic-specific nature of the KOH etch. The extent of the nitride membrane is thus determined by the thickness and crystallographic orientation of the starting silicon wafer. As will be recognized, the membrane dimensions can therefore be controlled as-desired.

[**0049**] Referring to **FIGS. 2D-2E**, the remaining layer **32** of silicon nitride opposite the membrane layer can then removed if desired by, e.g., conventional reactive ion etching, and then a layer of silicon dioxide **41** is optionally

grown on the exposed silicon surfaces, if electrical insulation of the silicon wafer is desired for a given application. Conventional wet or thermal oxide growth can be preferred over a CVD oxide layer such that oxide is only formed on the silicon surfaces in the manner illustrated. If, however, a composite membrane is desired, e.g., for mechanical stress control, then a CVD or other deposition process can be employed to produce an oxide layer on both the silicon wafer and the lower silicon nitride membrane surfaces, or on the nitride membrane surface alone.

[**0050**] In a next step of the process, referring to **FIG. 2F** and referring back to **FIG. 1A**, a cavity is formed in a selected surface of the membrane. In one example cavity formation process, an etching process, as illustrated, a layer of resist **42** is formed on the lower membrane surface, i.e., the membrane surface opposite that in the pyramidal wafer well. The resist is then patterned to define the cavity to be formed in the membrane. This choice of surface for the cavity can be preferable for enabling a selected lithography technique on a flat surface; it can be difficult to effectively pattern a layer of photoresist provided on the membrane surface at the bottom of the silicon pyramidal well. If desired for a given application, however, the cavity can be formed on such a surface with lithographic techniques specific to such a configuration. The invention contemplates the use of photolithography, electron beam lithography, and other suitable lithographic processes for defining the cavity pattern. It is to be recognized that the selected lithographic process is preferably suited to the dimensions of the cavity; e.g., electron beam lithography can be preferred over conventional photolithography for cavities having submicron dimensions.

[**0051**] As explained above, the sidewall profile of the cavity to be formed in the membrane can be specified to produce a selected limiting aperture geometry. The lithographic step defining the cavity, as well as the nature of the cavity etch process itself, can also be employed to define the cavity sidewall profile. In one example scenario, the selected lithographic cavity pattern is continuous, e.g., as a circle, and a relatively isotropic etch process, e.g., an isotropic reactive ion etch process, is carried out to form a bowl-shaped cavity **12** in the nitride membrane **36**, as shown in **FIG. 2G**. An isotropic reactive ion etch process inherently forms the bowl shape extending from a circular photolithographic pattern.

[**0052**] The invention contemplates the use of substantially any cavity pattern for achieving a desired cavity geometry. Square, rectangle, hexagonal, or other pattern, symmetric or asymmetric, can be employed. Due to the batch nature of lithographic processes and other microfabrication processes employed in the aperture forming method, arrays of cavities, of varying extent and geometry, can be defined in a single structure such as the membrane illustrated. Because the aperture formation process of the invention relies on structural thinning, rather than lithography, to define the final limiting aperture geometry, the largest lateral dimension of the cavity can be much greater than the desired limiting aperture extent; in general, the largest cavity pattern dimension can be two or more orders of magnitude larger than a selected limiting aperture diameter. Preferably, given the characteristics of a selected cavity etch process, the cavity pattern extent is correspondingly selected to produce a desired extent at the cavity bottom, and to produce a range of cavity expanses between the cavity bottom and the material surface.

[**0053**] Any suitable cavity etch process can be employed, including, e.g., plasma etching, focused reactive ion etching, focused ion beam etching, wet chemical etching, or other selected technique. Whatever etch process is selected, it is to be controlled to enable termination of the etch at a cavity bottom located at some distance within the membrane thickness or other structure in which the cavity is formed, i.e., at a point between the surfaces of the structure. For etch processes that are fully characterized for the structural material being employed, this can be accomplished by a timed etch; conventional diagnostic techniques otherwise can be employed in the conventional manner to produce a cavity bottom at a selected location in a membrane other structure. It is not required in accordance with the invention to precisely position the cavity bottom at a known, a priori depth in the structure. The progressive structural thinning process of the invention is particularly advantageous in this regard; no precise control or knowledge of the depth of the cavity is required to precisely produce an aperture. In addition, a combination of etch processes can be employed as-necessary for cavity formation in a given material or composite of materials. For example, where a composite membrane is formed of silicon nitride and silicon dioxide layers, the chemistry of a selected cavity etch, such as a plasma etch, can be adjusted over the course of the etch based on the material to be etched at a given time in formation of the cavity. Similarly, a combination of etch processes can be employed to alter the cavity sidewall profile as a function of cavity depth. For example, a combination of isotropic and anisotropic wet etches can be employed to produce selected curvature and slant of cavity sidewalls formed in a nitride or silicon layer or membrane. A combination etch such as this enables the formation of asperities or other distinct features to be located at the limiting aperture.

[**0054**] Referring back to **FIGS. 1B-1D**, once a cavity has been formed in the selected membrane or other structure, thinning of the structure is then carried out on the structure surface opposite that in which the cavity was formed, employing an appropriate procedure to open a limiting aperture in the structure. The invention contemplates a wide range of thinning processes and is not limited to a particular thinning technique; all that is required is the ability to etch back the structure from a surface opposing that in which the cavity was formed.

[**0055**] For many applications, a particularly well-suited thinning process is ion beam sputtering. In such a process, a beam of ions is directed to the structure surface to be thinned to sputter etch away material from that surface. In typical ion beam sputtering processes at relatively low beam energies, e.g., in the range of keV, for every incident ion, on average, a single atom of material is ejected from the sputtering target; sputtering may thus be considered as an atomic-scale version of "sand blasting." In the case of, e.g., a silicon nitride membrane, such sputter etching results in the removal of about one atomic layer of silicon nitride from the membrane per second for incident ion fluxes between about 10^{14}-10^{15} ions/cm^2/sec. When the surface exposed to

the sputtering beam has been sufficiently thinned that the surface intersects with the cavity bottom, a limiting aperture is formed.

[0056] The invention contemplates a wide range of additional thinning processes, including ion beam assisted etching, ion beam induced etching, electron beam etching or assisted etching, plasma and reactive ion etching, wet etching such as electrochemical etching, chemomechanical polishing, and other fabrication and manufacturing processes that enable controlled thinning of a structure to intersect a cavity on a surface opposite that being thinned. These aperture formation processes can be advantageous for many applications because during the thinning etch, the etch species, e.g., a sputtering ion beam or reactive plasma environment, need not be focused on a particular location of the structure surface being thinned. A blanket exposure of the structure surface can be employed to thin the entire extent of the structure. All that is required is that the structure surface including the cavity be isolated, i.e., shielded, from the etch species attacking the opposing surface. This results in nano-regime precision in feature formation without the requirement of nano-regime control of the etch apparatus and species.

[0057] Whatever thinning process is selected, the inventors herein have discovered that highly precise aperture formation can be accomplished by implementing a feedback mechanism during the thinning process. This feedback mechanism is based on detection of a physical species provided during the thinning etch in a manner that is indicative of the physical dimensions of a feature, e.g., an aperture, that is being produced by the etch. Such feedback enables real time control of the aperture formation process, whereby a precise and prespecified aperture diameter can be reliably and reproducibly formed. As explained later in the description, this feedback mechanism can in general enable precise sculpting of nanometric features and nanostructures, and finds wide application for micro- and nano-systems.

[0058] Considering feedback control in the aperture formation process of the invention more specifically, when an etch species, such as a beam of sputtering ions, thins a structure to the point that an aperture is formed, ions from the beam are at that point in time enabled to pass through the aperture. Thereafter, the number of ions passing through the aperture per unit time is proportionally related to the increasing diameter of the aperture as the thinning etch continues. Detection and quantification, e.g., by counting, of the rate and/or number of ions passing through the aperture thereby is indicative of the aperture diameter at any given time during the etch.

[0059] As a result, a selected aperture diameter can be prespecified based on a rate and/or number of ions expected to pass through the aperture before the selected diameter is produced. During a thinning etch process, a first passage of ions through a newly-formed limiting aperture can be detected, and the number of ions passing through the aperture as its limiting aperture dimension enlarges can be individually detected and quantified. When the prescribed number of ions pass through the aperture, a controlling signal can be sent to the sputtering ion beam controller to terminate the etch process at the desired aperture dimension. In addition, it is recognized in accordance with the invention that detection of a physical species can be carried even prior to the time at which an aperture is formed. For example, the level of X-rays produced by the ion beam gun that are detected as passing through the structure being thinned can be expected to increase as the thickness of the structure decreases. Detection of ions similarly can be made even prior to aperture opening. This enables control of the process even prior to the final opening of the aperture.

[0060] Referring to **FIGS. 3A-3B** there is schematically shown a system **50** for implementing this feedback-controlled sputtering process. The system includes an ion gun **52**, e.g., an ion gun capable of producing an ion beam with an energy range and diameter suitable for a given application. In general, an energy between about 1 eV and about several hundred KeV and a beam diameter between about a few nanometers to spatially very broad beams can be employed. A vacuum etch chamber **55** is provided in which the etch process can be carried out. Preferably, the etch chamber pressure is well-controlled such that etch environment pressures of less than about 10^{-8} Torr can be maintained during the etch process. A turbomolecular pump **57** is provided for pressure control and maintenance. Optionally, a mass spectrometer can be provided for monitor and analysis of the etch environment species.

[0061] A structure holder **54** is provided for supporting a structure **10** in which an aperture is to be formed, e.g., employing clips to maintain the position of the structure. Preferably, the holder **54** is thermally conductive and provides structure temperature control, e.g., by a liquid heat exchange loop, employing a thermocouple positioned on the holder or on the structure itself. For many applications, it can be preferable that the holder also be electrically conductive to enable voltage charge control of the structure and to enable monitor of incident ion beam current.

[0062] The holder includes a central aperture **56** corresponding to the location at which an aperture is to be formed in the structure **10**. With this configuration, a beam of ions **58** directed from the ion gun toward the structure **10** thins the structure to form therein an aperture, after which time the ion beam **58** traverses both the structure aperture and the holder aperture.

[0063] Referring to **FIG. 3B**, an electron flood gun **59** can be included in the arrangement to direct a beam of electrons at the structure being etched during the etch process. For structures such as a silicon nitride membrane that are electrically insulating, positive electrical surface charge can accumulate on the structure due to positively-charged ion beam irradiation. Electron beam irradiation of the structure can be carried out to neutralize this surface charge, if necessary for a given application.

[0064] If the thinning etch process is to be controlled by a feedback mechanism in accordance with the invention, then the stream of a species traversing the etched aperture is to be detected and quantified in the manner described below. If no such feedback control is desired for a given application, then no additional apparatus is necessary, and the sputtering can be carried out in a conventional sputtering chamber under conditions selected for a given etch.

[0065] In accordance with the invention, species detection and quantification systems can be included to provide a desired degree of feedback control. Given a scenario where the selected sputtering beam ions employed for the thinning

etch are electrically charged, ion focusing optics **60** can be provided for focusing the ions once they traverse the aperture, to facilitate ion detection by a detector that is relatively distant from the structure aperture through which the ions traversed. X-Y deflection optics and Einzel lenses can be employed in conventional configurations to produce a desired focusing of the ions. In the conventional manner, optics design software can be employed to produce a customized focusing configuration for a given detection arrangement. It is to be recognized that such focusing configuration may not be required for configurations where the ion detection system is relatively near to the holder aperture.

[**0066**] If employed, the focusing configuration preferably directs the output ion beam to an ion energy analyzer **62** for filtering the beam for the selected species to be detected and quantified by, e.g., counting. In general, it can be expected that the ion beam sputtering process will include and produce a wide range of physical species and radiation, including, e.g., sputtered silicon nitride atoms, etch species scattering in the etch chamber, and X-rays emanating from the ion gun. To enable highly precise etch control, the species to be detected is preferably filtered out from the produced radiation, produced etch species, and background radiation. Such background can be minimized by, e.g., isolating the ion beam gun, the structure to be etched, and the downstream optics from further downstream components such as detectors, as described below, by an electrostatic energy filter or other suitable filter. In addition, it can be preferable to maintain the ion beam gun, structure, and optics at reduced temperature conditions in a suitable vessel, as shown in **FIG. 3B**, whereby thermal effects can be controlled. Such a cooling configuration is also useful to maximize cleanliness of the etch and beam detection environment and to control structure temperature. It can also be advantageous to maintain the structure at an elevated temperature to influence materials modification phenomena during ion irradiation.

[**0067**] The employment of an ion energy analyzer **62** or other species-specific filtering system is advantageous in that it enables redirection of a species to be detected out of the line of sight of the sputtering trajectory. The species detection location can then be distant and out of line from bombardment by background and produced radiation such as X-rays. For example, as shown in **FIGS. 3A-3B**, the electrostatic energy analyzer employed produces a 90° bend in the trajectory of the ion species to be detected, whereby that species is separated from the other species and radiation coming from the etched structure. If the detection resolution and speed desired for a given etch process do not require a low background noise environment, then the ion energy analyzer is not required for many applications.

[**0068**] The filtered species of interest output from the electrostatic energy analyzer is directed to a detector **64**. For the detection of an electrically charged ion species, it can be preferable to employ a high-resolution, single ion detector, e.g., a Channeltron 4860 detector from Gallileo Electro-Optics of Sturbridge, Mass. Such a detector can be configured to produce one electrical output pulse per detected ion. Such single ion detection and associated counting can be preferred for many applications to enable nanometric-scale precision in production of a solid state feature such as an aperture. While a typical sputtering beam current density is about 10 ions/nm^2/sec, etching of a nanometer-range aperture requires counting of the passage of no more than about 10-20 ions through the aperture. Thus, a single ion detection and counting system, or another system of equivalent resolution, is preferred to reproducibly implement nano-regime control of feature production. If the features to be produced for a given application do not require nanometric dimensional control, then a more coarse detection mechanism can be employed.

[**0069**] Given a single ion detector configuration, a fast pulse amplifier **66** can be employed to modify the electrical output of the detector to facilitate an ion counting process. A suitable pulse preamplifier can be constructed in a conventional manner or a suitable commercial system, e.g., the VT120 Fast Preamp from EG&G Ortec of Oak Ridge, Tenn., can be employed. In one example scenario, given the production of a 10 mV ion detection pulse by the ion detector, the pulse amplifier **66** can be configured to amplify the pulse voltage to about 1 V. This amplified detection pulse is directed to a counting system, e.g., a universal counter such as the HF53131A by Hewlett Packard, for producing an electrical signal indicative of the number of detected ions. It is recognized that detection pulse amplification may not be required for a given pulse counter configuration, and that the pulse amplification, if implemented, is preferably controlled based on requirements of the counting system.

[**0070**] The electrical output of the pulse counter **68** is directed to a controller **70** that implements, e.g., monitor and control software for enabling an operator to monitor the thinning etch process in real time and for producing an ion gun control signal. In one example, the controller is implemented in software employing, e.g., Labview, from national Instruments of Austin Tex. Whatever controller implementation is selected, it preferably provides ion beam control signals based on the ion feedback. For example, the controller can be implemented to initiate ion beam sputtering of the structure for a specified time interval and to configure the counter to count the number of ions received at the detector during the specified time interval. At the end of the interval, the number of ions counted is determined by the controller and the extent of the aperture can at that point be calculated based on this ion count and the known ion flux. The number of ions counted during the interval is then employed by the controller to determine if a further interval of ion beam sputtering is to be initiated to continue etch of the structure.

[**0071**] In one advantageous configuration, a computer system including monitor, memory, and associated input/output and printing systems is provided for enabling visual monitoring and recording of the etch process progression. Display of the ion count rate and aperture extent over time, and storage of count rate and other system values can be preferable for many applications.

[**0072**] The output of the controller **70** is directed to an ion gun control system **72** for controlling the sputtering etch itself. In one example implementation, ion gun feedback control is effected by control of the ion gun's X-Y deflection plates to deflect the ion beam away from the structure **10** at the time when the desired aperture dimension is produced. This can be a preferable control technique because of the rapid speed at which the beam can be deflected, typically in much less than a millisecond. It is recognized, however, that alternative beam control mechanisms can be employed. For example, an electrostatic grid can be located between the

gun and the structure holder. In this scenario, the grid is energized in response to an ion beam termination control signal to return the beam back toward the ion gun. In a further technique, the accelerating electron impact voltage of the ion gun can be controlled in response to an ion beam termination control signal to terminate production of the ion beam. These techniques are advantageous in that they suppress all sputtering after the desired aperture dimension is produced, whereby possible contamination of the sample is eliminated.

[**0073**] With a sputtering system and feedback/control hardware configuration in place, a feedback calibration curve can be produced for a given ion beam species, structure material, and aperture geometry to be produced: Such a calibration curve enables specification of the relationship between ion count number and/or rate and limiting aperture dimension, and can be established empirically, to specify for a particular structural material and thickness a relation between number of measured counts per time and actual limiting aperture dimension.

[**0074**] It is found that for many configurations, the relationship between limiting aperture dimension and ion count is generally linear. For this and other generally-predictable relationships, an extrapolated calibration curve can be produced based on a few measurements. To produce each such measurement, a thinning etch is carried out for a prescribed duration, during which an ion count is made and at the end of which an aperture dimension is physically measured by, e.g., transmission electron microscopy. Multiple etch durations and dimensional measurements can be carried out on a single aperture as that aperture is increased from etch to etch. A calibration curve can then be produced based on the ion count and aperture measurements and extrapolated to lower and higher ion counts. With such a calibration curve in hand, the controller system of the feedback configuration can be programmed to direct a controlling etch termination signal to the ion gun when the prescribed ion count corresponding to a desired aperture dimension is reached.

[**0075**] It is to be recognized that etch environment temperature and pressure, mechanical stress and temperature of the structure being etched, and feature dimensions and structural aspects can influence the relationship between detected ion count rate and physical feature dimensions. For example, the residual mechanical stress in a silicon nitride membrane can impact its etch characteristics. Similarly, the density of apertures in an array to be formed, the aperture proximity to each other, and other aspects can impact etch characteristics. It is therefore to be recognized that the calibration curve preferably is produced with consideration for various physical and etch environment parameters that can impact etch characteristics.

EXAMPLE 1

[**0076**] A 50 nm-thick silicon nitride membrane having a cavity formed on one surface was produced by the process outlined in FIGS. 2A-G. The silicon nitride was deposited by low pressure chemical vapor deposition. The cavity bowl was etched in the membrane by a reactive ion etch process. **FIG. 4A** is an electron micrograph of the cavity formed in the membrane.

[**0077**] The membrane surface opposite that including the cavity was exposed to an argon ion beam etch at an energy of about 3 KeV, and a flux of about 3 $Ar^{+}sec/nm^{2}$. The ion beam diameter was about 200 μm and the membrane temperature during the etch was maintained at about −120° C. The ion beam was directed toward the membrane for 1 sec during each 5 sec interval. During the etch process, ion detection and counting was carried out.

[**0078**] **FIG. 4B** is an electron micrograph of the membrane cavity including a **10** nm limiting aperture formed by thinning of the membrane. **FIG. 4C** is a plot of argon ion count/second as a function of sputtering time. This plot includes that time when the ion beam was directed to the membrane, not when the beam was deflected away from the membrane. As indicated by the plot, the number of counted ions/sec was substantially zero until at point in time, at **25** sec, when the limiting aperture was opened. Then as the limiting aperture diameter increased, the ion counts correspondingly increased. This enables control of the aperture formation process.

[**0079**] In this example, precise and controlled etch of the aperture was enabled by detection and counting of electrically charged ions that traversed the aperture once it was opened. Here the species operating as an etchant also operated as the species to be detected. In accordance with the invention, this dual role of the ion beam is not in general required. In an alternative scenario provided by the invention, the etchant species is selected and operates distinctly from the detection species. For many applications, such a decoupling of the etchant and detection species can be advantageous in enabling a broader range of candidate species for both etchant and detection species.

[**0080**] Considering an atom beam etch species, if the beam is electrically neutral rather than electrically charged, detection of the atoms can be difficult. A distinct non-etching detection species such as an electron beam can in this case advantageously be employed for controlling formation of a prespecified aperture diameter. Such a scenario can be preferable where the structure being etched may become electrically charged by the impinging sputter beam, thereby warranting the use of an electrically neutral beam. For many applications, it can be preferable to employ an electrically charged detection species, for facilitating beam bending, filtering, and detection and counting with conventional techniques. Electrically neutral detection species can be employed, however, when such is optimal for a given application. For example, laser fluorescence of electrically neutral transmitted atoms can be employed for detecting and counting control functions.

[**0081**] When employed, a separate detection species is preferably one that can be directed in some manner toward a feature being produced and whose movement in the vicinity of the feature is indicative of changing dimensions of the feature. This enables detection of the species in a manner that is indicative of changes in the feature's dimensions. For example, in the case of formation of a membrane aperture, direction of an electron beam toward the membrane, such that electrons traverse the membrane aperture once it is formed, enables counting of electrons in the manner of ion counting described above. The invention does not require the use of a single detection species; more than one detection species can be employed. For example, X-rays produced by the ion gun can be monitored as the structure thins to predict and indicate a the time of a further aperture

formation event. Thereafter, ions, electrons, or other species can be employed to monitor changes in aperture diameter. Neutral species and other species suited to a given application can similarly be employed together to provide precise detection and feedback mechanisms.

[0082] In addition, the invention does not require that the detection species be directed orthogonally to the plane of a feature being produced. For example, electron beam diffraction detection and the diffraction patterns produced by a material can be employed as a feedback mechanism. In such a case, e.g., where a feature in an upper layer is formed by removal of the upper layer to expose a lower layer or substrate, detection of the electron beam diffraction pattern characteristic of the lower layer can be employed as the feedback mechanism. Here the electron beam makes a glancing angle with the material. Similarly, in the case of formation of, e.g., an aperture, diffraction can be detected as a function of the aperture diameter by diffraction rings indicative of changes in aperture periphery. The diffraction feedback mechanism here occurs at the aperture periphery rather than as a trajectory through the aperture.

[0083] In a further example, an electron beam can be directed parallel to the upper structure surface being thinned in formation of an aperture, whereby the withdrawal of surface material is indicated by an increase in electron count in a direction parallel to that surface.

[0084] The invention contemplates alternative detection species. For example, atoms in a meta-stable state, e.g., an electronic meta-stable state, can be directed toward a feature being formed and detected once past the feature. Such meta-stable atoms, e.g., excited states of helium or argon, are electrically neutral and do not decay until hitting a solid surface, at which time an electron is liberated and can be detected and counted. Whatever detection species is selected, it preferably is one that can be detected and counted on a time scale that is commensurate with the desired dimensional scale of control in the feature being produced. For example, where nanometric feature dimensions are of importance, microsecond detection and counting processes are preferable to enable high sensitivity and resolution in the feedback mechanism. Less strict sensitivity and resolution requirements need be placed on detection species for micro- and macro-scale feature control.

[0085] The invention contemplates application of physical species detection and counting for feedback control in a wide range of fabrication processes. Many fabrication processes that are conventionally carried out in open loop fashion, i.e., without feedback control, can be adapted to enable nanoscale dimensional feature control with the incorporation of the highly sensitive and precise feedback mechanisms provided by the invention. For example, in the aperture formation process described above, reactive ion etching in a plasma, rather than sputter etching, can be employed to thin a structure surface in formation of a limiting aperture. In such a plasma etch process, the structure surface including a cavity is isolated from the plasma environment by a suitable fixture. The opposing structure surface is fully exposed to the plasma environment. As the plasma etch progresses to thin the structure and eventually produce a limiting aperture and growing aperture, ions traversing the aperture are detected by, e.g., a channeltron positioned on the isolated side of the structure. Accordingly, in the manner of the ion sputtering etch described above, feedback control can be imposed on the plasma etch process based on the detection and counting of plasma ions traversing the aperture.

[0086] In a further example process contemplated by the invention, physical detection and feedback control can be imposed on a wet etch process employed to produce a feature. For example, in formation of an aperture in a structure, electrodes can be provided near to the cavity formed in the structure. Here the structure surface opposite the cavity is exposed to a wet etch environment, e.g., an electrochemical environment, and the structural surface which includes the cavity is isolated from the etch environment. As the wet etch progresses to thin the structure and open an aperture, ions in the liquid that traverses the aperture can be detected and counted at the cavity-side electrodes. This enables feedback control for terminating the electrical stimulus of the etch at a time when the desired aperture dimension is attained.

[0087] The invention contemplates implementation of physical species detection and feedback process control for enabling fabrication of a wide range of structural, solid state features. The feedback mechanism is not limited to the aperture formation process described above. As explained above, an aperture, slit, trench, hole, or gap between two feature edges can be precisely formed, by any of a wide range of processes, in a precise and controllable manner with the feedback mechanisms of the invention.

[0088] For example, in a membrane aperture formation process employing, e.g., focused ion beam or plasma etching techniques where a hole is formed directly through the thickness of the membrane from one surface to the other of the membrane, feedback can be employed to control and monitor the formation. Similarly, the invention contemplates a membrane aperture formation process where a cavity is formed in one surface of the membrane and then that membrane surface, including the cavity, is exposed to, e.g., an ion sputtering etch. Because the thickness of the membrane between the cavity bottom and the opposing surface is much less than at other membrane regions, such etching opens a limiting aperture at the base of the cavity before completely etching away other regions of the membrane. The feedback mechanisms of the invention enable precise control and monitoring of this process.

EXAMPLE 2

[0089] A silicon nitride membrane of about 50 nm in thickness was produced in the manner of **FIGS. 2A-2E**. An aperture was formed through the entire thickness of the membrane by reactive ion etch. This resulted in a 37 nm-wide aperture, an electron micrograph of which is shown in **FIG. 5A**. The membrane and aperture were then exposed to an argon ion beam at a flux of about 1.7 $Ar^+/nm^2/sec$ and an energy of about 3 KeV. The ion beam was directed toward and away from the membrane to sputter for 1 second during each 5 second interval. The membrane was maintained at a temperature of about −102° C. during the ion beam exposure.

[0090] **FIG. 5B** is an electron micrograph of the 58 nm-wide aperture that resulted from 180 seconds of sputtering. **FIG. 5C** is a plot of counted ions/sec as a function of

time. A generally linear relationship between ion counts as a function of time is demonstrated.

[0091] The invention does not require that the process being controlled by feedback be a subtractive process as in Example 2; additive processes can also be controlled by the feedback techniques of the invention. For example, an aperture, trench, or hole of a given dimension can be diminished or narrowed, by a suitable process, during which the physical species detection and feedback process control of the invention is imposed to control the diminishing process.

[0092] Sintering, heating, material deposition, material growth, and other suitable processes are contemplated as being controllable by the feedback mechanism of the invention. Similarly, oxidation, swelling, material flow and transport as described in detail below, condensation, evaporation, electroplating, ion- or electron-assisted deposition or growth, and other such additive processes can be controlled in accordance with the invention. The only requirement of the process to be controlled, whether additive or subtractive, is that the process accommodate the introduction of some detection species near to the structural feature being processed in a manner that enables detection of that species as an indicator of changing feature dimensions. As explained above, the features can be produced in a membrane, in a layer or layers provided on a support structure, or in a structure itself, e.g., a silicon wafer. Whether the process being controlled is additive or subtractive in nature, the advantages of the control processes of the invention can be most fully exploited and realized in the formation of nanometric scale feature dimensions and dimensional tolerances.

[0093] This capability can be particularly advantageous for producing a field of nanometric features, e.g., in formation of a lithographic mask plate. Here, e.g., a starting membrane can be processed with selected geometries to ultimately form wires, pads, and other mask plate geometries by additive or subtractive processes. This enables precise formation of the mask plate features in an efficient and effective process.

[0094] In another aspect of the invention, the inventors herein have discovered that the conditions of interaction between an ion beam and a solid can be controlled for manipulating nanoscale feature dimensions in solid state materials. These controlled ion beam interaction techniques enable solid state material topology to be adjusted, rather than necessarily removed. Specifically, under selected process conditions provided by the invention, solid state material can be caused to transform such that feature edge locations are precisely and controllably produced and/or modified by atomic transport mechanisms that are locally additive or subtractive.

[0095] Referring to **FIGS. 6A-6C**, in a first example of this ion beam feature control, a limiting aperture **24** in a structure **10** is caused to be adjusted from a first diameter, D_1, to a smaller diameter, D_2 or D_3. The starting aperture is formed in a selected structure in any suitable fashion, e.g., by the methods described above and shown in **FIGS. 1A-1D** and **FIGS. 2A-2G**, in, e.g., a membrane, layer, substrate, or other structure. The structure surface **18** in which the limiting aperture was formed is then exposed to ion beam irradiation, employing, e.g., the system described above and illustrated in **FIGS. 3A-3B**.

[0096] As shown most dramatically in **FIG. 6C**, for selected ion beam irradiation conditions, the inventors have discovered the unexpected result that the material is added to the periphery, or boundary, of the limiting aperture **24** exposed to the irradiation, causing the diameter of the limiting aperture to decrease. This condition can be predictably and precisely imposed by enforcing structure temperature, ion flux rate, and ion energy conditions conducive to material addition at the aperture rim. Given that the ion beam irradiation is generally considered to be a sputtering/material removal process, it is particularly unexpected that this material movement and addition condition can effectively progress, even in the presence of the atomic sputtering erosion, to result in a change in the physical dimensions of a feature.

EXAMPLE 3

[0097] A silicon nitride membrane of about **500** nm in thickness was produced in the manner of the process outlined in FIGS. **2**A-E. An aperture was formed through the entire thickness of the membrane by reactive ion etching. **FIG. 7A** is an electron micrograph of the 95 nm-wide aperture that resulted from the etch.

[0098] The membrane and its aperture were then exposed to an argon ion beam flux at an energy of about 3 KeV, and a flux of about 47 Ar^{+}/sec/nm^2. The membrane was maintained at a temperature of about 20° C. during ion flux exposure. The ion beam was directed to the membrane for 250 ms for each 1 sec time interval.

[0099] **FIG. 7B** is an electron micrograph of the membrane after exposure to the argon ion beam reduced the aperture diameter to about 3 nm. **FIG. 7C** is a plot of counted argon ions/sec as a function of time. A generally linear count rate is indicated for midpoints in the process.

[0100] Without being bound by theory, the inventors herein understand that the mechanisms underlying the ability of an ion beam to cause material build up at an ion-irradiated aperture rim may be related to atomic transport through the bulk of the structure; ion-induced changes in viscosity, electronic surface charge, mechanical stress generation, and lateral swelling of the structure; and/or atomic surface transport caused by ion-induced surface atom excitation or supersaturation of mobile adsorbed ionic species on the structure surface. At sufficiently low ion energies the ion penetration depth is much less than the structure thickness, resulting in a domination of surface transport processes. The invention does not require a specific material transformation mechanism, but rather, provides distinguishing process control parameters that impose predictable material transformation results.

[0101] Considering the process parameters to be controlled, it is found that the temperature of the structure being exposed to the ion beam irradiation directly impacts the ability to impose material movement and the rate at which material moves. It is found that for a specific structural material, there is a characteristic temperature above which material of the structure is found to move, resulting in an adjustment, or change, in feature dimensions and below which material is instead removed by sputtering from the structure. For given ion beam energy and flux conditions, control between material removal and dimensional feature adjustment can therefore be imposed by structural temperature control.

EXAMPLE 4

[0102] Referring to the graph of **FIG. 8**, there is plotted the ion counts/second detected by an ion sputtering system like that of **FIG. 3A** as a function of time for a 500 nm-thick silicon nitride membrane in which was initially fabricated a square aperture of about 72 nm in length. The membrane was fabricated based on the process shown in **FIGS. 2A-2F** and the aperture was fabricated by a focussed ion beam directed at the membrane to form an aperture that extended completely through the membrane. Each region of the graph indicates the temperature at which the membrane was maintained during bombardment by an argon ion beam. The beam flux was 14 Ar^+/sec/nm^2 and the beam energy was 3 KeV. The on/off duty cycle of the ion beam being directed toward the membrane was such that the beam was directed to the membrane for 200 msec during each 1 sec interval.

[0103] As a function of time, an increase in ion count/second indicates an increase in the aperture dimension, while a decrease in ion count/second indicates a decrease in the aperture dimension. The plotted data clearly indicate an increasing rate of aperture shrinkage under the ion beam irradiation as the membrane temperature is increased above about 5° C. In contrast, at membrane temperatures below about 4° C. the aperture dimension increases rather than decreases. At membrane temperatures between about 0° C. and about −10° C. no appreciable temperature dependence in the rate at which the aperture dimension decreases is indicated.

[0104] With this experimental data, it is indicated that for a silicon nitride membrane, two distinct temperature regimes exist; the first temperature regime, at or above about 5° C., imposes material movement and feature addition by ion beam irradiation, the second temperature regime, at or below about 4° C., imposes material sputtering and removal by ion beam irradiation, both regimes for given ion beam species, flux, and energy conditions. This analysis for a silicon nitride membrane is an example of the empirical analysis contemplated by the invention to determine that temperature above which a material of interest can be made to move and augment features. It is recognized that this transition temperature can vary widely from material to material.

[0105] The plotted data also indicate that within the regime for imposing material movement and addition, the rate of material transport in altering feature topology is temperature dependent. At relatively higher temperatures, the transport process proceeds more rapidly than at relatively lower temperatures. Knowledge of this temperature-dependent transport rate enables precise process control and characterization.

EXAMPLE 5

[0106] Five silicon nitride membranes of about **500** nm were fabricated in the manner of the process outlined in FIGS. **2**A-E. Apertures each of about 1400 nm^2 in area were produced in the membranes by focused ion beam etching. The membranes were then exposed to an argon ion beam at an energy of about 3 KeV for various total doses at five ion beam fluxes. Each membrane was maintained at a temperature of about 22° C. during the ion beam exposure. Each ion beam exposure was controlled to sputter for 200 msec during each 1 second interval.

[0107] Referring to the graphs of **FIGS. 9A-9B**, there is plotted the area of the apertures in nm^2 as a function of total argon ion beam dose, in ions/nm^2, for five different argon ion beam fluxes, and the aperture area decrease per dose, as a function of argon ion beam flux, respectively. From the plotted data, it is indicated that as a function of total argon ion beam dose, the aperture shrinks more rapidly at low incident fluxes relative to higher incident fluxes. In other words, the lower the flux, the less dose is required to shrink an aperture. The strong nonlinearity indicates that the amount of material mass transport produced by the ion beam irradiation per incident ion may be suppressed at high incident fluxes. This characterization enables operation at a selected mass transport rate. In a manner analogous to the temperature dependence analysis provided above, the invention contemplates empirical analysis of flux dependence for a selected material, to enable precise control of the material movement.

EXAMPLE 6

[0108] A 50 nm-thick layer of silicon nitride was deposited by low pressure chemical vapor deposition on a silicon wafers. The silicon nitride layer was patterned by electron beam lithography to produce trenches of about 50 nm in width through the entire thickness of the silicon nitride layer. The bottom of each trench thereby exposed the underlying silicon surface. **FIG. 10A** is a scanning electron micrograph of the trenched silicon nitride layer on the silicon wafer.

[0109] The trenched silicon nitride layer was exposed to an argon ion beam at an energy of about 3 KeV and a flux of about 20 Ar^+/nm^2/sec, where the ion beam was sputtering for 0.5 seconds for each 2 second interval. The silicon wafer was maintained at a temperature of about 20° C. during the ion beam exposure. **FIG. 10B** is a scanning electron micrograph of the trenched silicon nitride layer after about 200 seconds of sputtering. Note that silicon nitride material has been moved to the trenches, whereby the trenches have been partially filled in. This indicates that for the process conditions here employed, material is transported from the silicon nitride layer to the trenches.

[0110] A second 50 nm-thick trenched silicon nitride layer like the one just described was exposed to an argon ion beam at an energy of about 3 KeV and an ion flux of about 30 Ar^+/nm^2/sec, with the ion beam sputtering for one second during each two second interval, for a total sputtering time of about 300 seconds. The silicon wafer was maintained at a temperature of about −100° C. during the ion beam exposure. **FIG. 10C** is a scanning electron micrograph of the trenched silicon nitride layer. Here, the silicon nitride material at the top of the trenches has been etched away, as indicated by the rounding of the trench edges, but the bottom of the trenches are not at all filled in.

[0111] This example demonstrates the temperature control that can be imposed to predictably produce material transport and feature adjustment or material removal by sputtering as desired for a given application.

[0112] Turning to additional material transport control mechanisms provided by the invention, it is understood that the energy of the ion beam can impact the nature of material transport. Specifically, for a given structural material and temperature, a given ion beam current density, and a given time structure of the ion beam exposure, as discussed below,

there exists an ion beam energy above which material transport is effectively induced in the manner described above and below which sputtering in the conventional manner occurs. This juncture between the two distinct operational regimes can be empirically determined for a given material and ion beam exposure system, and can be employed as an important control technique for precisely enabling and disabling the material transport processes.

[0113] Further in accordance with the invention, it is found that the time structure of the ion flux exposure, i.e., the sequence of intervals in which the ion beam is controlled to enable interaction with a material and then controlled to not interact with the material, impacts the nature of material transport and dimensional feature change. Specifically, the imposition of an on/off duty cycle on the ion flux is found to impact the ability to cause material movement and corresponding dimensional feature change.

EXAMPLE 7

[0114] A 500 nm-thick silicon nitride membrane was produced in the manner of the process outlined in FIGS. **2**A-E. A 95 nm-wide aperture was formed through the entire thickness of the membrane by focused ion beam etch. The membrane and aperture were then exposed to an argon ion beam at an energy of about 3 KeV and a flux of about 14 $Ar^+/sec/nm^2$. The membrane was maintained at a temperature of about 16° C. during the ion beam exposure. During the exposure, the amount of time that the ion beam was directed to the membrane was varied. Six different time structures were employed: 100 msec on for each 1 second interval; 200 msec on for each 1 second interval; 400 msec on for each 1 second interval; 600 msec on for each 1 second interval; 600 msec on for each 2 second interval; and 600 msec on for each 4 second interval. During the ion beam exposure, ion detection and counting was carried out as an indication of the reduction or enlargement of the aperture in response to the various ion beam exposure cycles.

[0115] **FIG. 11** is a plot of argon ions counted/second as a function of sputtered time. The plot indicates that the 400 msec/1 second interval and the **600** msec/l second interval time structures increased the aperture diameter, while all other time structures decreased the aperture diameter. This demonstrates that at about room temperature, control between material transport processes and sputtering processes can be achieved, by control of the ion beam exposure time structure, to result in a desired degree of mass transport stimulation. Such stimulated mass transport processes are herein referred to as ion beam sculpting, or ion sculpting, to distinguish over conventional ion stimulated sputter erosion of a target material.

[0116] The invention provides an understanding, based on experiments using periodically pulsed ion beams, for directly determining the time scale of material transport on ion sculpted materials, including dielectric materials such as silicon dioxide and silicon nitride. Experimental measurements produced in accordance with the invention demonstrate that ion sculpting can indeed be successfully applied to the technologically important oxide of silicon, and further demonstrate a discovery of the invention, that ion sculpting material transport time scales can be surprisingly long, indicating that the materials do not necessarily relax to their equilibrium condition until seconds after a stimulating ion beam has been extinguished. This effect can be used advantageously in applications of ion sculpting to predictably control the sculpting process for a desired dimensional result.

[0117] In accordance with the invention, additional samples for ion beam sculpting were prepared as 500 nm-thick, freestanding SiO_2 or SiN membranes supported on a silicon frame. The SiO_2 membranes were thermally grown on Si(100) substrates, then capped for further processing by depositing a 200 nm-thick layer of Si_3N_4 by low pressure chemical vapor deposition. Photolithography and anisotropic wet chemical etch processing of the silicon substrates was then carried out to create free-standing 90 μm×90 μm SiO_2 membranes. The Si_3N_4 capping layer was then removed by etching in hot phosphoric acid, and then the oxide surface was cleaned by exposing it to an oxygen plasma. Silicon nitride membranes were fabricated by first depositing a 500 nm-thick layer of low-stress SiN directly on Si(100) substrates by LPCVD, followed by similar photolithography and etching steps as described above for the oxide membranes. A single initial hole of a selected diameter was then milled near the center of each SiO_2 or SiN membrane by a focused ion beam milling process.

[0118] The thusly produced oxide and nitride membranes were individually exposed to an argon ion beam at an energy of about 3 keV in the apparatus of **FIG. 3A**, with the ion beam impinging the membrane surface in the normal direction. Ions transmitted through the open holes were detected by a Channeltron single ion detector after electrostatic focusing and energy analysis in the manner described previously. The ion beam exposure of the membrane was varied in the manner described above, to produce a periodic time structure of pulsed ion exposure. This was specifically controlled by electrostatically deflecting the ion beam on and off a membrane for the desired "on" and "off" times, referred to as T_{on} and T_{off}, respectively. Pulses of 200 volts were applied to deflection plates at the exit port of the ion gun to steer the beam about 5 mm away from a hole being processed within about one microsecond. The term "pulsed ion exposure" is thus herein meant to refer to the direction and removal of an ion beam at the hole.

[0119] In a first experiment with a silicon dioxide membrane, a 55 nm-wide hole in an SiO_2 membrane was exposed to the pulsed argon ion beam at a temperature of about 28° C. A range of beam "off" times of 0.1 s, 0.4 s, 0.9 s, and 1.9 s was employed with a constant beam "on" time of 0.1 s per cycle, as shown in the plot of **FIG. 16**. In this experiment, the instantaneous ion beam flux was kept constant at 15.7 $Ar^+nm^{-2}s^{-1}$. The initial duty cycle of the beam was 0.1 s "on", 0.9 s "off". Without interrupting the experiment, the "off" time was changed to 0.1 s, 1.9 s, 0.1 s, 0 s, i.e., continuous exposure, 0.9 s, 0.1 s, then 0.4 s, each for 100 cycles.

[0120] The hole area in the SiO_2 membrane was found clearly to decrease with increasing ion beam exposure, at a rate of hole decrease that depended on the "off" time of the pulsed beam. Whereas the continuous beam tended to open the hole, remarkably a pulsed beam with an "off" time of 0.1 s or longer acted to close the hole. The rate at which the hole area closed per unit fluence, referring to the negative slope in the figure, and given as "closing rate" for short, represents

the efficiency, ξ, with which the ion beam closed holes. It is clearly an increasing function of "off" time up to 1-2 seconds.

[0121] In a similar experiment, a 100 nm-wide hole in a SiN membrane, fabricated as described above, was exposed at a temperature of about 28° C. to varying ion beam exposure cycles of a pulsed ion beam having an instantaneous flux of 11.2 Ar+nm^{-2} $^{s-1}$. The resulting hole area is plotted in **FIG. 17**, revealing a duty-cycle dependence similar to that exhibited by the hole in the SiO_2 membrane. The ion sculpting efficiency was found to clearly increase as the ion beam "off" time was increased from 0.5 s through 1.5 s and 3.5 s, and was unchanged at 5.5 s all while the beam "on" time was held constant at 0.5 s.

[0122] Based on these experimental results, it is understood in accordance with the invention that the rate of hole closure, i.e., the rate of material transport, can be controlled by increasing the beam "off" time, and specifically can increase the material transport rate. The efficiency with which a pulsed ion beam sculpting process reduces a hole diameter is further found to increase with the beam "off" time, i.e., T_{off}, as an increasing function of T_{off}, independent of ion beam flux, processing temperature, or the initial conditions of a hole being ion beam sculpted. In addition, it is found that the efficiency with which a pulsed ion beam sculpting process reduces a hole diameter can be enhanced, to promote reduction of the hole, by lowering the flux of the ion beam or by raising the processing temperature, given a selected ion beam exposure duty cycle.

[0123] In addition, in the SiN experiments, it was also found that continuous ion beam exposure increased, rather than decreased the hole diameter in the SiN membrane at various temperatures. This demonstrates a discovery in accordance with the invention that the lateral transport of matter by ion sculpting can be "frozen out" at low temperatures, at which point sputter erosion of a pore dominates the process. The 0.1 s "on", 0.9 s "off" pulsed beam that closed the hole at 28° C. opened it at a rate of 2.9 nm^2/Ar$^+$nm^{-2} at −100° C. Thus, in accordance with the invention, an increase in process temperature can be employed to increase the rate of material transport.

[0124] It is further recognized, based on these experiments, in accordance with the invention, that pulsed ion beam sculpting can be precisely controlled by the initial conditions of a hole being exposed to a pulsed ion beam, as well as the surface topography of the membrane in which the hole is formed, in conjunction with the duty cycle of the pulsed ion beam. More specifically, the closing efficiency of a hole being ion sculpted by a pulsed ion beam is directly controlled by the initial condition of the hole, including the size of the hole and the surface topography of the membrane in which the hole is formed. For example, a large initial hole, e.g., of about 150 nm in diameter, can be enlarged under the same pulsed ion sculpting conditions that reduce the diameter of a smaller hole, e.g., of about 50 nm in diameter, given a fixed ion beam flux and processing temperature.

[0125] As explained previously, without being bound to theory, it is understood in accordance with the invention that on a microscopic scale ion beam sculpting can involve the motion of independent atoms along the surface of the material, and/or the collective motion of many atoms in a surface layer, to account for the lateral transport of matter under the influence of low-energy ion beams. To describe the time-dependent behavior of pulsed ion beam sculpting of the invention, at first ignoring the effect of sputter erosion, the material response is parameterized with a rise time, τ_{rise}, and a decay time, τ_{decay}. Within the time scale description, the closing rate of a hole approaches a steady-state closing rate value, i.e., a continuous beam closing rate value, R_{ss}, as $(1-e^{(t-t_0)/\tau(rise)})R_{ss}$ when the ion beam is turned on, and decays as $e^{-t/\tau(decay)}$ when the beam is turned off, where t is time and t_0 is the initial time. An exponential rise and decay of the hole closing rate is the simplest phenomenological model that incorporates material response time scales. Such time scales are common to microscopic models that are understood to provide a description of the pulsed ion sculpting phenomenon of the invention, including surface diffusion or viscous flow models.

[0126] In accordance with the invention it is required that the closing rate of a hole being sculpted be a continuous function of time that is assumed to reach a quasi-steady state condition where the closing rate at the beginning of each ion pulse, given as time t=0 in the equations below, is the same. Then the closing rate of the hole area, A, is given by:

$$\frac{dA}{dt} = R_{ss}\left(1 - e^{-\frac{t}{\tau_{rise}}}\left(\frac{1 - e^{-\frac{T_{off}}{\tau_{decay}}}}{1 - e^{-\frac{T_{off}}{\tau_{decay}} - \frac{T_{on}}{\tau_{rise}}}}\right)\right) 0 \le t < T_{on} \tag{1a}$$

$$\frac{dA}{dt} = R_{ss}\left(1 - e^{-\frac{T_{on}}{\tau_{rise}}}\left(\frac{1 - e^{-\frac{T_{off}}{\tau_{decay}}}}{1 - e^{-\frac{T_{off}}{\tau_{decay}} - \frac{T_{on}}{\tau_{rise}}}}\right)\right) e^{-\frac{(t-T_{on})}{\tau_{decay}}} T_{on} \le t \le T_{off} \tag{1b}$$

[0127] A hole closes during the entire beam pulse cycle, i.e., during both ion beam "on" and "off" durations. The area change induced by the cycle is thus integrated over the "on" and "off times of (1a) and (1b) above. The ion sculpting efficiency, ξ, for flux ϕ is:

$$\xi = \frac{1}{\phi T_{on}} \int_{cycle} \frac{dA}{dt} dt = \frac{R_{ss}}{\phi}\left[1 + \frac{(\tau_{decay} - \tau_{rise})}{T_{on}} \frac{\left(1 - e^{-\frac{T_{on}}{\tau_{rise}}}\right)\left(1 - e^{-\frac{T_{off}}{\tau_{decay}}}\right)}{1 - e^{-\frac{T_{on}}{\tau_{rise}} - \frac{T_{off}}{\tau_{decay}}}}\right] \tag{2}$$

[0128] This expression accounts for duty cycle dependence in ion beam sculpting through the relative lengths of the material response time scales. The experimental results in the plots of **FIGS. 16 and 17** suggest that the intrinsic decay in material response, τ_{decay}, i.e., the material response decay when the ion beam is off during a pulse cycle, for both SiO_2 and SiN, is on the order of seconds, and fitting the results to the exponential time scale model given above indicates that the rise time in material response, τ_{rise}, is shortened by the incident ion beam relative to the decay in material response, τ_{decay}.

[0129] In accordance with the invention, it is understood that the pulsed ion beam sculpting process of the invention is characterized by a condition in which ion-stimulated

mobile species cause the rise time in material response, τ_{rise}, to decrease with increasing ion beam flux. The mechanism by which τ_{rise} is reduced by increasing beam flux is understood to be a function of incoming ions ejecting mobile surface species, i.e., sputter erosion, thereby reducing the intrinsic time for such species to be trapped on the surface. Ion sputter erosion is known to arise from momentum transfer in atomic collision cascades that last on the order of a picosecond. But the time scale for a material to respond in ion beam sculpting is unusually long—on the order of seconds.

[**0130**] For a given material, the extent to which a pulsed ion beam reduces the material response rise time, τ_{rise}, relative to the material response decay time, τ_{decay}, can be determined by measuring the ratio of ion sculpting efficiency, ξ, for continuous beam exposure and pulsed beam exposure. The expression for ion sculpting efficiency, ξ, can be approximated by $\xi \approx R_{ss}/\phi[1+(\tau_{decay}-\tau_{rise})(\tau_{decay}+\tau_{rise})^{-1}]$ for a pulsed beam whose "on" and "off" times are the same and are assumed to be much shorter than τ_{decay} and τ_{rise}.

[**0131**] With this expression, the ion sculpting efficiency, ξ, is given as R_{ss}/ϕ for continuous ion beam exposure. As the material response rise time, τ_{rise}, decreases, the ion sculpting efficiency of the pulsed beam therefore tends to twice that value, regardless of the material, for a 50% duty cycle of ion exposure. This is a surprising discovery provided by the invention, and implies that the same amount of hole closing can be induced by half the ion fluence in the same amount of time by using a periodically pulsed beam at a 50% duty cycle, in the manner described above.

[**0132**] This enhancement of ion sculpting efficiency of a pulsed beam over a continuous beam was experimentally measured in accordance with the invention for the SiO_2 and SiN membranes described above. The measured the results are shown in the plot of **FIG. 18**. The experiment was performed by switching between continuous ion beam exposure and a periodically pulsed beam with 10 ms "on" and "off" times. The incident ion flux was 8.3 $Ar^+nm^{-2}s^{-1}$ for the nitride membrane hole, and 2.2 $Ar^+nm^{-2}s^{-1}$ for the oxide membrane hole.

[**0133**] The ion sculpting efficiency was found to be clearly enhanced by the periodically pulsed beams in both materials. For the SiO_2 membrane, the measured value of efficiency, ξ, increased from 0.3 for the continuous beam exposure to 1.4 for the pulsed beam exposure, in units of $nm^2/(Ar^+nm^{-2})$. The measurement was repeated on the same SiO_2 sample to find the efficiency, ξ, enhanced from 0.5 for continuous beam exposure to 1.3 for pulsed beam exposure. The measured value of efficiency, ξ, for the SiN membrane was found to increase from 1.6 for continuous ion beam exposure to 5.8 for pulsed beam exposure, then returned to 3.5 when the continuous beam exposure measurement was repeated.

[**0134**] Based on the model described above, when continuous ion beam exposure is switched to a pulsed beam exposure, the ion sculpting efficiency, ξ, should be enhanced by at least a factor of 2 if the material response rise time, τ_{rise}, negligibly small, and again neglecting sputter erosion effects. The experimentally determined ξ-enhancement factors were observed to be 3.4 for the SiO_2 membrane, and 2.3 for the SiN membrane, by averaging the slopes for continuous or pulsed segments of the data from the beginning and the end of each experiment, which likely differ due to surface material changes affected by significant argon irradiation.

[**0135**] The measured values of ξ then are preferably corrected for the competing effect of pore opening by sputter erosion by using the low temperature data in **FIG. 18**. Sputter erosion is assumed to contribute a constant hole opening rate of 2.9 $nm^2/(Ar^+nm^{-2})$ because the sputter yields of SiO_2 and SiN are very similar, weakly flux-dependent, and presumed to be independent of duty cycle. The corrected experimental efficiency ξ-enhancement factors are 1.3 for the SiO_2 membrane and 1.6 for the SiN membrane. These values are less than the predicted value of 2 because the material response rise time, τ_{rise}, although significantly diminished relative to the material response decay time, τ_{decay}, is not negligibly small. From equation (2), it is found that the material response rise time, τ_{rise}, is reduced to 0.6 times decay for an SiO_2 membrane by a 2.2 $Ar^+nm^{-2}s^{-1}$ ion beam. Similarly, a 8.3 $Ar^+nm^{-2}s^{-1}$ ion beam reduces the material response rise time, τ_{rise}, to one quarter of the material response decay time, τ_{decay}, for the SiN membrane.

[**0136**] These experimental results in accordance with the invention indicate that dynamics of hole closing, and correspondingly, material transport, in SiO_2 and SiN membranes are strongly dependent on the rest time between ion beam pulses, indicating that in general, a significant amount of hole closing, and material transport, occurs when no beam is incident on the material surface. This discovery has bearing on ion beam sculpting nanofabrication techniques of the invention in enabling control of ion beam time structure and control of the ion dose necessary to close holes, i.e., to impose material transport, on a feature being ion sculpted. It further determines whether holes can be made smaller at all by influencing the competition between the hole-closing and hole-opening processes of ion-induced lateral matter transport and sputter erosion, respectively. The dynamics of pulsed ion beam sculpting can be described by an exponential rise and decay of the hole closing rate. The incident ion beam must shorten the material response time in order to account for the enhanced sculpting efficiency of pulsed beams.

[**0137**] Based on these ion sculpting control mechanisms, the invention provides techniques for real time monitoring of an ion sculpting process in a manner that enables highly precise control of the process parameters. As explained above, the time signature of periodic ion exposure, the ion beam species, the target material temperature, and other process parameters can have a dramatic impact on an ion sculpting process. Monitoring of an ion sculpting process in an ion counting feedback loop configuration like that of **FIG. 3A** enables a high degree of process control.

[**0138**] For many applications, it can be preferred to augment this ion counting feedback control technique to enhance the accuracy of the process control it enables. It is found that various ion sculpting factors can effect the ion counting process of the feedback control. For example, as an ion sculpting process progresses, the number of ions counted, in the feedback loop, per time increment, i.e., the ion count rate, can change dramatically; in one example, as the diameter of an aperture is reduced, the ion count rate can fall to a very low level. Measurement of very low ion count

rates can be limited by statistical variations in the observed ion rate and/or the ion detector efficiency, leading to a low signal-to-noise ratio (S/N) in the measured ion count rate and a corresponding degree of inaccuracy in the ion sculpting process control. Specifically, an ion sculpting control paradigm for indicating if a measured ion count rate meets a prespecified ion count threshold can be limited in accuracy by a low signal-to-noise ratio. In addition, near to the threshold condition, this paradigm may not always enable sufficient process time for making adjustments in process parameters just prior to meeting the threshold condition, thereby limiting the ability to accurately produce a desired feature size.

[**0139**] The steps of a first process provided by the invention for enhancing the accuracy in ion counting feedback control is provided in **FIGS. 19A-19B**. Referring first to **FIG. 19A**, in the enhanced feedback control method **100** of the invention, a termination threshold of measured ion rate, or other suitable indicator, is selected **102** for a given ion sculpting process. As explained above, such a threshold can be set based on established calibration data for a selected material, starting features, process temperature, ion parameters, and desired final feature size. For example, given an ion sculpting process for producing a 5 nm-wide pore in a silicon nitride membrane from a 100 nm-wide starting pore, it can be established from calibration data that a termination threshold of, e.g., 100 ions counted per second, can be employed as an indicator for controlling the ion beam to produce the 5 nm-wide pore.

[**0140**] At a next step, process parameters are selected **104** for the ion sculpting process to be undertaken. Such parameters include, e.g., the duty cycle of periodic ion exposure, the on/off ratio of periodic ion exposure, ion energy, ion species, structure temperature, process pressure, and other parameters, as described above, including prespecification of adjustments to such parameters in real time during the sculpting process. For the example described here with regard to **FIGS. 19A-19B**, it is assumed that a periodic ion exposure sequence is employed, with a number of ions delivered as an ion packet during an ion packet duration, that duration referring to the "on" time of ion exposure during a periodic sequence duty cycle, with a nonexposure duration following each ion packet duration. With the termination threshold and process parameters in place, the feedback loop of **FIG. 3A** can be initiated to begin the sculpting process, by sending **106** a first ion packet to a target material being processed.

[**0141**] In the manner described previously, ions delivered to a target structure that is provided in the ion sculpting configuration of **FIG. 3A** cause material transport at the target, with material motion **108** occurring on the target surface. Once passing the target, the ions can be counted, as described previously, to measure **110** an ion rate. Specifically, the rate of counted ions proceeding from the target material is measured, producing an ion count and an ion count rate. This measured ion rate, or alternatively, the ion count, can then be stored **112** for use in refining **114** the measured ion rate, e.g., to compensate for the S/N ratio of the measured ion rate and/or to enable predictive process control, both described in detail below.

[**0142**] With this ion rate measurement, the ions that are sculpting the structure are also acting as a physical detection species for feedback control of the process. The current example being described employs ions in these dual roles, but such is not required by the invention. As explained previously, distinct ion sculpting and detection species can be employed. In addition, the detection species need not be directed at the location of the feature being ion sculpted. Rather, a separate and distinct designated structural location can be employed to which a physical detection species is directed and from which the species proceeds and is counted. Further, in the current example being described, the dual role of ions results in the sculpting species and the physical detection species being directed to the target structure simultaneously; i.e., the detection species is directed to the structure during the ion beam exposure of the structure. The invention contemplates separation of these tasks. For example, the ion sculpting process can be paused and the detection species directed to the target material at a time when the structure is not exposed to the ion beam; the ion sculpting process can then resume. In this manner, ion sculpting and detection species measurement can be carried out alternately, with each process alternating in time.

[**0143**] Referring back to **FIG. 19A**, based on the refinement of the measured ion rate, a query **116** is made to determine if at the current time in the process the selected termination threshold has been met. If so, the ion sculpting process can be ended **119**. Prior to ending the sculpting process, the fabrication process conditions can be adjusted **117**, in the manner described below, and an additional one or more ion packets can be sent **118** to the target, here with the feedback loop disabled. The process conditions can be adjusted prior to each sending of an ion packet. This end-stage, open-loop processing can be employed when, e.g., it is known that once a selected termination threshold is reached, specific adjustments to the process parameters and/or one or more final ion packets will more precisely produce a desired sculpting result than would an automatic threshold technique.

[**0144**] If the threshold query **116** determines that the termination threshold has not been met, the ion sculpting process is continued. Prior to sending **106** an additional ion packet to the target, the model employed for refining the measured ion rate can be adjusted **120** and/or the process parameters of the process can be adjusted **122**, both based on the fitted ion rate measurements, as described in detail below. Such is not required, but as explained in more detail below, these adjustments can be preferred in some applications for enhancing high-accuracy processing as well as predictive process control.

[**0145**] The flow diagram of **FIG. 19B** details the process steps of an example technique for refining **114** a measured ion rate. In this technique, the measured ion rate is input **124** to a processor configured for the refinement process. Then a number, n, of ion rate measurements that were previously acquired and stored during the current ion sculpting process are employed with the current ion rate measurement in a selected mathematical model fitting. Fitting of the n ion rate measurement points to a mathematical model results in a refined, more accurate indication of ion rate values for the time span over which the n ion rate measurements were acquired and can enable extrapolation of the fitted measurement points, as described below, for controlling the fabrication process conditions.

[0146] A wide range of mathematical models can be employed for the fitting process. Simple models such as statistical models, like a simple or weighted average taken over a number, n, of ion rate measurements, fitting of ion rate measurements to a straight line or polynomial expression, or other statistical model can be employed. Alternatively, more complex models of the ion sculpting process can be employed, as described below.

[0147] Whatever model is selected, it is preferred that the number, n, of ion rate measurements employed in the fitting process be chosen based on the current process conditions and the degree of refinement required, and tradeoffs of such. For example, as the number of included ion rate measurements is increased, the S/N of the refined ion rate measurements is also increased, but the refined measurements may be unnaturally biased by the characteristics of the model if the measurements significantly deviated from the model. As the number of included ion rate measurements is reduced, the more true the refined measurement values are to the actual nature of the ion sculpting process conditions, but the S/N of the refined measurement values is decreased. Thus, a tradeoff can be required in selecting the number, n, of ion rate measurements to be included in the model fitting process. For any number of ion rate measurements selected to be fit, it is preferred that all ion rate measurements included in a given fitting process reflect the ion sculpting conditions of the current ion rate measurement.

[0148] Beyond the simple statistical models described above, a fitting model can be produced having a functional form that is selected to reflect characteristics of the ion sculpting process. Specifically, physical arguments describing the ion sculpting process can be considered for producing a corresponding mathematical model of the process. Unknown details of the process can be reflected by mathematical parameters included in the general functional form of the selected model. This parametric description enables guiding of the ion rate measurement fit to the true nature of the ion sculpting process, and implicitly generates a set of fitting parameters that are more mathematically efficient for the ion sculpting process than are simple statistical parameters.

[0149] Mathematical modeling of a periodic beam ion sculpting process was previously described, and is further described in detail below. For purposes of an ion rate measurement fitting model, it can be preferred to generate a simple parameterized model. In an example of such a model for the ion sculpting of an aperture having an extent that is reduced from a starting extent to a prespecified final extent, it is assumed that transport of material on the surface of a target structure to the reducing aperture edge during ion beam exposure is proportional to the instantaneous extent of the aperture during the sculpting process. A corresponding constant of proportionality sets a first fitting parameter for the model.

[0150] In this aperture sculpting example, a further parameter can be specified based on an assumption that the instantaneous radius of the aperture through which the ions traverse, which is the boundary through which ions are incident, can be increased by a distance corresponding to the mean free path of incident species. This introduces an additional fitting parameter to the model. With these considerations, the rate of material transport, F(t), reducing the aperture extent can be modeled as:

$$F(t)=\tilde{\alpha}[2\pi(r+\xi)]\equiv\alpha A^{1/2}+\xi \quad (3)$$

[0151] where α is the proportionality factor described above, ξ is related to the molecular mean free path, and A is the instantaneous area of the aperture. This aperture area, A, can be modeled as:

$$A(t)=A(0)-\beta\int_0^t F(t')dt' \quad (4)$$

[0152] where A(0) is the starting area of the aperture, and , β is a final fitting parameter describing the effective size of the molecules of material transport that reduce the aperture extent. With the models represented by expressions (3) and (4), these expressions can be simultaneously solved by standard techniques to provide the following solution for rate of material transport at an aperture edge, F(t) as:

$$F(t)=F(0)-\frac{\beta\alpha^2}{2}t+\xi\ln[F(t)/F(0)] \quad (5)$$

[0153] This model for fitting ion rate measurements is thus shown to employ three fitting parameters, namely, F(0), the initial rate of aperture extent reduction; $\beta\alpha^2/2$, which sets the time scale, and ξ, which sets the mean free path of transporting molecules. With the solution of expression (5), expression (4) can be employed to determine the instantaneous aperture extent, and thus a refinement of a measured ion rate per aperture area, during the sculpting process. By fitting the expressions to a selected number, n, of ion rate measurements during a sculpting process, the parameters can be set, enabling the determination of refined ion rate measurements across the span of measurements.

[0154] The example above provides one technique for modeling the ion sculpting process in a manner that enables relatively straightforward parameterization and ion rate measurement data fitting. The invention does not require the use of a specific model, however, and it is recognized that a wide range of statistical and process-based modeling can be employed.

[0155] Referring back to **FIG. 19B**, with the last n ion rate measurement points fit **126** to a selected model, the modeled, or fitted data is employed to obtain an estimate **128** of what the current ion rate would be based on the model. This estimate is then output **130** as the refined ion rate measurement **114** as shown in **FIG. 19A**. The sculpting process of **FIG. 19A** then continues, with a query as to reaching the ion rate termination threshold **116**. By employing a step to produce a refined ion rate measurement that is used in the termination threshold query, the threshold query makes a determination based on ion rate measurement data that can be rendered less noisy, more accurate, and more realistic than the ion rate measurement data as-acquired. As a result, the accuracy of the feedback control system is enhanced and the ion sculpting process reliability and repeatability is correspondingly enhanced.

[0156] As explained above and shown in **FIG. 19A**, if the termination threshold is found to not have been reached, then if desired, the refinement model can be adjusted **120** prior to the next delivery of ions to the target. Such a model

adjustment can consist of changes to a model's parameters, including adding or deleting parameters, weighting or changes to weighting of parameters and/or the n ion rate measurements, as well as complete substitution of a new model for the current model. For example, as an ion sculpting process progresses, the sculpting mechanism may differ during various times. Distinct models can be employed for each sculpting regime to enable ion rate measurement refinement in a way that accurately reflects the process dynamics.

[0157] Also as explained above and shown in **FIG. 19A**, if the termination threshold is found to not have been reached, then if desired, the process parameters can be adjusted **122** prior to the next delivery of ions to the target. The invention contemplates a wide range of process parameter adjustments that can be employed. For example, ion packet length, ion packet duty cycle, ion energy, ion species, target temperature, chamber pressure, and other process parameters, including those described previously, can be adjusted. Thus, the termination threshold query can be employed to gauge the progress of a sculpting process and provide information to correspondingly alter the parameters of subsequent process durations.

[0158] In the example process of **FIGS. 19A-19B**, it is assumed that a periodic ion exposure paradigm is employed, with a duty cycle including a packet duration which ions are directed to a target and a nonexposure duration during which no ions are directed to the target. As explained previously, it is understood in accordance with the invention that such a periodic ion exposure can be particularly advantageous for enabling precisely controlled ion sculpting. This periodic ion exposure paradigm also enables ion rate measurement, threshold termination query, model adjustment, and process parameter adjustment to be carried out during the nonexposure duration. As a result, real time monitoring and adjustment of the ion sculpting process can be carried out for each ion packet. But the invention contemplates a range of other process paradigms. For example, the ion rate measurement refinement, threshold query, and model and process adjustments can be made in real time during a continuous ion exposure, rather than a periodic exposure. These steps can also be carried out at a point when a continuous process is paused and then restarted after completion of the steps. No particular ion exposure paradigm or process monitoring and adjustment correspondence is required.

[0159] This flexibility enables a wide range of applications for the control techniques of the invention. One particularly useful application is the extrapolation of fitted ion rate measurement data to enable predictions about and predictive control of ion sculpting subsequent to an ion rate measurement. Referring to the flow diagram of **FIG. 20A**, a first example of such an extrapolation control technique is outlined, here for the example scenario of periodic ion exposure of a target and an ion counting feedback loop configuration like that of **FIG. 3A**. In this extrapolation control technique **135**, an ion sculpting process is begun in the manner previously described, with a termination threshold selected **102**, and ion sculpting process parameters selected **104**. The ion sculpting is initiated by delivering **106** an ion packet to the target, causing material transport motion **108** on the target surface.

[0160] Once an ion packet has been sent to a target and has traversed the target, the current rate counted ions proceeding from the target is measured **110** and the measured value stored **112** in the manner described above. A process for fitting measured ion rate data to a selected model is then undertaken as described above but here employed in extrapolation of the ion rate data for predicting **140** the time at which the termination threshold will be met for the ion sculpting process. **FIG. 20B** is a flow diagram of the steps for this extrapolation and prediction technique. In a first step, the measured ion rate is input **150** to a processor for making the extrapolation and prediction. Then a selected number, n, of ion rate measurements that have been previously acquired are fit **126** to a selected model in the manner previously described.

[0161] Once the ion rate measurement data is fit to the model, the ion rate measurement data is extrapolated **152** to estimate the future time at which an ion rate measurement will meet the selected ion rate termination threshold. The predicted future time at which the termination point is expected to be reached is then output **154**. This prediction enables a decision as to how best to control the progression of the ion sculpting process. Referring back to **FIG. 20A**, with the expected termination time known, there can be made a query **142** as to whether to remain in a measurement-guided, feedback loop control regime or whether to end the feedback control.

[0162] Such a query can be implemented, e.g., as a threshold query or other parameter. For example, when the ion rate reaches a level that is close to, but not at, the threshold, the feedback control can be discontinued. Such a scenario could be advantageous where, e.g., it is expected that further ion sculpting as the threshold is approached might actually overshoot the threshold. Referring to **FIG. 20A**, in such a scenario, if it is determined that no, it will be best if the process not remain in the measurement-guided regime, then the process parameters can be adjusted **144** as desired, based on the current state of the sculpting, and one or more final ion packets delivered **146** to the target, with the feedback loop control suppressed. As shown in the diagram, the adjustment of process parameters can be carried out after each ion packet delivery, if desired. The ion sculpting process is then ended **148** at a user-defined time.

[0163] If the query **142** as to whether to remain in a measurement-guided, feedback loop control regime or whether to end the feedback control indicates that the yes, the feedback loop control should continue, then as shown in the diagram, the ion rate refinement model can be adjusted **120**, and the process parameters can be adjusted **122** in the manner described above. The next ion packet is then delivered **106** to the target and the feedback loop control is continued.

[0164] The predictive control process of **FIGS. 20A-20B** enables an intelligent decision as to if and when automatic feedback control of the process should be halted, and further enables a continuous update as to the expected end point of the ion sculpting. It is not required that the feedback loop be halted during the ion sculpting as in the flow diagram of **FIG. 20A**, however. If it is determined during the process that the feedback loop should remain in control of the sculpting until the termination threshold is reached, then the process reverts to that shown in the diagram of **FIG. 19A**, where the query **116** as to reaching the termination threshold is made and based on the query, the process is either ended

118, or the process is continued in the feedback loop with adjustment of the refinement model **120** and process parameters **122**, if desired.

[**0165**] A further example of an extrapolation control technique provided by the invention is shown in the flow diagrams of **FIGS. 21A-21B**. Here as above it is assumed that periodic ion exposure of a target and an ion counting feedback loop configuration like that of **FIG. 3A** are employed. In this extrapolation control technique **160**, an ion sculpting process is begun in the manner previously described, with a termination threshold selected **102**, and ion sculpting process parameters selected **104**. The ion sculpting is initiated by delivering **106** an ion packet to the target, causing material transport motion **108** on the target surface.

[**0166**] Once an ion packet has been sent to a target and has traversed the target, the current rate of ions proceeding from the target is measured **110** and the measured value stored **112** in the manner described above. A process for fitting measured ion rate data to a selected model is then undertaken as described above but here employed in extrapolation of the ion rate data for predicting **162** the ion rate for a future point in time during the sculpting process. **FIG. 21B** is a flow diagram of the steps for this extrapolation and prediction technique. In a first step, the measured ion rate is input **166** to a processor for making the extrapolation and prediction. Then a selected number, n, of ion rate measurements that have been previously acquired are fit **126** to a selected model in the manner previously described.

[**0167**] Once the ion rate measurement data is fit to the model, the ion rate measurement data is extrapolated **168** to estimate the ion rate for a selected future point in time during the sculpting process. In other words, the ion rate at a future time is predicted based on the selected model and the fit of the n previous ion rate measurements to that model. It is recognized that the accuracy of extrapolated ion rate values may not be as high as that of refinements for previously measured ion rate values; it can therefore be preferred to not extrapolate to times very far in the future. To aid in the accuracy of the ion rate prediction, it can be preferred to employ a mathematical model of the ion sculpting process rather than a simple statistical approach.

[**0168**] Referring back to the flow diagram of **FIG. 21A**, once the predicted ion rate is determined, a query **142** is made as to whether to remain in a measurement-guided, feedback loop control regime or whether to end the feedback control. Such a query can be implemented, e.g., as a threshold query or other parameter. For example, when the ion rate reaches a level that is close to, but not at, the threshold, the feedback control can be discontinued. Such a scenario could be advantageous where, e.g., it is expected that further ion sculpting as the threshold is approached might actually overshoot the threshold. Referring to **FIG. 21A**, in such a scenario, if it is determined that it will be best if the process not remain in the measurement-guided regime, then the process parameters can be adjusted **144** as desired, based on the current state of the sculpting, and one or more final ion packets delivered **146** to the target, with the feedback loop control suppressed. As shown in the diagram, the adjustment of process parameters can be carried out after each ion packet delivery, if desired. The ion sculpting process is then ended **164** at a user-defined time.

[**0169**] If the query **142** as to whether to remain in a measurement-guided, feedback loop control regime or whether to end the feedback control indicates that the yes, the feedback loop control should continue, then as shown in the diagram, the ion rate refinement model can be adjusted **120**, and the process parameters can be adjusted **122** in the manner described above. The next ion packet is then delivered **106** to the target and the feedback loop control is continued in the manner described above.

[**0170**] These example extrapolation techniques are provided to highlight the wide range of control paradigms contemplated by the invention. The predictive nature of the extrapolation techniques enables an increase in ion sculpting control and accuracy. For example, the ion rate termination threshold can be set slightly off from that corresponding to a selected final feature size, so that once the threshold is met, one or a few final ion packets can be delivered, under adjusted process conditions if desired, to meet the selected feature size under manual, rather than automatic, control. Further, the ion process can be continuously monitored for predicted progress, enabling adjustments to the process parameters if warranted. Additionally, by enabling a prediction of when the termination threshold will be met, the current process parameters can be adjusted to ensure that the threshold is not overshot under automated feedback control. As described above, aside from the predictive control techniques, the ion rate measurement refinement of the invention enables real time data noise reduction and an increase in S/N ratio, resulting in a corresponding increase in accuracy of process control and termination decisions. As discussed previously, the invention does not require the use of ions as a feedback detection species. Other selected species can be employed so long as the selected species is compatible with the ion sculpting process conditions. Alternating ion sculpting and detection species measurement intervals can be employed as well.

[**0171**] The feedback control techniques just described can be implemented in any suitable hardware configuration, e.g., that shown and described with regard to **FIG. 3A**. While it is preferred that a processor be provided that enables real time measurement refinement and extrapolation, as explained above an ion sculpting process can be paused while the analysis is carried out and then restarted. Whatever time correspondence is employed, the techniques enable enhancement of the control and accuracy of an ion sculpting process.

[**0172**] The ion rate measurement, data refinement, and extrapolation control techniques of the invention for imposing feedback control on ion irradiation mass transport is advantageous for many applications for enabling precise feature formation, but is not required by the invention. Once a mass transport process is characterized, and for processes that do not require very fine feature control, feedback control of the system may not be required. All that is required is the exposure of the material to an ion beam under conditions that impose processes such as mass transport for adjusting dimensions of structural features of the material by local material addition or subtraction.

[**0173**] This structural material adjustment process provided by the invention can be applied to a wide range of structural features, including holes, slits, apertures, and gaps in general, and in trenches and other such features where a distinct feature rim or wall is present and can be adjusted. It further can be applied to fabrication of protruding features such as hillocks and asperities.

[0174] In one example of such a fabrication technique, the ion flux and dose and the temperature of a membrane are selected to produce a protrusion on the membrane by exposure to ion beam flux. One membrane surface is exposed to the ion beam flux under the selected conditions. This results in formation of a protrusion on the membrane surface opposite that exposed to the ion flux.

EXAMPLE 8

[0175] A silicon nitride membrane of about 500 nm in thickness was produced by a LPCVD process following the fabrication sequence outlined in **FIG. 2**. The membrane was exposed to a gallium ion beam at an energy of about 50 KeV and a dose of about 4 nanocoulombs/μm^2. Five different isolated exposure areas on the membrane were defined, namely, 0.12 μm^2, 0.14 μm^2, 0.16 μm^2, 0.18 μm^2, and 0.20 μm^2.

[0176] **FIG. 12** is an atomic force micrograph of the nitride membrane surface opposite that which was exposed to the gallium ion beam. In this image, brightness level corresponds to topology; the brighter a region in the image, the "taller," or higher, is the topology of that region. As noted in the image, both of the 0.16 μm^2, 0.18 μm^2, and 0.20 μm^2 membrane areas, and one of the 0.14 μm^2 membrane areas were opened by the ion beam exposure, i.e., an aperture through the thickness of the membrane resulted from the ion beam exposure in that area. The other 0.14 μm^2 membrane area and the 0.12 μm^2 membrane area were not opened by the ion beam exposure and instead exhibit hill-like protrusions formed on the membrane surface opposite that exposed to the ion beam. This example demonstrates that dose can be controlled to cause mass transport in a manner that produces a protrusion on the surface of a structure. This example further demonstrates that the ion beam species can impact the nature of feature formation and adjustment; in this example gallium ions were employed as opposed to the argon ions employed in earlier examples. It is understood in accordance with the invention that ion species can be selected to control aspects of feature formation processing. Similarly, it is understood in accordance with the invention that the ambient gas species present during the ion interaction with a material can be selected to control the nature of the interaction.

[0177] The features formed by and/or having dimensions adjusted or changed by the processes of the invention can be provided on the surface of a structure, in a layer provided on a support structure or a free-standing membrane, or other surface which can be irradiated by an ion beam. Composite material structures can be processed. There is no restriction on the fabrication sequence employed to produce the starting structures for which dimensional adjustment is to be carried out.

[0178] The invention provides a model of the various ion beam processes described above for enabling control of the process parameters. Such process control provides an ability to, in effect, ion beam sculpt nanoscale features with a precision not previously attainable. Solutions to analytical expressions of the model, as-obtained with appropriate parameter values for a given sculpting process, can be employed in accordance with the invention to produce prespecified nanoscale features in a precise, predictable manner, and in open-loop fashion, i.e., without the need for closed-loop ion counting rate feedback control like that provided by the feedback system of **FIG. 3A** described above. As explained in detail below, the invention provides a recognition that the ion beam sputtering and mass transport phenomena discussed above compete during an ion beam sculpting process. The methodology of the invention provides the ability to control these phenomena such that one can be made to dominate over the other in a manner to enable production of a desired nanoscale feature or geometry.

[0179] The invention provides analytical model expressions that are based on process parameters which generally depend on the properties of a material being ion beam sculpted, e.g., the specific material composition, the initial geometry of a structure or feature at the material surface, material defects, and doping impurities, as well the local environment around the sculpting process, for example the gaseous ambient environment, the temperature of the material, the incident ion species, ion flux, and ion energy, and other parameters that characterize the incident ion beam. It is recognized in accordance with the invention that the process parameters therefore are to be adjusted based on a particular ion beam sculpting application to achieve desired process results, in the manner described below.

[0180] For clarity, the following discussion is directed to a process model based specifically on ion beam sculpting of a nanopore of a selected diameter, or area. As explained in detail below, however, the invention is not limited to such. The analytical process model expressions provided by the invention can be adjusted to control formation of a wide range of geometries, e.g., slits or irregularly-shaped holes, trenches, or other geometry, extending through the entire thickness of a material or through only a portion of the thickness. In addition, positive features, rather than negative features such as apertures, can be formed on a material surface or in a material, in the manner previously described. Features such as lithographic mask features, ion beam doping profiles accompanied by mass transport, or buried layer profiles can further be produced in accordance with the process model provided by the invention. Further, the dimensions of existing features can be controlled, or changed, in accordance with the invention. There is no fundamental geometric symmetry or pattern to which the process control model is limited. Whatever geometry or feature is being formed, controlled, and/or changed, it is the nanoscale control of that geometry by the methodology of the invention that is universally applicable.

[0181] As explained above, the model employed by the invention for use in controlling ion beam sculpting is based on a recognition that distinct processes are likely to compete during the sculpting. Considering ion beam sculpting of a nanopore to reduce a starting diameter of a pore to a selected reduced diameter, a first such competing process tends to open the pore and is understood to likely be driven by ion beam-sputter erosion of a pore edge. This erosion process is understood to be dominant at low temperatures and high ion beam fluxes. Established sputtering phenomenology can be employed for most applications to account for and control sculpting processes that are dominated by sputtering in this regime.

[0182] A second, competing process tends to cause motion of matter, i.e., mass transport, and can operate to a degree

necessary for reducing the starting pore diameter. Without being bound to theory, it is understood that more than one view can explain this phenomenon. A first theory understood in accordance with the invention takes the view that a very thin, e.g., about **5** nm-thick, stressed viscous surface layer can be created by the energy and matter deposited on a material surface by an ion beam. An enhanced collective motion, driven by a reduced viscosity and/or enhanced stress owing to implantation effects or surface tension, may cause the layer to flow or relax, whereby material is transported across a surface.

[0183] Although this "viscous flow" model has merit, in accordance with the invention a preferred ion beam sculpting control model reflects a process theory in which incident ions create as well as annihilate excess, independent, and mobile species such as adatoms, ad-dimers, ad-molecules, molecular clusters and surface vacancies that are present at the surface of a material exposed to an ion beam. For most applications, it is understood to be reasonable to assume a single mobile species which, for simplicity, will here be called an "adatom." The changing concentration of surface adatoms, C(r,t), is modeled in accordance with the invention as a function of distance, r, along the surface, and time, t, governed by a two dimensional diffusion expression as:

$$\frac{\partial}{\partial t}C(r,t) = FY_1 + D\nabla^2 C - \frac{C}{\tau_{trap}} - FC\sigma_C, \tag{4}$$

[0184] where C is the concentration of adatoms on a two-dimensional surface, r=(xmy) is the radial surface position, t is time, F is the ion flux, Y_1 is the number of adatoms created per incident ion, D is the adatom surface diffusivity, τ_{trap} is the average lifetime of an adatom before thermally-activated adatom annihilation occurs at a surface defect, and σ_c is the cross-section for adatom annihilation by incident ions.

[0185] **FIG. 13** schematically illustrates the competing mechanisms modeled by this expression. Changes in concentration of surface adatoms, $\partial C/\partial t$, depends firstly on a rate of generation of adatoms that results from the ion flux, F, with Y_1 indicating the number of created adatoms per incident ion. The second modeled term is a mass transport term, driving the adatom transport by diffusion along the surface and within the structure, and thus depending on the adatom surface diffusivity, D, and the adatom concentration gradient. This transport term models the reduction in a nanopore radius by mass transport of material from around the pore, in the manner described and demonstrated above.

[0186] Further as shown in **FIG. 13**, the surface adatom concentration change is determined by adatom annihilation that can occur at a surface defect, or trap; τ_{trap} is correspondingly defined as the average lifetime of an adatom before such annihilation at a trap occurs. The final term models ion beam annihilation of adatoms; here σ_c reflects the cross-section for adatom annihilation by the incident ion beam itself. It is also understood that annihilation of adatoms occurs at the pore edge as the pore is filled by the mass transport phenomena; this annihilation mechanism is treated as a boundary condition for Expression (4) above.

[0187] The first and last terms on the right hand side of Expression (4) above reflect an understanding provided by the invention that each incident ion resets a surface patch of area given as σ_C to an adatom concentration given as Y_1/σ_c that is independent of its previous state. The presence of a nanopore of an initial diameter in the material being subjected to an ion flux is represented by adding an adatom sink at the nanopore edge, for a nanopore radius, R, and by including the second term on the right hand side of the expression to model long-range material diffusion to the pore edge. Adatoms annihilated at the nanopore boundary are turned into new, stable matter at the boundary.

[0188] The magnitudes of the parameters Y_1, D, τ_{trap}, and σ_c can be estimated for a given ion beam sculpting application from experience with suitable materials and can be determined by independent experiments. For example, a matrix of pore-closing experiments can be conducted, preferably including both steady state and transient conditions, and employing the feedback system of the invention described previously for making precise determination of the influence of each parameter on feature formation, e.g., pore-reduction rate, and other characteristics. One or more "test" ion flux exposures of a material structure can be carried out under a variety of test process conditions, with each "test" exposure monitored by the ion counting feedback loop previously described above. This monitoring enables an indication of feature fabrication dependence on the test process conditions. In turn, the magnitudes of the model parameters, and corresponding optimal process conditions, can then be determined and selected based on the accumulated test process results. It is recognized in accordance with the invention that the values of the model parameters can be manipulated by adjusting not only temperature, ion beam flux, and ion beam energy, but also by adjusting the ambient gas species and pressure, ion species, material properties, e.g., concentrations of trace impurities on the material surface, material defects, and impurity doping. The parameters are therefore treated here as being fully adjustable to enable selection based on test process results, if desired, and to enable precise control of the ion beam sculpting process for a given application.

[0189] By comparison with the trapping annihilation term of the right hand side of Expression (4) above, the ion impingement annihilation term of the right hand side of Expression (4) above corresponds to an average adatom lifetime before ion impingement-induced annihilation as $\tau_{ion}=1/(F\sigma_c)$. Thus, the effective surface lifetime, τ, of an adatom in the presence of both annihilation mechanisms can be given as:

$$\frac{1}{\tau} = \frac{1}{\tau_{trap}} + F\sigma_C \tag{5}$$

[0190] It is understood that under some circumstances, one of the two annihilation terms of the right hand side of Expression (4) above will be insignificant compared to the other, but this may not necessarily always be the case, and is not required for the analysis of the invention.

[0191] An additional annihilation mechanism, namely, adatom annihilation by joining of adatoms and precipitation into adatom islands, is not represented in Expression (4) for simplicity so that this partial differential equation is linear, rather than nonlinear, for ease of analytical mathematical

solution. It is understood, however, that applications for which this annihilation channel cannot be neglected are more precisely modeled with the addition of another term to the right hand side of Expression (4) that would be proportional to $-C^n/\tau_{island}$; where n is the number of adatoms in an critical island of a critical size, i.e., a size just large enough to be more likely to grow than to shrink, and τ_{island} is a characteristic time constant for adatom island formation. Thermal generation of adatoms, thermal desorption of adatoms into a surrounding vacuum, and deposition of adatoms from an ambient vapor are additional mechanisms that have also been neglected for clarity but can be readily incorporated, when necessary for a given application, in the manner of the mechanisms described above.

[0192] Expression (4) above expresses an understanding provided by the invention that far from a feature, e.g., a nanopore, steady ion beam irradiation of a material surface creates on the surface and at the near-surface a spatially uniform, steady state adatom concentration $C_{SS}=FY_1\tau$. The pore boundary, or nanopore edge, is taken to be a "perfect sink" for adatoms, which are there transformed to a thin layer of accumulating matter that accounts for pore reduction. If the nanopore edge is taken as a sink for adatoms then the adatom supersaturation drops as the nanopore edge is approached. Expression (3) above implies that the normalized difference, n(r,t), between C_{SS} and C(r,t), given as $n(r,t)\equiv(C_{SS}-C(r,t))/C_{SS}$, obeys a diffusion equation as:

$$\frac{\partial n(r,t)}{\partial t} = D\nabla^2 n - \frac{n}{\tau}. \tag{6}$$

[0193] The assumption that the pore boundary is a "perfect sink" for adatoms implies that the adatom concentration, C, vanishes at the pore boundary, shown as in **FIG. 13** to be of radius R. This is the simplest boundary condition that accounts for a net accumulation of adatoms at the pore, and thus for reduction of pore diameter. It is recognized in accordance with the invention, however, that because of its interaction with the ion beam, the pore boundary could be a net source of surface vacancies while producing this pore-reducing effect if vacancies, rather than adatoms, dominate surface transport. The invention is therefore not limited to an adatom "perfect sink" boundary condition. An alternative boundary treatment contemplated by the invention employs a surface accommodation velocity to describe a partial sink for adatoms at the pore boundary, in a manner analogous to surface recombination velocity factors employed in semiconductor modeling of charge carriers interacting with surfaces. These pore boundary conditions can be directly generalized to other feature location characteristics.

[0194] The diffusion model employed by the control method of the invention is thus found to be phenomenological in nature, relying on several idealizations and assumptions to compensate for uncertainty in aspects of many microscopic properties of matter under ion beam exposure. Nevertheless, it is understood by the inventors that studies of pulsed and continuous ion beam exposures at different temperatures, gas ambients, and material conditions can be employed for a given application in conjunction with the model to permit the determination of materials-specific parameters like diffusivity, D, ion-induced adatom population Y_1, area of adatom annihilation by ion impingement σ, and adatom lifetime prior to trap annihilation, τ_{trap}, for a given application. Such analysis enables prespecified and precise ion beam sculpting of the material in the production of useful nanoscale devices.

[0195] In addition, practitioners of ion beam sculpting can use the model provided by the invention in both quantitative and qualitative ways. That is, by knowing the qualitative as well as quantitative nature of the solutions to the analytical model expressions and their dependence on various parameters of the model that are subject to experimental control, the parameters can be adjusted to achieve desired dimensional control of structures for large classes of structures. For example, the model demonstrates a qualitative dependence of an ability to increase the rate of pore reduction, and even the possibility of reducing a pore diameter at all with ion sculpting, by increasing the material temperature or by decreasing the incident flux of incident ions. The model also provides a quantitative dependence of the precise degree of temperature increase or flux decrease required for a given application. In these examples, practitioners are guided to such action by noting that both of these actions increase the effectiveness of surface diffusion of adatoms over sputtering, by a temperature enhancement of the surface diffusion constant and a reduction in adatom sputtering, respectively.

[0196] Other qualitative and quantitative uses of the model include correlations between analytical predictions of the model and ancillary empirical observations. For example, an observation that nanopores, the area of which are reduced to a desired area more quickly under the ion beam sculpting process, may require a minimum initial diameter before the sculpting process can be effective, can be correlated to process conditions via the model. Although the model at any given stage of its solution evolution may not contain the details of the process controlling the pore diameter, it can be used to correlate the process control parameters, and thereby, e.g., control the process mechanisms.

[0197] In a further example, consider the reduction in diameter of a nanoscale pore from a starting pore diameter down to a selected final diameter in the manner described above with reference to the pore shown in the electron micrographs of **FIGS. 7A-7B**. A plot of pore area as a function of ion beam dose, as in **FIGS. 9A-9B**, demonstrates that for a given ion beam dose, as the incident ion beam flux is reduced, mass transport of material increases, thereby more quickly reducing the diameter of the pore. As explained above, the strong nonlinearity of this result indicates that at high ion beam fluxes, the mass transport mechanism captured by the model of the invention may become suppressed. Analysis and testing based on the model of the invention enables a correlation of this flux dependence for given material and ion beam characteristics.

[0198] **FIG. 14A** provides a similar plot of pore reduction data, here of nanopore area as a function of total ion beam dose for several ion beam fluxes and for continuous as well as pulsed ion beam exposure. The dotted plot points correspond to experimentally measured results, and the solid lines correspond to results produced by analysis of Expression (4) above, as explained in detail below. The slope of this data demonstrates that for continuous ion beam exposure, where the ion beam flux, F=0.53, 1.17, and 4.7 $Ar/sec/nm^2$, the efficiency of pore closing per incident ion is clearly greater at low fluxes than at high fluxes. This plotted data also

demonstrates that pulsed ion beam exposure, here at 100 ms/1 s, provides more effective mass transport, and a correspondingly increased rate in pore area reduction, than does a continuous ion beam at the same instantaneous flux. Particular control methodology provided by the invention for the plotted pulsed ion beam exposure data is described below.

[0199] Thus, as explained above, in accordance with the invention, ion beam sculpting process parameters can be adjusted for a given application, based on the process model provided by the invention, to enable prescription of nanoscale geometries produced by the sculpting process. As explained above, parameters will in general depend on the composition of the material being ion sculpted, the environment around the structure during the sculpting process, temperature, and on the incident ion species, energy, and other parameters that characterize the incident ion beam. The incident ion beam can be supplied as atoms, i.e., neutral ions, ions of a controlled charge state, molecules or clusters of incident atoms, or indeed any controlled energy source. It is recognized that differing model parameters will be required for various energy sources. In addition, the invention contemplates the use of multiple energy sources as well as adjustment of the charge state of the material surface at the start and during the sculpting process.

[0200] It is recognized in accordance with the invention that both the surface of a structure being ion sculpted and the ion-induced adatoms on the surface may be highly susceptible to the influence of the environment. By environment is meant a background ambient of a gas like oxygen, hydrogen, sulfur hexafluoride, or other selected gas. As a result the interaction of these gasses with surface atoms and/or adatoms, the transport of adatoms and/or the removal of surface atoms and adatoms can be greatly modified, relative to a process carried out in the absence of such gasses. Consequently, the rates and signs of ion sculpting mechanisms captured in the model provided by the invention will be dramatically modified by ambient gas species, and these modifications can be of great utility for precise control of the ion beam sculpting process.

[0201] It is also to be recognized that the state and chemical reactivity of the ambient gas, as well as the excitation state of the surface or charge state of the surface being acted upon, can be influenced by, or catalyzed by, the incident ion beam. This can result in removal or addition of adatoms and/or creation or elimination of surface defect traps, thereby influencing the mass transport and annihilation mechanisms of the ion sculpting process. Means other than an incident ion beam, such as an electron beam, laser beam, atomic beam, metastable excited atomic beam, mixtures of ion beams, or other energy source, can be used to control the sensitivity of the ion sculpting process to the ambient environment in which the process is carried out. Adjustment and control of these various influences are recognized in accordance with the invention to enable flexibility and reproducibility of prespecified and precise ion beam sculpted geometries of a material in the production of useful nanoscale devices.

[0202] As mentioned above, the charge state of an ion beam can be adjusted based on a particular ion beam sculpting application to achieve desired ion sculpting process results. Positive, neutral, or negative ions can be employed in accordance with the invention to produce a desired surface force between adatoms that are produced and transported along the surface during the sculpting process.

[0203] Turning to more quantitative solutions of the analytical model provided by the invention, and referring back to Expression (4) above, it is clear that the ion sculpting process can be specifically controlled by controlling the dominance of adatom creation and transport mechanisms relative to adatom annihilation mechanisms. Specifically, the adatom creation mechanism, represented by the term FY_1, along with the adatom mass transport mechanism, represented by the term $D\nabla^2 C$, can be controlled to dominate, or alternatively be dominated by, the adatom trapping annihilation mechanism, represented by the term C/τ_{trap}, together with the adatom ion impingement annihilation mechanism, represented by the term $FC\sigma_c$. This control accordingly enables a "starting" and "stopping" of an ion sculpting process to achieve a desired feature geometry.

[0204] Specifically, in accordance with the invention, process parameters that influence the ion flux, F, and adatom diffusivity, D, are selected relative to process parameters that influence surface defects and ion impingement characteristics, to control the adatom concentration and transport. For example, material temperature, material surface conditions, and other material dependent characteristics can be selected to increase adatom diffusivity, D, thereby to enhance mass transport to a feature being ion sculpted and to maximize the rate at which an ion sculpted feature is produced. Minimization of surface defects and other material trapping mechanisms can be carried out to minimize annihilation of adatoms by traps, thereby further enhancing the mass transport mechanism of the ion sculpting process.

[0205] Considering the influence of the ion beam flux, F, as explained above with reference to the plot of **FIG. 14A**, as ion beam flux is increased, adatom annihilation by ion impingement also increases, resulting in a reduction of adatom concentration and transport to a feature to be produced. But at the same time, as ion beam flux is increased, the number of adatoms created also increases. Ion beam flux is therefore preferably controlled to influence adatom creation and adatom annihilation, thereby to determine the availability of adatoms for the ion sculpting process. Control of incident ion species and energy, and control of the gaseous process ambient enable control of the factors Y_1 and σ_c similarly to control adatom creation and annihilation.

[0206] Specific solutions for the spatial adatom concentration profile given by the model in Expression (4) can be achieved under a quasi-stationary approximation in which the left hand side of Expression (4) is set to zero. This scenario is justified for applications in which the adatom concentration profile of a material being processed adjusts rapidly to changes in feature geometry, e.g., changing pore radius, R, and ion flux, F. With this assumption, the model yields a spatially uniform steady-state adatom supersaturation concentration far from the pore edge, decaying over a characteristic mass transport distance, X_m, to zero at the nanopore edge.

[0207] Because adatoms are being removed everywhere on the surface of a material exposed to ion beam irradiation, as well as being created by the ion beam, adatoms created within the mass transport distance, X_m, of a feature, e.g., a the pore edge, are more likely to diffuse to and add to the

material at the pore edge than be annihilated by incident ions; the opposite is true of adatoms created farther away. The mass transport distance, X_m, therefore decreases with increasing flux.

[0208] Obtaining Y_p, the effective cross section for sputter-erosion from the pore edge, from relevant data obtained at low temperature, where diffusion is expected to be insignificant, and taking Y_1, the number of adatoms created per incident ion, to be of order unity, then for a material thickness of about 10 nm for a silicon nitride sample, the model of Expression (4) yields the solid curves of the plots of **FIG. 14A** for each Argon flux given, at a temperature of about 28° C., which is a temperature experimentally verified to cause pores to be reduced.

[0209] From this data, a value of diffusivity, D, of about $10^3\ nm^{2\ s-1}$ is extracted, using a linear fit, with σ_c of about 0.1 nm^2 as a reasonable estimate. From this experimental data, it is found that the model therefore predicts that the maximum distance, X_m, from which adatoms are likely to diffuse to and add to material at a feature location, e.g., at the edge of a reducing pore, is linearly proportional to the adatom diffusivity, the trap lifetime, the ion beam flux, and the cross section for adatom annihilation, as:

$$\frac{1}{X_m^2} = \frac{1}{D\tau_{trap}} + \frac{\sigma_C}{D}F \tag{7}$$

[0210] and a linear relation is indeed observed, as demonstrated by the plotted data of **FIG. 14B**. **FIG. 14A** provides an indication of the corresponding mass transport distance, X_m, for each ion flux considered. The mass transport distance, X_m, thus is found to represent a characteristic distance from the pore edge within which adatoms are more likely to reach the pore than be annihilated by traps or ion beam flux erosion. Adatoms beyond a distance X_m from a feature to be formed, such as a pore edge, are more likely to be annihilated before they reach the pore edge.

[0211] Considering particular parameter effects, as the ion beam flux is increased, the number of produced adatoms is increased, but the distance from which adatoms can diffuse to and add to a pore edge is reduced. As the average lifetime of an adatom is increased by a reduction in surface defects, the maximum adatom diffusion distance also increases. As the temperature is increased, the diffusivity, and correspondingly, the maximum adatom diffusion distance, is increased. With the analytical understanding of these relationships provided by the invention, the model thereby enables an ability to prescribe a minimum distance, X_m, of material that must be provided around a starting feature, such as a nanopore, or around a location at which a feature is to be fabricated, to provide sufficient material for fully forming the feature, e.g., for reducing the radius of the nanopore to a desired final radius, R, under given processing conditions, and enables adjustment of processing conditions to accommodate a maximum diffusion distance X_m that is available for a given application.

[0212] The adatom flux, or current, j, at any location, r, of a surface being processed is given by

$$j(r) = -D\partial C/\partial r, \tag{8}$$

[0213] with r the radial coordinate, and the concentration gradient evaluated at the edge of the nanopore, at r=R, providing an indication of the adatom fluxj(R) to the edge of the nanopore material. Additionally, scraping of material off the edge of the nanopore, tending to increase the pore area, is accounted for by a characteristic cross section for sputter-erosion from the pore edge.

[0214] If each adatom reaching the nanopore fills the pore by a volume Ω, thereby reducing the extent of the pore, then the nanopore reduction rate is predicted by a volume balance given as:

$$\frac{d}{dt}(\pi R^2 H) = 2\pi R\Omega(-j(R) + FY_p), \tag{9}$$

[0215] where Y_p is an effective cross section for sputter-erosion from the pore edge, H is the thickness of a film that is formed as the nanopore is reduced, or filled in, and Ω is the atomic volume. Substituting Expression (8) above for the adatom current j(R) at the edge of the nanopore results in:

$$\frac{d}{dt}(\pi R^2) = -\frac{2\pi\Omega RF}{H}\left(Y_1 X_m \frac{K_1\left(\frac{R}{X_m}\right)}{K_0\left(\frac{R}{X_m}\right)} - Y_p\right), \tag{10}$$

[0216] where K_0 and K_1 are modified Bessel functions of the second kind.

[0217] This expression enables ion beam sculpting control, for a given set of process parameters characteristic of an ion beam environment, to produce a nanopore of a desired radius R. For example, it is found from this model that reduction of pore radius is enhanced with increasing temperature. This can be accounted for by a thermally activated adatom diffusion coefficient in the manner described above.

[0218] Based on this understanding, if the process parameters that influence adatom creation and mass transport are selected such that the first two terms of the right hand side of Expression (4) above dominate the second two terms of the right hand side of Expression (4), then ion sculpting to form a selected feature in a material being ion-irradiated proceeds. On the other hand, if the process parameters that influence adatom annihilation by traps and adatom annihilation by ion impingement are selected such that the second two terms of the right hand side of the Expression (4) dominate, then material sputtering and removal, rather than mass transport of the material from one surface location to another, is controlled to occur.

[0219] Thus, in accordance with the control method of the invention, with this methodology, Expression (10) can be employed to specify R_{max}, the largest starting pore radius that can be reduced at all under any particular set of processing conditions. This maximum starting radius, R_{max}, increases with increasing temperature and with decreasing ion beam flux. At a sufficiently high temperature and sufficiently low ion beam flux, R_{max} becomes infinite, in a

scenario that determines the conditions under which an open pore can be closed. The maximum radius, R_{max} is thus given by:

$$Y_1 X_m \frac{K_1\left(\frac{R_{max}}{X_m}\right)}{K_0\left(\frac{R_{max}}{X_m}\right)} - Y_p = 0. \tag{11}$$

[0220] With X_m, Y_1, and Y_p provided as constants, the ratio of

$$\frac{K_1\left(\frac{R}{X_m}\right)}{K_0\left(\frac{R}{X_m}\right)}$$

[0221] gets smaller with increasing pore radius, R, so that at $R=R_{max}$ and above, the pore radius cannot be reduced. Analysis of this expression thereby enables adjustment of processing conditions to produce a desired R_{max} or to accommodate a maximum radius, R_{max}, that is fixed by a given application.

[0222] It has been observed empirically that the thickness, H, of a growing membrane or film produced as a nanopore radius is reduced and a pore is filled in depends on the rate of reduction, $d(\pi R^2)/dt$, where R is the radius of the nanopore. Higher pore reduction rates result in thinner films than lower pore reduction rates. In addition, higher ion beam energies result in thicker films than lower ion beam energies. Based on the expressions given above, the invention provides the ability to prescribe a selected film thickness by selecting ion beam sculpting process conditions, and particularly ion beam energy, that result in a desired pore reduction rate and film thickness.

[0223] As explained above, it is understood in general in accordance with the invention that different regions of the perimeter of an arbitrarily-shaped aperture will also open and close according to Expressions 4-7 above. In addition, Expressions 7-11 above can be generalized in an obvious manner to remove the cylindrical symmetry assumed in the example given here, to enable modeling and process control of arbitrarily-shaped features. Thus, as stated above, the invention is therefore not limited to a particular feature geometry.

[0224] Time dependent solutions of the adatom diffusion model can be employed in accordance with the invention to describe an ion sculpting process employing a pulsed ion beam having a selected duty cycle. In order to model conditions when the incident ion beam is turned off, a steady state condition is assumed for the initial concentration profile. That is, the ion beam flux is set to F=0, and the initial concentration of the adatoms on the surface is given, for the nanopore example above, as:

$$C(r, t=0) = C_{ss}\left[1 - \frac{K_0\left(\frac{r}{X_m}\right)}{K_0\left(\frac{R}{X_m}\right)}\right], \tag{12}$$

[0225] where C_{ss} is the steady state adatom concentration far from the pore edge. Substitution of this initial concentration into Expression (4) above then provides:

$$\frac{\partial}{\partial t} C(r, t) = D\nabla^2 C - \frac{C}{\tau_{Trap}}, \tag{13}$$

[0226] with assumed boundary conditions for the adatom concentration, C, as:

$$\begin{aligned} &C(R, t) = 0 \\ &C(b = NX_m, t) = C_{ss} e^{-\frac{t}{\tau_{Trap}}}, \end{aligned} \tag{14}$$

[0227] where b is an outer boundary condition, far from the pore edge, i.e., N>>1. In practical calculations, N=5 is typically sufficiently large, but it is recognized that for some applications, a larger value of N can be required for increased accuracy.

[0228] Solutions to Expression (13) above provide time dependent solutions of the adatom concentration on the surface of a material being processed after the beam is off, as:

$$C^{off}(r, t) = C_{ss}\left[\frac{\ln\left(\frac{r}{R}\right)}{\ln(b/R)} + \sum_{n=1}^{\infty} A_n U_0(\alpha_n r) e^{-\alpha_n^2 D t}\right] e^{-\frac{t}{\tau_{Trap}}}, \tag{15}$$

$$\text{where } A_n = \frac{\pi^2 \alpha_n^2}{2} \frac{J_0^2(\alpha_n R)}{J_0^2(\alpha_n R) - J_0^2(\alpha_n b)} = \int_R^b r\left[1 - \frac{K_0\left(\frac{r}{X_m}\right)}{K_0\left(\frac{R}{X_m}\right)} - \frac{\ln\left(\frac{r}{R}\right)}{\ln(b/R)}\right] U_0(\alpha_n r)\, dr.$$

$$\text{Given: } U_0(\alpha r) = J_0(\alpha r) Y_0(\alpha b) - J_0(\alpha b) Y_0(\alpha r)$$

$$\text{and } U_0(\alpha_n R) = J_0(\alpha_n R) Y_0(\alpha_n b) - J_0(\alpha_n b) Y_0(\alpha_n R) = 0,$$

[0229] to provide the roots of α_n, J_0 and Y_0 are Bessel functions of the first kind.

[0230] The rate at which the area of a pore decreases when the ion beam is off, or the material is not being irradiated by the beam, is given as:

$$\frac{\partial}{\partial t}(\pi R^2) = -\frac{2\pi\Omega R}{H} D \frac{\partial C^{off}}{\partial r}\bigg|_{r=R} \tag{16}$$

[0231] When a material being processed is not irradiated by the ion beam, i.e., just after the beam is extinguished or the material is shielded from the beam, mobile adatoms remain on the surface of the material, but the adatom annihilation mechanism associated with the incident beam flux is no longer present. Thus, once the material is not exposed to the ion beam, those adatoms remaining on the material surface can diffuse to the pore periphery from a greatly increased X_m. This condition is discovered to significantly increase the efficiency per ion for pore radius reduction. Indeed, as shown in the plot of **FIG. 14A**, a pulsed ion beam irradiation process is found experimentally to be more efficient in forming a feature, here in reducing the radius of a pore, than continuous exposure conditions.

[0232] In accordance with the invention, Expression (16) can be employed in combination with Expression (10) above to predict and then control the rate of feature formation or change, e.g., nanopore diameter reduction, when a pulsed ion beam sculpting process is employed. Specifically, the pulsed ion beam time structure, i.e., the pulse rate and duty cycle, can be adjusted in accordance with the invention to achieve control over the sign and rate of change of structural dimensions.

[0233] It is recognized in accordance with the invention that as with the conditions when the beam is turned off, there is also a transient solution when the beam is first turned back on or the structure is again exposed to the beam. This transient may be important under some conditions, but it is understood that for most applications, the "beam-on" transient is significantly shorter than the "beam-off" transient and therefore can be ignored. If for a given application such is not the case, then the "beam-off" transient analysis given above is preferably extended to the "beam-on" analysis. Then the duty cycle of the ion beam irradiation can be particularly selected to achieve desired ion sculpting results.

[0234] To demonstrate the effectiveness of the process control methodology of the invention, a nanopore was sculpted in a Si_3N_4 membrane for use as a single-molecule electronic detector of DNA. Proteinaceous nanopores, or channels, have been inserted into lipid bilayers in aqueous solutions where they serve as electronic sensors to identify and characterize single molecules. But proteins in lipid bilayers are labile and the channel diameters they provide cannot easily be adjusted. Robust, solid-state nanopores provided in accordance with the invention, fashioned to any desired diameter, enable a yield of new data and understanding of transport in confined spaces, and make it possible to produce robust single-molecule-sensing devices to characterize molecules of DNA and other biopolymers at unprecedented speeds.

[0235] A 5 nm-diameter pore in a silicon nitride membrane was produced in accordance with the process parameters and process control described above. Then, using electrophysiology techniques, the pore was tested with double-stranded DNA. After applying a voltage bias that would draw the negatively charged DNA molecules through the nanopore, diminutions of the ionic current were observed, as shown in **FIG. 15**, in a manner analogous with the ionic-current blockages observed when single strands of DNA are translocated through the channel formed by α-hemolysin in a lipid bilayer. Because no such reductions in current were observed during one hour of monitoring before adding DNA, and because the reductions in current ceased to occur when the voltage bias was reversed, the reductions in current are attributed to interactions of individual DNA molecules with the nanopore. The duration of these reductions in current was found to be on the order of milliseconds, and to consistently fall to a current value of about 88% of the open-pore current value. This last value is commensurate with translocation of a rod-like molecule whose cross-sectional area is 3-4 nm^2.

[0236] The experimental observations, model considerations and control methodology, and experimental electronic device results all described above indicate that the ion beam-sculpting control method of the invention represents a superior approach to nanoscale fabrication. Specifically, the invention enables control of sputtering and mass transport processes that compete during an ion beam sculpting process. With the feedback control techniques described above, reproducibility does not depend on precisely matching all conditions and starting dimensions. If, however, such can be achieved, then the control model of the invention enables open loop processing without reliance on ion rate counting or other feedback control. The invention therefore is not limited to features or geometries that can accommodate an ion counting feedback loop.

[0237] The ion beam-sculpting control method of the invention is particularly useful for fabricating a wide variety of nanoscale semiconductor devices, masks, and mechanical features, and as explained above is not limited to formation of a pore or a through-hole. Slits, trenches, crosses, doping profiles, resist patterning, buried layer profiles, and other geometries and features can be produced and dimensionally controlled, or changed. Similarly, a wide range of materials can be employed, including microelectronic materials such as Si, SiO_2, Si_3N_4, Al, and a wide range of others. Furthermore, it is recognized that next-generation ion-source arrays and mask technologies, combined with multichannel ion detectors, can be employed to enable highly parallel applications of the nanoscale ion beam sculpting control methods of the invention.

[0238] This discussion highlights the wide range of applications of the solid state feature formation and dimensional control processes of the invention. The subtractive and additive materials processing techniques of the invention, in conjunction with the physical species detection and feedback control of the invention, enable reproducible and highly precise feature formation. The advantages of this precision and control are most apparent when applied to nanometric feature dimensions and dimensional tolerances. It is recognized, of course, that those skilled in the art may make various modifications and additions to the processes of the invention without departing from the spirit and scope of the present contribution to the art. Accordingly, it is to be understood that the protection sought to be afforded hereby should be deemed to extend to the subject matter of the claims and all equivalents thereof fairly within the scope of the invention.

We claim:

1. A method for controlled fabrication of a solid state structural feature, comprising:

providing a solid state structure;

exposing the structure to an ion beam under fabrication process conditions for producing the structural feature;

directing a physical detection species toward a designated structure location;

measuring a rate at which the detection species proceeds from the designated structure location;

fitting detection species rate measurements to a mathematical model; and

controlling the fabrication process conditions based on the fitted detection species rate measurements to fabricate the structural feature.

2. The method of claim 1 wherein measuring detection species rate comprises making a measurement of count of the species as the species proceeds from the designated structure location.

3. The method of claim 1 further comprising storing detection species rate measurements.

4. The method of claim 1 further comprising adjusting the mathematical model based on the fitted detection species rate measurements.

5. The method of claim 1 wherein fitting detection species rate measurements comprises fitting a selected number of previously acquired detection species rate measurements.

6. The method of claim 1 wherein the mathematical model includes parameters reflecting characteristics of the fabrication process.

7. The method of claim 1 wherein the mathematical model is a polynomial expression.

8. The method of claim 1 wherein the mathematical model is a statistical average of previously acquired detection species rate measurements.

9. The method of claim 1 wherein controlling the fabrication process conditions is based on determining if a preselected detection species rate has been met.

10. The method of claim 9 wherein if a preselected detection species rate has been met, then the ion exposure is continued without further measurement of detection species rates.

11. The method of claim 9 wherein if a preselected detection species rate has been met, then the fabrication process conditions are adjusted to complete the structural feature fabrication.

12. The method of claim 1 wherein controlling the fabrication process conditions is based on determining if measurement of detection species rates is to be continued.

13. The method of claim 1 wherein controlling the fabrication process conditions is carried out during the ion exposure.

14. The method of claim 1 wherein the ion exposure comprises periodic ion exposure with a duty cycle of an ion packet duration and a nonexposure duration.

15. The method of claim 14 wherein controlling the fabrication process conditions comprises controlling ion packet duration.

16. The method of claim 14 wherein controlling the fabrication process conditions comprises controlling ion exposure duty cycle.

17. The method of claim 1 wherein controlling the fabrication process conditions comprises controlling ion energy.

18. The method of claim 1 wherein controlling the fabrication process conditions comprises controlling ion species.

19. The method of claim 1 wherein controlling the fabrication process conditions comprises controlling structure temperature.

20. The method of claim 1 wherein controlling the fabrication process conditions comprises controlling process pressure.

21. The method of claim 1 wherein controlling the fabrication process conditions comprises terminating exposure of the structure to the ion beam at a time when the fitted detection species rate measurements indicate completion of the structural feature fabrication.

22. The method of claim 1 wherein the physical detection species comprises ions.

23. The method of claim 1 wherein the structure comprises a semiconductor substrate.

24. The method of claim 1 wherein the structure comprises a membrane.

25. The method of claim 1 wherein the structure comprises a substrate including a layer in which the structural feature is to be fabricated.

26. The method of claim 1 wherein the structural feature is an aperture in the structure and the designated structure location is through the aperture.

27. The method of claim 26 wherein the aperture comprises an array of apertures.

28. The method of claim 26 wherein the fabrication process conditions are selected to reduce an initial aperture diameter.

29. The method of claim 26 wherein the fabrication process conditions are selected to increase an initial aperture diameter.

30. The method of claim 26 wherein the fabrication process conditions are selected to etch the aperture in the structure.

31. The method of claim 1 wherein the structural feature is a gap between at least two structural edges and the designated structure location is through the aperture.

32. The method of claim 31 wherein the fabrication process conditions are selected to reduce an initial gap in the structure.

33. The method of claim 31 wherein the fabrication process conditions are selected to increase an initial gap in the structure.

34. The method of claim 1 wherein the physical detection species is directed toward a designated structure location during ion beam exposure of the structure.

35. The method of claim 1 wherein the physical detection species is directed toward a designated structure location at a time when the structure is not exposed to the ion beam.

* * * * *